INFORMATION TO USERS

This manuscript has been reproduced from the microfilm master. UMI films the text directly from the original or copy submitted. Thus, some thesis and dissertation copies are in typewriter face, while others may be from any type of computer printer.

The quality of this reproduction is dependent upon the quality of the copy submitted. Broken or indistinct print, colored or poor quality illustrations and photographs, print bleedthrough, substandard margins, and improper alignment can adversely affect reproduction.

In the unlikely event that the author did not send UMI a complete manuscript and there are missing pages, these will be noted. Also, if unauthorized copyright material had to be removed, a note will indicate the deletion.

Oversize materials (e.g., maps, drawings, charts) are reproduced by sectioning the original, beginning at the upper left-hand corner and continuing from left to right in equal sections with small overlaps. Each original is also photographed in one exposure and is included in reduced form at the back of the book.

Photographs included in the original manuscript have been reproduced xerographically in this copy. Higher quality 6" x 9" black and white photographic prints are available for any photographs or illustrations appearing in this copy for an additional charge. Contact UMI directly to order.

UMI®

Bell & Howell Information and Learning
300 North Zeeb Road, Ann Arbor, MI 48106-1346 USA
800-521-0600

INFLUENCE OF ROAD ROUGHNESS AND DIRECTIONAL MANEUVERS ON THE DYNAMIC PERFORMANCE OF HEAVY VEHICLES

RAJU ISAAC SAMUEL RAJ

A Thesis

In

The Department

of

Mechanical Engineering

Presented in Partial Fulfillment of the Requirements

for the Degree of Master of Applied Science at

Concordia University

Montreal, Quebec, Canada

June 1998

Abstract

Influence of Road Roughness and Directional Maneuvers on the Dynamic Performance of Heavy Vehicles

Raju Isaac Samuel Raj

The gross vehicle weight (GVW) and dimensions of articulated freight vehicles have been considerably relaxed during the past few decades, which have contributed to many concerns related to highway safety and preservation of the roadways. The directional dynamics of articulated heavy vehicles is investigated to study the influence of road roughness on the directional performance measures and the road damage potentials of the vehicle undergoing a directional maneuver. The directional performance characteristics and the road damage potentials are investigated for low speed cornering and high-speed directional maneuvers. A number of measured road profiles are analyzed to identify three groups of roads, namely: smooth, medium and rough roads based on their roughness index (RI) values. A detailed analysis of the road roughness data is carried out to derive correlation between the right and left wheel excitations. A range of performance measures are formulated to study the influence of road roughness on the directional dynamics and the influence of steering maneuver on the pavement damage. The equations of motion of the vehicle are solved for typical low-speed cornering, and high-speed lane-change and evasive maneuvers. The results of the study show that the

road roughness affects some of the directional performance measures of the vehicle in a significant manner, specifically the lateral load transfer ratio related to dynamic rollover potential of the vehicle. The study also revealed that the multiple excitations arising from the tire-road interactions and the directional maneuvers, significantly contribute to the dynamic wheel loads transmitted to the pavement. The contributions of excitations arising from directional maneuvers to the dynamic wheel load are presented in terms of different measures, which have been related to the road damaging potentials of heavy vehicles. These measures include dynamic load coefficient, the dynamic road stress factor and the peak tire force.

Acknowledgement

The author is sincerely grateful to his supervisors Dr. Subhash Rakheja and Dr. A. K. W. Ahmed for their enthusiastic guidance and continuous support, encouragement and guidance during the course of this work.

The financial support provided by my supervisors from their NSERC and FCAR grants are greatly acknowledged.

Thanks are due to the colleagues, faculty and staff of CONCAVE Research Center, Department of Mechanical Engineering, Concordia University, for their contribution to this effort.

Finally, the author would like to express his special thanks to the members of his family for their understanding and support. I dedicate this work to my beloved parents.

Contents

List of Figures

List of Tables

Nomenclature

$\vec{a}_c$	Fifth Wheel acceleration (m/s^2)
$\vec{a}_{mui}$	Acceleration of the i^{th} unsprung mass (m/s^2)
$\vec{a}_{msk}$	Acceleration of the k^{th} sprung mass (m/s^2)
$\vec{a}_{mui/Ri}$	i^{th} unsprung mass acceleration with respect to the roll center (m/s^2)
$\vec{a}_{Ri/msk}$	Acceleration of the i^{th} roll center with respect to the center of gravity of the k^{th} sprung mass (m/s^2)
AT_{ij}	Aligning torque generated at the tire-road interface of the j^{th} tire on the axle i (N-m)
a_y	Lateral acceleration (g's)
A_i	Dual tire spacing on axle i (m)
F_{ij}	Force due to the j^{th} suspension spring on axle i (N)
F_r	Approximate lateral force at the tractor drive axles (N)
F_{Ri}	Force acting through the roll center in a direction parallel to the $\vec{j}_u$ axis (N)
F_{si}	Suspension force transmitted to the sprung mass for axle i (N)
F_{yi}	Total lateral force at the tire-road interface of axle i (N)
F_{yij}	Lateral force at the tire-road interface of the j^{th} tire on axle i (N)
F_{zij}	Vertical force at the tire-road interface of the j^{th} tire on axle i (N)
g	Gravitational acceleration (9.81 m/s^2)
h	Height of the vehicle center of gravity above ground level (m)
HR_i	Vertical distance of roll center from the ground plane (m)

H_{ui}	Vertical distance of the center of gravity of the i^{th} unsprung mass from the ground plane (m)
I_{xxsk}	Roll mass moment of inertia of the sprung mass k ($kg.m^2$)
I_{yysk}	Pitch mass moment of inertia of the sprung mass k ($kg.m^2$)
I_{zzl}	Total yaw mass moment of inertia of the tractor ($kg.m^2$)
I_{zzsk}	Yaw mass moment of inertia of the sprung mass k ($kg.m^2$)
K_{ij}	Vertical stiffness of the j^{th} suspension spring on axle i (N/m)
KRS_i	Auxiliary roll stiffness of the suspension spring on axle i (N.m/rad)
KT_{ij}	Vertical stiffness of the j^{th} tire on axle i (N/m)
m_l	Total mass of the tractor (kg)
M	Inertia matrix
m_{sk}	Sprung mass k (kg)
m_{ui}	Unsprung mass of axle i (kg)
p_{sk}	Roll rate of the k^{th} sprung mass (rad/s)
p_{ui}	Roll rate of the i^{th} unsprung mass (rad/s)
q_{sk}	Pitch rate of the k^{th} sprung mass (rad/s)
r_{sk}	Yaw rate of the k^{th} sprung mass (rad/s)
r_{ui}	Yaw rate of the i^{th} unsprung mass (rad/s)
R_i	Rolling radius of the tires on the axle i (m)
s_i	Half of the lateral distance between suspension springs on axle i (m)
T_i	Half of the lateral distance between the inner tires on axle i (m)
U_{sk}	Longitudinal velocity of the k^{th} sprung mass (m/s)
$U_{tire_{ij}}$	Forward velocity of the j^{th} tire on the axle i (m/s)

V_{axle_i}	Lateral velocity of axle i (m/s)
V_{sk}	Lateral velocity of the k^{th} sprung mass (m/s)
W_{sk}	Vertical velocity of the k^{th} sprung mass (m/s)
W	Total weight of the sprung and unsprung masses (N)
W_{si}	Weight of the i^{th} sprung mass (N)
W_{ui}	Weight of the i^{th} unsprung mass (N)
$\ddot{\vec{x}}$	Acceleration vector (m/s^2)
x_{Ri}	Longitudinal distance between the roll center i and the center of gravity of the sprung mass (m)
x_{ui}	Longitudinal distance from the sprung mass center of gravity to axle i (m)
x_5	Longitudinal distance between the tractor center of gravity and the fifth wheel (m)
y_i	lateral displacement of axle i due to the lateral compliance of the tire (m)
Z_{Ri}	Vertical distance between the sprung mass center of gravity and the roll center of axle i (m)
Z_{ui}	Vertical distance between the roll center and the center of gravity of axle i (m)
Z_{uoi}	Vertical distance between the i^{th} roll center and i^{th} axle center of gravity at t = 0 (m)
Z_{5i}	Vertical distance from the fifth wheel coupling to the ground plane (m)
α_{ji}	Sideslip angle of the j^{th} tire on axle i (rad)
δ	Front wheel steer angle (rad)
Δ_{ij}	Vertical deflection of the j^{th} tire on axle i (m)

Δ_{oi}	Vertical deflection of the axle i at t = 0 (m)
Δz_{sk}	Vertical deflection of the k^{th} sprung mass center of gravity along the inertial axis $\bar{k}_n$ (m)
ϕ	Roll angle (rad)
ϕ_{sk}	Roll angle of the k^{th} sprung mass (rad)
ϕ_{ui}	Roll angle of the i^{th} unsprung mass (rad)
ψ_{sk}	Yaw angle of the k^{th} sprung mass (rad)
θ_{sk}	Pitch angle of the k^{th} sprung mass (rad)
γ	Articulation angle (rad)
$\dot{}$	First derivative with respect to time
$\ddot{}$	Second derivative with respect to time

Chapter 1

Introduction

1.1 General

For reasons of economy, the freight transport industry has indicated a continuing interest in increasing the sizes and load carrying capacities of freight vehicles. The gross vehicle weight (GVW) and dimensions of these vehicles have been considerably relaxed during the past few decades. The use of multiple axle semitrailers has been increasing steadily to carry heavier loads. The population of articulated vehicles with four-, five- or six axle semitrailers has grown considerably, specifically in Quebec and Ontario. Such variation in vehicle configurations, weights and dimensions has raised many concerns related to highway safety and preservation of damage to the roadway infrastructure. The directional control and stability limits of articulated vehicles are known to be significantly lower than those of other road vehicles, due to their excessive weights and dimensions, and high location of the sprung weight center of gravity. Many studies have established that the directional stability limits and dynamic wheel load characteristics of such vehicles are distinctly sensitive to certain size and weight variables [1]. The directional stability and control, dynamic wheel loads, and ride vibration characteristics of such vehicles have been extensively investigated and reported in the literature. The high GVW and load per

axle, coupled with vertical dynamics of the vehicle, impose high magnitudes of dynamic wheel loads to the pavements and bridge leading to their rapid fatigue and premature failure. These studies, in general, focus on a single performance measure, such as directional stability, dynamic wheel loads, or ride quality, while neglecting the couplings between different measures, and corresponding excitations. All the studies, irrespective of their focus, however, have established that increase in vehicle weights and dimensions affects the above performance measures in an adverse manner.

In view of the high costs associated with maintenance of the roadways, the dynamic wheel loads of heavy vehicles transmitted to the roadway structure have been extensively investigated in many analytical and experimental studies. These studies, invariably, focus on the vertical and pitch plane dynamics of the vehicle subject to excitations arising from the random road surfaces. The contributions due to dynamic lateral load transfer within an axle, caused by the directional response of the vehicle under a steering excitations, are considered negligible. The directional dynamic response characteristics of the vehicle, on the other hand, are analyzed under steering inputs, assuming perfectly smooth road roughness.

The increased concerns on the highway safety risks associated with lower directional dynamic stability limits of heavy vehicles have prompted the development of various performance measures address all aspects of directional dynamics, including: steady and dynamic rollover, lower and high-speed jackknife, tire-road friction demand, offtracking, etc. These performance measures, however, are evaluated from the

directional response of the vehicle moving on a perfectly smooth surface (zero roughness).

The primary focus of this dissertation research is to investigate the influence of multiple excitations arising from the tire-road interactions, and directional maneuvers on the directional performance measures and the dynamic wheel loads. A methodology to study the contribution of road roughness induced dynamics of the vehicle to the directional performance measures is proposed. The road damage potentials of an articulated vehicle during directional maneuvers are also investigated as a function of the road roughness, steering input and speed.

1.2 Review of Previous Investigations

The handling, directional control and dynamic stability characteristics of heavy trucks and articulated vehicles have been extensively investigated during past two decades. VLK [2] presented a comprehensive review of the reported studies on the lateral dynamics of articulated vehicles. The influence of size and weight variables on the dynamic stability and control characteristics of heavy trucks and trailer combinations have been investigated by Ervin et al. [1]. The analytical models, validated through limited field tests, clearly established that directional performance characteristics of these vehicles are quite sensitive to variations in vehicle parameters. A large number of studies on the vehicle-road interactions have further concluded that heavy vehicles transmit excessive dynamic tire loads to the pavements leading to their premature failure [3]. The

road damaging potentials of heavy vehicles have been related to a number of vehicle and road design factors. The large variations in commercial vehicle configurations, weights and dimensions, and their aggressivity towards the roads, and unreasonable safety risks posed by accidents involving such vehicles, have prompted numerous analytical and experimental studies. A review of previous investigations, relevant to the directional dynamics and tire loads performance characteristics, is presented in the following subsections to develop the scope of the dissertation.

1.2.1 Directional Dynamics of Heavy Vehicles

The directional dynamics of heavy vehicles are investigated to establish the handling, directional control and directional stability characteristics of vehicles under steady and transient steering maneuvers. Between the application of steering input and the attainment of steady state motion, the vehicle is considered to be in a transient state. The overall handling qualities of a vehicle depend, to a great extent, on its transient behavior. In analyzing the transient response, the inertia properties of the vehicle must be taken into consideration. During a turning maneuver, the vehicle is in translation as well as in rotation. Steady state handling performance is concerned with the directional behavior of a vehicle during a turn under non-time varying conditions. While the steady-state directional dynamics determines the vehicle handling and rollover immunity under steady turning maneuvers, the transient directional dynamic response is concerned with roll and yaw instabilities under transient maneuvers, such as lane change and obstacle avoidance. The steering induced dynamic roll stability limits of such vehicles are known to be

considerably low due to high c.g. location, and large weight and dimensions. The yaw instabilities of the vehicle related to jackknife and trailer swing are primarily caused by steering and braking inputs.

Huber and Dietz [4], and Dietz [5,6] performed the earliest documented research on directional dynamics of truck-trailer combinations. The experimental study involved testing of scale model of laterally constrained trailers, on an endless moving belt and was specially concerned with the lateral stability of straight running vehicle configurations with two axle tow bar trailers equipped with either turn table or Ackerman steering. The study concluded that the trailer yaw oscillations could be most effectively suppressed by introducing viscous damping within the turntable. While the coulomb damping within the turntable was observed to be somewhat undesirable. This experimental study was followed by a complementary theoretical effort by Ziegler [7,8], by considering the tire forces similar to the coulomb damping. The directional stability of truck-trailer vehicles, investigated by Laurien [9], also concluded that the trailer yaw oscillations could be most effectively suppressed by the introduction of coulomb damping at the hitch and at the trailer steering mechanism. The trailer with Ackerman steering was observed to be more prone to lateral oscillations than the trailer with turntable (dolly) steering.

The interdependence between truck and trailer motions, investigated by Schimid [10] and Jindra [11], concluded that the yaw oscillations of the trailers increase with an increase in the yaw moment of inertia of the trailer body. Gerlach [12] analyzed a similar mathematical model incorporating turntable offset, coulomb and / or viscous damping at

the hitch and the turntable. The study concluded that a truck-trailer combination with high cornering stiffness of the tire, either coulomb or viscous damping at the hitch, long drawbar and the turntable center located ahead of the dolly axle, lead to good dynamic stability.

Nordstrom et al. [13] developed vehicle dynamics simulation programs to study the lateral and roll dynamic stability of heavy vehicles, including tank tracks. Several full-scale tests were performed to validate the simulation program, and to develop test methods to assess the directional performance of heavy vehicles. A comprehensive digital computer program was further developed to simulate for directional dynamics of various combinations incorporating up to three articulations, a maximum of nine axles, driving or braking forces, lateral load transfer, etc. [14]. The eight degree-of-freedom analytical model was developed assuming fixed roll axles, linear suspension springs, negligible interaction between lateral and longitudinal tire forces, negligible pitch and longitudinal load transfer [15]. Based upon the simulation results for a lane change directional maneuver, it was concluded that a satisfactory lane change behavior can be achieved with long trailer wheel base, low normal load on the tires, short distance between the truck rear axle and the tow pin, and roll understeer on the trailer rear axle. A longer drawbar, however, resulted in large amplitude lateral oscillations.

Bakhmutskii and Gineburg [16] have investigated the directional response characteristics through road tests performed with various vehicle combinations and drivers. The handling characteristics of the vehicle and the driver-vehicle systems were

derived from the test data. The tests were performed under step steer and lane-change maneuvers and a linear four degrees-of-freedom mathematical model was used for the theoretical analysis. Mallikarjunarao and Fancher [17] developed a similar linear yaw-plane model to study the directional response of tractor-semitrailer combinations with multi-axled and multi-articulated tanker trucks, while neglected the roll dynamics. An eigen value analysis was performed to determine the natural modes of oscillation and the directional stability limits of the vehicle. The study concluded that the lateral acceleration of the pup trailer of the Michigan double tanker is significantly larger, when compared to that attained by the tractor, during the obstacle-avoidance maneuver performed at highway speeds. This rearward amplification of lateral acceleration was considerably reduced by increasing the rigidity of the pintle hook connection.

VLK[2] indicated that while many studies have described the development of various computer simulation models to analyze the lateral dynamics of articulated vehicles, there exist relatively few published studies on comparison of these models. Further more, the in-plane vehicle models discussed above assume linear tire cornering forces. The influence of size and weight variables on the stability and control of heavy trucks and tractor-trailer combinations was examined by Ervin et al. [1], using computer simulations. The computer simulation studies were validated through a limited number of field tests. These models clearly predicted the periodic yaw response of the trailer about its equilibrium, but did not yield information about a periodic trailer swing and jackknife due to lack of a bounded and nonlinear tire model.

The research efforts, in the recent years, have been directed towards development of increasingly sophisticated computer simulation models to handle complex tire models. Since the directional dynamics of a vehicle combinations is strongly related to the forces and moments generated at the tire-road interface, nonlinear tire models have been used in the lateral stability analysis of heavy vehicles subject to braking and steering maneuvers [18]. A comprehensive three-dimensional simulation program, referred to as YAW/ROLL model, was developed by the Road and Transport Association of Canada (RTAC) and University of Michigan Transportation Research Institute (UMTRI) [19]. The simulation program incorporated nonlinear cornering characteristics of tires, nonlinear suspension forces, and closed-loop driver model, while the forward speed was assumed to be constant. The model has been extensively used to evaluate roll, yaw and lateral directional responses of heavy vehicle combinations, comprising up to 4 units and 11 axles, and different articulation mechanisms.

The above model was further enhanced to study the vehicle response to simultaneous steering and braking inputs [19]. The model, referred to as PHASE IV, incorporated nonlinear braking and turning properties of tires using look-up tables, nonlinear suspension forces, and comprehensive brake system dynamics. A nonlinear vehicle model to evaluate the performance in view of various current design features, such as fifth wheel reactions and antilock brake system, has also been developed by Susemihl and Kranter [20].

Directional dynamics models of heavy vehicles, reported in the literature, range from simple two-degrees-of-freedom (DOF) models to several DOF models. Simple models have been used to assess the performance of vehicle systems or subsystems in the linear range, under constrained directional motion. More comprehensive models are employed to derive the vehicle response with appropriate consideration of highly complex and nonlinear force generating subsystems, such as tires, suspension, articulation mechanisms, and brake systems. All the reported models and computer simulation codes, however, are formulated to derive the response characteristics of each unit of the vehicle combination under pure steering input, defined either in terms of open-loop front wheel steer angle or in terms of closed-loop path-following parameters. The contribution of tire interactions with randomly rough roads to the directional dynamics of the vehicle, is completely ignored. The dynamic tire forces generated at the tire-road interface, along all the three axis, are strongly influenced by dynamic vertical loads and tire-road adhesion. Both the tire-road adhesion, and dynamic vertical tire loads are in turn strongly influenced by the road roughness and the speed.

1.2.2 Performance Measures Related to Directional Dynamics

Although the directional dynamics of heavy vehicle combinations have been extensively reported in the literature, the results of these studies did not address the most important safety related concerns of the regulators and operators. Majority of the studies reported analytical models, analytical methods, and influence of various design and operating

parameters on the directional response behavior of specific vehicle configurations. Moreover, majority of the studies was conducted under varying steering and operating speeds. The studies did not permit relative performance evaluations of different vehicle configurations, due to lack of standardized and controlled inputs and performance measures. In light of extensive variations in commercial vehicle configurations, tires and suspension designs, and operating limits, a need to develop well defined performance measures was identified to establish their relative dynamic stability and safety performance under representative steering inputs [21].

A series of performance measures related to roll, yaw and lateral dynamics of heavy vehicle combinations, have evolved in the recent years [14]. The first set of performance measures, used in a significant way, was developed for the Canadian Vehicle Weights and Dimension Study, conducted by RTAC [19]. The performance measures, primarily derived from the YAW/ROLL and PHASE IV simulation programs, were used to assess the impact of relaxed weights and dimensions regulations in Canada. These measures attempted to address the concerns related to directional stability, control, offtracking and braking performance of vehicles. Although not formally adopted by RTAC, this set of measures continues to be referred to as 'RTAC measures'. They were used to provide the scientific and technical basic for regulatory changes introduced in most Canadian Provinces following the Weights and Dimensions Study. These regulations were designed to encourage the use of preferred vehicles – those judged superior to other configurations from a safety performance point of view. E.I.Gindy [21] reviewed the existing performance measures for commercial heavy vehicles, and summarizes the

methods for their evaluation. The study further proposed the pass/fail criteria based upon target values for each measure.

EI-Gindy and Woodrooffe [14] established the significant effects of certain tractor design parameters and proposed a set of modified performance measures. In light of these modifications, the studies recommended a comprehensive review of all existing performance measures, and formulated eight stability and control measures as follows:

a. Handling performance measure, to assess the relative handling quality of the vehicle.
b. Static rollover threshold (SRT), to assess the rollover limits of heavy vehicles under steady turns.
c. Dynamic rollover stability in terms of Load Transfer Ratio (LTR) and Rearward Amplification (RWA), to assess the dynamic roll stability limits under transient maneuvers.
d. Yaw Damping Ratio (YDR), to assess the rate of decay of yaw oscillations of the trailer.
e. Friction Demand of the drive-axle tires, to assess the low and high-speed jackknife potentials of vehicle combinations.
f. Lateral friction utilization, to assess the low and high-speed lateral slippage potentials.
g. Low and high-speed steady-state, and transient offtracking, to assess the maneuverability at tight intersections, and safety risks on the highways.

h. Braking performance, to assess the braking efficiency, stopping distance, response time and jackknife potentials of vehicle combinations.

Some of the above performance measures, considered relevant to the scope of the dissertation, are further discussed below.

Handling performance measure:

This performance measure describes the handling characteristics of the vehicle in terms of understeer coefficient (K_{us}) and critical value of the understeer coefficient K_{uscr} [22]. A 'three-point measure' was proposed to characterize the handling diagram of a vehicle over a wide range of operating parameters. The understeer coefficient is derived from the handling diagram, a plot of lateral acceleration (a_y) Vs the steering parameter ($L/R-\delta$), where L is the wheelbase, R is turn radius and δ is the front wheel steer angle. It is proposed that the K_{us} of the vehicle under the specified directional input must be larger than its K_{uscr}, which is gL/U^2, where U is the forward speed of the vehicle.

Dynamic rollover stability measures:

The rollover immunity of heavy vehicles is known to be considerably lower than other road vehicles, which is primarily attributed to high c.g. location, high axle loads and large sizes of the vehicles. The roll stability of vehicles under a steady turn is evaluated in terms of its static rollover threshold (SRT), the maximum level of constant lateral acceleration a vehicle can withstand without rolling over. A limiting SRT value of 0.35g has been proposed in many studies [23]. Heavy vehicles also exhibit roll instability during a transient steering maneuver, and the dynamic roll stability limits are known to

considerably different from the SRT of the respective vehicle. A number of dynamic rollover measures have been defined in the literature, including dynamic rollover threshold (DRT), roll safety factor (RSF), load transfer ratio (LTR), and rearward amplification (RWA) [24].

The LTR is defined as the ratio of the absolute value of the difference between the sum of the right wheel loads and the sum of the left wheel loads, to the sum of all the wheel loads. The DRT and RSF measures are also derived from the LTR. The rearward amplification ratio (RWA) is a frequency dependent measure, defined as the ratio of the peak (positive or negative) lateral acceleration at the c.g. of the rearmost trailer to the amplitude of controlled lateral acceleration of 0.15g at the center of front axle of the lead unit (tractor). The proposed measures require evaluation of LTR and RWA under a lane-change maneuver performed at a speed of 100 km/h. The vehicle is considered to be acceptable, if LTR < 0.6 and RWA < 2.2 [21].

Apart from the above measures, the directional response behavior of heavy vehicles is often assessed by its Roll, Yaw and Pitch rates which are related to LTR, jackknife, trailer swing and dynamic load transfer during transient maneuver [22]. It should be noted that the proposed performance measures are evaluated from the simulation programs. The measures thus do not incorporate the influence of vehicle dynamics attributed to interactions between tire and road.

1.2.3 Dynamic Wheel Loads Transmitted to the Pavements

The vertical loads of heavy vehicles transmitted to the pavements comprise two components: the static axle loads and the dynamic tire loads arising from vibration modes of the vehicle and dynamic tire-road interaction. The static component of the tire load depends on the weight distribution and geometry of the vehicle, and the static load sharing characteristics of the suspension system. Uneven load sharing can result in unnecessarily high average tire forces with consequently high stresses and strains in the road surface and additional road damage. Multiple axle groups of heavy trucks generate dynamic tire loads that are greatly in excess of their static loads. Dynamic tire forces are caused by vibration of the vehicle, when it is excited by roughness of the road surface. They normally occur at frequencies below 20 Hz and predominate around the vertical mode resonant frequencies of the sprung and unsprung masses. Dynamic tire forces generate additional dynamic stresses and strains in the pavements, which are believed to accelerate road surface deterioration, although the damage mechanisms are not well understood.

There is considerable literature concerned with experimental and theoretical studies of road damage caused by heavy vehicles, however it is mostly based on the notion that vehicles apply constant (static) tire forces to the road surface [25]. These studies have achieved mixed success due to extremely complex nature of the road damage problem. Comparatively few researchers have investigated the influence of

vehicle suspension design features on static and dynamic tire forces and the consequent effects on the pavement damage [26]. A large number of analytical and experimental studies have been carried out in recent years, in an attempt to establish the road damaging potentials of heavy vehicles. Most of these studies are directed to study the influence of various design and operating variables on the relative dynamic tire loads. The study represented by Kulakowski [27], perhaps is the most comprehensive one, which describes the influence of several vehicle parameters on the dynamic tire loads, such as DLC, peak tire force are, invariably, evaluated under straight driving conditions. The influence of dynamic load transfer encountered during directional maneuvers is entirely ignored, while only pitch-plane models are considered to account for only vertical and pitch modes of vibration of the vehicle [28,29]. The lateral dynamic loads encountered during directional maneuvers are known to be quiet significant, and may contribute to rapid determination of the roads, specially on the turning ramps.

1.2.4 Performance Measures Related to Dynamic Wheel Loading

Although dynamic tire forces of heavy vehicles are known to accelerate the pavement fatigue, the methods to quantify the road damaging potentials have not yet been established. Alternatively, a number of performances measures have been proposed to assess the relative agressivity of the heavy vehicles, and to assess the influence of various design and operating factors [27]. Some of these performance measures are described below.

Dynamic Load coefficient (DLC)

The relative road damaging potentials of heavy vehicles, and the design and operating parameters are frequently expressed in term of dynamic load coefficient (DLC). The DLC describes the magnitude of variations in the tire forces, and is defined as:

$$DLC = \frac{\text{Root Mean Square of dynamic tire force}}{\text{Static tire force}}$$

Many studies have concluded that the DLC strongly depends on the road surface roughness, vehicle speed, vehicle configuration, geometry and mass distribution, axle loads, properties of the suspension and tires, and the vehicle vibration modes. It is recommended by David Cebon [3] that under normal operating conditions, the DLC of 0.1 - 0.3 are typical. Experimental study by Sweatmen [30] and Woodrooffe et al [31] reported DLC value up to 0.4 for particularly poor tandem suspensions. The recommended and measured values are only applicable to straight line driving.

Road Stress Factor (RSF)

Eisenmann [32] proposed a measure known as 'road stress factor', Φ, assuming that the road damage is related to fourth power of the instantaneous (dynamic) wheel force at a point on the road. The formulation was based upon the comprehensive study undertaken by AASHO road test [33]. Assuming that the dynamic wheel forces are Gaussian (normal distribution), Eisenmann showed that the expected value of the fourth power of the instantaneous wheel force is given by:

$$\Phi = E\,(1+6S^2+3S^4)\,P^4_{stat}$$

Where P_{stat} is the static tire force, and S is the Coefficient of variation of dynamic tire force (essentially the DLC). In 1978, Eisenmann [34] proposed a modified version of the above equation which accounted for the effects of wheel configuration and tire pressures where the dynamic road stress factor, v is given by:

$$v = 1+6S^2+3S^4$$

For typical highway conditions of roughness and speed, Sweatman [30] measured the dynamic road stress factor v in the range 1.11 to 1.46 depending on the suspension system. It is expected that suspension should rank in the same order whether the wheel loads are compared in terms of road stress factor or DLC.

1.3 Scope of the Thesis

From the literature review, it is evident that while extensive efforts have been mounted on the directional stability of articulated vehicles, the influence of road roughness on the directional stability remains the subject of concern. Moreover, large number of recent studies conducted on the dynamic pavement loading do not account for the contribution due to steering induced dynamic tire forces. The primary objectives of this dissertation research are thus formulated to investigate the influence of road roughness on the

directional stability of the articulated heavy vehicle and the influence of directional maneuver on the dynamic pavement loading. The specific objectives of the study are:

(i) To develop the analytical model of an articulated freight vehicle comprising non linear tire-road interactions to study the directional dynamic performance of the vehicle under excitations arising from both the steering input and tire interactions with randomly rough roads.

(ii) Analyze the road roughness data to determine the correlation between the right and left wheel excitations, and the spectra of road-induced roll excitations.

(iii) Investigate the influence of road roughness on the various directional performance measures of the vehicle.

(iv) Investigate the influence of transient directional maneuver on the dynamic tire loads transmitted to the pavement, and propose suspension damping characteristics to reduce the road damaging potentials.

In Chapter 2, the vehicle model is presented and the equations of motion for the model are derived. Various assumptions made in the formulations are also presented. A comprehensive database on vehicle geometry, and commercially employed suspension and tires are compiled. The variables of road inputs are incorporated in the equations to study the influence of road inputs on the vehicle stability. The performance measures related to the influence of road roughness and directional maneuvers on the dynamic performance of heavy vehicles are discussed in detail.

In Chapter 3, the characterization of road roughness is done on the basis of RI values to investigate the vehicle performance under different road conditions and the statistical analysis of road roughness are also discussed. The different types of maneuvers that are to be considered to evaluate the performance measures are also discussed. The methodology of the study is charted out.

In Chapter 4 & 5, the simulation is carried out as per the simulation matrix and the related performance measures are studied and discussed about the influence of road roughness, the vehicle speed and the maneuver that encountered. The road damaging potential, which is caused by, dynamic tire forces are quantified and discussed.

The conclusions drawn from the study are summarized in Chapter 6, and recommendations on future studies are also proposed.

Chapter 2

Development of Vehicle Model and Performance Measures

2.1 General

Numerous in-plane and three-dimensional models of varying complexities have been developed and analyzed to determine the yaw, lateral and roll directional dynamics of heavy vehicles. The analytical models vary from a simple linear yaw-plane model to a sophisticated 71 degrees-of-freedom nonlinear model. As discussed in the literature review, a number of vehicle dynamics simulation programs have been developed to evaluate the directional response characteristics of heavy trucks and truck-trailer combinations subject to steering and braking inputs. In selecting a model for a given analysis it is essential to identify the complexity necessary for effective simulation of a vehicle system. The present investigation involves dynamic performance analyses and prediction of pavement load due to road roughness and directional maneuvers. It is therefore essential to incorporate nonlinear cornering characteristics of the tires and nonlinear properties of suspension of the vehicle. Furthermore, it is necessary to adapt a

three dimensional model with yaw, roll and lateral degrees-of-freedom to derive performance measures under road and steering inputs.

A comprehensive three-dimensional yaw/roll plane vehicle simulation program developed by UMTRI [19] is quite adequate for the proposed investigation. The simulation program incorporates nonlinear tire and suspension characteristics which can be used for the simulation of yaw, roll and lateral directional response of vehicle combinations comprising up to four units and 11 axles, with a choice of articulation mechanism. A major limitation of the program is that it assumes the road to be perfectly smooth.

The yaw/roll model of a articulated vehicle combination is thus considered to study the role of road roughness on the directional performance, and the role of steering inputs on the dynamic wheel loads. The vehicle model is thoroughly reviewed and discussed in this chapter. The equations of motion for the vehicle model are revised to incorporate the tire forces developed due to their interactions with rough roads. The selected vehicle configuration is further discussed together with a number of performance measures to assess the directional response and pavement load characteristics of the vehicle, while the road roughness data is analyzed in chapter 3.

2.2 Yaw-Roll Model

The yaw-roll model is one of the simulation programs developed by UMTRI [19] to study the directional response characteristics of multi-articulated vehicles to dynamic

directional maneuvers. The model was originally conceived to simulate a road train of up to four units, with up to eleven axles distributed in any arbitrary configuration, except for a single tractor front axle. In order to investigate the directional dynamics of a tractor-semitrailer combination, the yaw-roll analysis, limited to a maximum of two units and six axles, is used in this investigation.

The highlights of the yaw-roll vehicle model include nonlinear cornering characteristics of the tires and nonlinear suspension characteristics. The nonlinear cornering forces and aligning moments of the tires are computed as a function of normal load and side slip angles, using look-up tables. The nonlinear suspension characteristics such as backlash are presented in the form of load-deflection tables. The leaf springs tend to twist in the roll plane and hence produce an additional roll resisting moment when a relative roll motion takes place between the sprung mass and the axles. This property of the leaf-spring suspension is represented by an auxiliary roll stiffness parameter. The vehicle model may be analyzed in either the closed-loop or open-loop steering modes. In the open-loop mode, the time history of the steering input is provided as input to the model, while the closed -loop mode, requires the description of desired trajectory to derive the steering input at the front wheels using a driver model incorporating preset preview time and time delays. The present investigation consider both open- and closed-loop steering inputs, and road inputs for evaluation of directional performance and dynamic pavement loading characteristics of the vehicle. Detailed equations of motion for a tractor with three axles coupled with a trailer with two axles are derived in order to incorporate the road inputs arising from randomly rough roads. Various assumptions

associated with the model development together with the final form of the equations of motion are presented in the following subsections.

2.2.1 Assumptions

Various assumptions made are consistent with those described in the UMTRI yaw/roll model [19]. In view of constant forward speed, it is assumed that the pitch angles of the sprung masses and the relative roll angles between the sprung and unsprung masses are further assumed to be small, such that the small angle assumption, $\mathrm{Sin}(\cdot) \approx 0$ and $\mathrm{Cos}(\cdot) \approx 1$, holds well. Further, the principal axis of inertia of the sprung and unsprung masses are assumed to coincide with their respective body fixed coordinate systems. The model further assumes that each unit (tractor and trailer) consists of a rigid body sprung mass and a number of beam axles, represented by unsprung masses, connected to the sprung mass through a complaint suspension system. The vehicle is assumed to move at a constant forward speed on a horizontal surface with uniform frictional characteristics. The relative motion between the sprung and unsprung masses are assumed to occur about the roll center of each axle. The roll center is assumed to be located directly underneath the sprung mass and free to move in the vertical axis of the unsprung mass. Each suspension is independent of other suspension, such that inter-axle load transfer or load-sharing is neglected. The fifth wheel coupling allows each unit to roll, pitch, and yaw with respect to one another. The relative roll motion between the two units, however, is limited by the nonlinear moment-deflection characteristics of the fifth wheel. Unlike the UMTRI yaw/roll model, here the road is considered to have random irregularities of

varying magnitudes. The vertical tire forces developed due to their interactions with randomly rough roads are formulated as a function of the road elevation, tire stiffness, and the geometry, which describes the phase relationship between the various tire forces. The tire forces, thus developed, are incorporated within the roll and vertical equations of motion for the model.

2.2.2 Equations of Motion

Figure 2.2 illustrates the schematic of a tractor-semitrailer combination considered in this study, along with its axis systems. In the model, each sprung mass is treated as a rigid body with five degrees-of-freedom, namely: lateral, vertical, yaw, roll and pitch. Since the tractor forward velocity is assumed constant, the longitudinal degree-of-freedom is neglected. Each axle is permitted to roll and bounce with respect to the sprung mass, each unsprung mass is thus modeled as a two-degrees-of-freedom system. The development of the yaw-roll model is organized under the following systematic stages:

-- Axis Systems,

-- Suspension Forces,

-- Equation of Motion for the Sprung Masses,

-- Equation of Motion for the Unsprung Masses,

-- Constraint Force and Moment Equations, and

-- Tire Forces

Axis system

Three axis systems namely: (i) an inertial axis system fixed in space, (ii) axis system fixed to each of the sprung masses, and (iii) axis system fixed to each of the axles, are needed in developing the equations of motion.

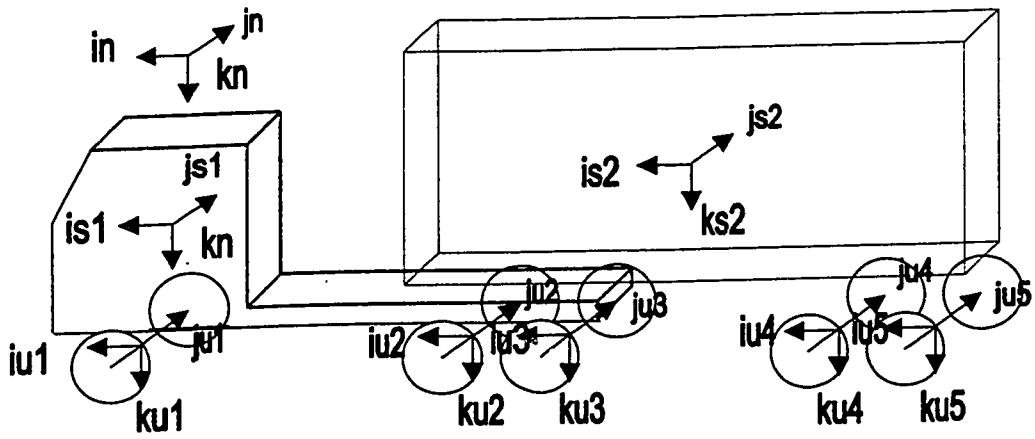

Figure 2.1: Tractor-semitrailer configuration and its axis systems

Three Euler angles, yaw (ψ_s), pitch (θ_s) and roll (ϕ_s) are used to describe the orientation of each of the sprung mass axis system with respect to inertial axis system. Sprung mass pitch angles are assumed to be small during directional maneuvers at constant forward speed, such that $\sin\theta_s = \theta_s$ and $\cos\theta_s = 1$. The transformation matrix relating the body fixed sprung mass axis system to the inertial axis system can be obtained as [35]:

$$\begin{Bmatrix} \vec{i}_s \\ \vec{j}_s \\ \vec{k}_s \end{Bmatrix}_k = \begin{bmatrix} \cos\psi_s & \sin\psi_s & -\theta_s \\ -\sin\psi_s\cos\phi_s + \theta_s\cos\psi_s\sin\phi_s & \cos\psi_s\cos\phi_s + \theta_s\sin\psi_s\sin\phi_s & \sin\phi_s \\ \sin\psi_s\sin\phi_s + \theta_s\cos\psi_s\cos\phi_s & -\cos\psi_s\sin\phi_s + \theta_s\sin\psi_s\cos\phi_s & \cos\phi_s \end{bmatrix}_k \begin{Bmatrix} \vec{i}_n \\ \vec{j}_n \\ \vec{k}_n \end{Bmatrix}_k ; \quad k = 1, 2 \tag{2.1}$$

The subscripts k = 1 and k = 2 in the above equation refers to the sprung mass of the tractor and trailer, respectively. Each axle is allowed to roll and bounce only with respect to the sprung mass to which it is attached. The orientation of the axle with respect to the inertial axis system is therefore defined by the yaw angle, ψ_s, and the roll angle, ϕ_u. The transformation matrix relating the axis systems located on the sprung and unsprung masses respectively can be derived as [35]:

$$\begin{Bmatrix} \vec{i}_u \\ \vec{j}_u \\ \vec{k}_u \end{Bmatrix}_i = \begin{bmatrix} 1 & \theta_{sk}\sin\phi_{sk} & \theta_{sk}\cos\phi_{sk} \\ -\theta_{sk}\sin\phi_u & \cos(\phi_{sk} - \phi_u) & -\sin(\phi_{sk} - \phi_u) \\ -\theta_{sk}\cos\phi_u & \sin(\phi_{sk} - \phi_u) & \cos(\phi_{sk} - \phi_u) \end{bmatrix}_i \begin{Bmatrix} \vec{i}_s \\ \vec{j}_s \\ \vec{k}_s \end{Bmatrix}_k \tag{2.2}$$

where i represents the axle number, i = 1, 2, 3 for k = 1 and i = 4, 5 for k = 2.

The equations of motion of each sprung mass are written in terms of the body-fixed translational $(u_s, v_s, w_s)_k$ and angular velocities $(p_s, q_s, r_s)_k$, and their derivatives. The Euler angular velocities $(\dot{\phi}_s, \dot{\theta}_s, \dot{\psi}_s)_k$, defined along the $\{\bar{i}_{sk}, \bar{j}'', \bar{k}_n\}$ directions, are equated to the body-fixed velocities and expressed [35]:

$$\begin{aligned}
\dot{\phi}_{sk} &= p_{sk} + (q_{sk} \sin \phi_{sk} + r_{sk} \cos \phi_{sk}) \theta_{sk} \\
\dot{\theta}_{sk} &= q_{sk} \cos \phi_{sk} - r_{sk} \sin \phi_{sk} \\
\dot{\psi}_{sk} &= q_{sk} \sin \phi_{sk} + r_{sk} \cos \phi_{sk}
\end{aligned} \tag{2.3}$$

Equations (2.3) are numerically integrated to obtain the Euler angles.

Suspension Forces

Figure 2.2 illustrates the roll plane of three dimensional vehicle model. Each axle suspension is assumed to consist of a pair of nonlinear springs and each sprung mass rolls about a roll center. The suspension springs are assumed to remain parallel to the $\bar{k}_{ui}$ axis of the unsprung mass, and are capable of transmitting either compressive or tensile forces only. All the roll plane forces perpendicular to the suspension springs are assumed to act through the roll center located at a fixed distance, Z_{Ri}, beneath the sprung mass as shown in Figure 2.2. The roll center is allowed to slide along the $\bar{k}_{ui}$ axis of the unsprung mass. The force due to suspension of axle i transmitted to the sprung mass is thus expressed as:

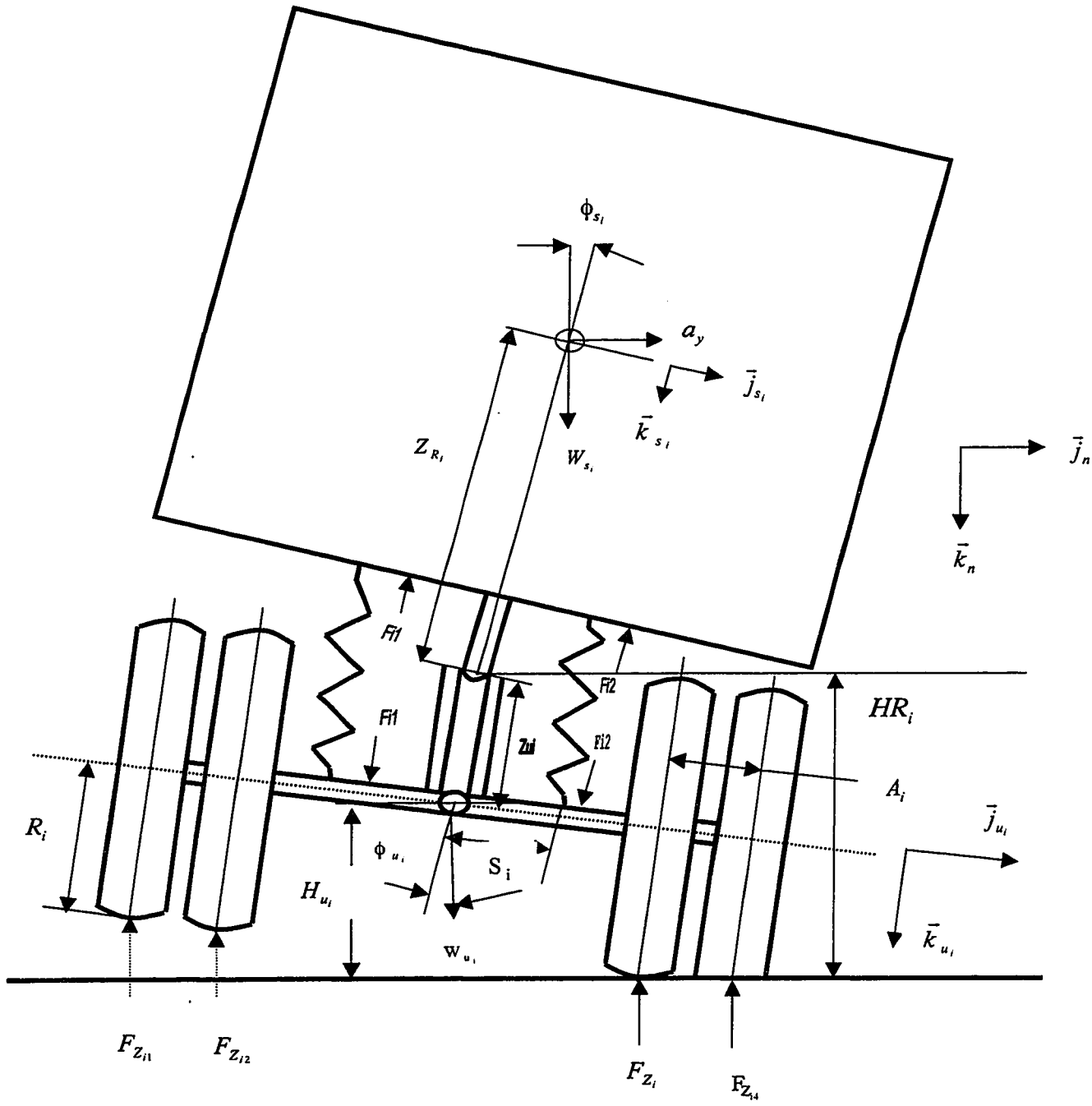

Figure 2.2: Forces and Moments Acting in the Roll Plane of the Vehicle (Rear View)

$$F_{si} = F_{Ri}\,\vec{j}_{ui} - (F_{i1} + F_{i2})\,\vec{k}_{ui}$$

where F_{i1} and F_{i2} are forces due to left and right springs and dampers of axle suspension i, and F_{Ri} is the lateral force through the roll center. It should be noted that the yaw/roll program developed by UMTRI considers only viscous suspension damping. The suspension dampers in general develop nonlinear and asymmetric damping forces in compression and rebound. The suspension forces in this study are formulated as combinations of components of nonlinear spring and damping forces. While the nonlinear spring forces (F_{si}) are derived as a function of the spring deflection using the measured force-deflection characteristics expressed by a look-up table, the damping force (F_{Di}) component is derived from the relative velocity across the spring (v_{sp}):

$$F_{Di} = \begin{cases} C_1 v_{sp}; 0 < v_{sp} < v_c \\ C_1 v_c + C_2 (v_{sp} - v_c); v_{sp} > v_c \\ C_3 v_{sp}; v_e < v_{sp} < 0 \\ C_3 v_e + C_4 (v_{sp} - v_e); v_{sp} < v_e \end{cases}$$

where C_1 and C_3 are the damping coefficients in compression and rebound, respectively, corresponding low velocities. C_2 and C_4 are the coefficients in compression and rebound at higher velocities. v_c and v_e are transition velocities in compression and rebound, respectively. The typical force-velocity characteristics of dampers, shown in Figure 2.3 and Figure 2.4, show that dampers in general develop considerably higher forces in rebound. The dampers provide high damping coefficient at low velocity due to bleed flow, and considerably lower damping coefficient at higher velocity due to flows through blow-off valves. The suspension forces are defined in the sprung mass coordinate system

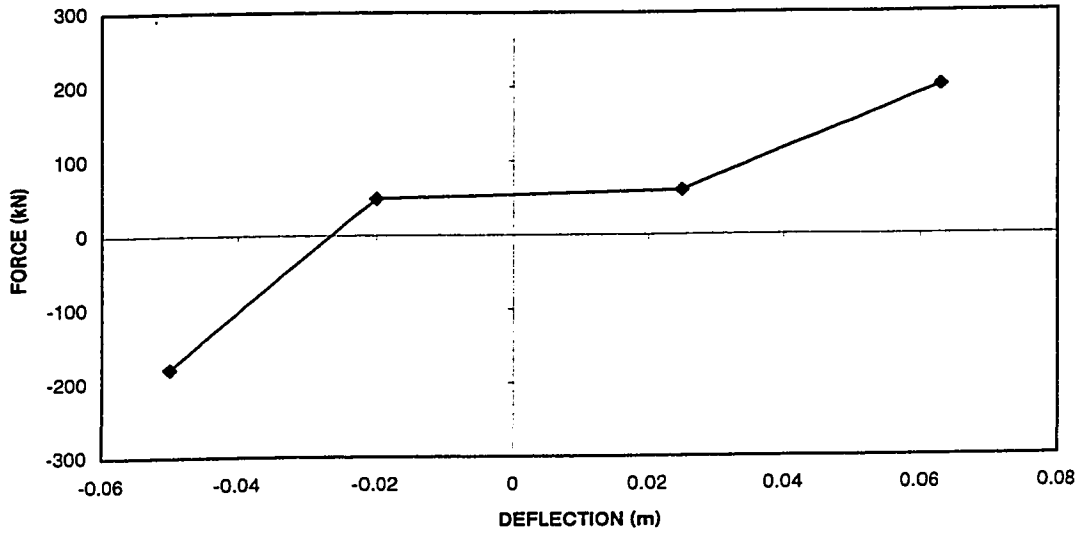

Figure 2.3: Force-Displacement Charecteristics of the Neway AR95.17 24K Suspension Spring.

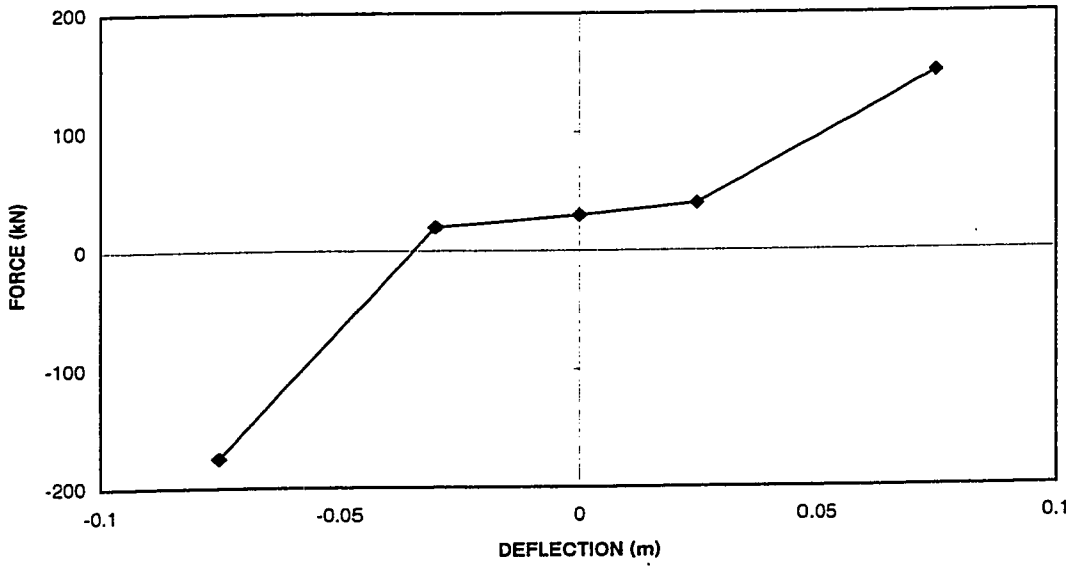

Figure 2.4: Force-Displacement Charecteristics of the Neway ARD224 16K Suspension Spring.

by applying the coordinate transformation expressed in equation (2.2). Upon applying the transformation, the suspension force can be expressed as:

$$\begin{aligned} F_{si} = & [-F_{Ri}\theta_{sk}\sin\phi_{ui} + (F_{i1}+F_{i2})\theta_{sk}\cos\phi_{ui}]\,\vec{i}_{sk} \\ & + [F_{Ri}\cos(\phi_{sk}-\phi_{ui}) - (F_{i1}+F_{i2})\sin(\phi_{sk}-\phi_{ui})]\,\vec{j}_{sk} \\ & - [F_{Ri}\sin(\phi_{sk}-\phi_{ui}) + (F_{i1}+F_{i2})\cos(\phi_{sk}-\phi_{ui})]\,\vec{k}_{sk} \end{aligned} \tag{2.4}$$

The force , F_{Ri} , acting through the roll center is an internal force which is eliminated by inspecting the dynamic equilibrium of the axle in the $\vec{j}_{ui}$ direction. The equation for the lateral equilibrium of the axle can be written as:

$$\begin{aligned} m_{ui}[\vec{a}_{mui}\cdot\vec{j}_{ui}] = & -F_{Ri} + (F_{yi1}+F_{yi2}+F_{yi3}+F_{yi4})\cos\phi_{ui} \\ & - (F_{Zi1}+F_{Zi2}+F_{Zi3}+F_{Zi4})\sin\phi_{ui} + m_{ui}\,g\sin\phi_{ui} \end{aligned} \tag{2.5}$$

Equation (2.5) is rearranged to express F_{Ri} as:

$$\begin{aligned} F_{Ri} = & -m_{ui}[\vec{a}_{mui}\cdot\vec{j}_{ui}] + (F_{yi1}+F_{yi2}+F_{yi3}+F_{yi4})\cos\phi_{ui} \\ & - (F_{Zi1}+F_{Zi2}+F_{Zi3}+F_{Zi4})\sin\phi_{ui} + m_{ui}\,g\sin\phi_{ui} \end{aligned} \tag{2.6}$$

where F_{yij} and F_{Zij} are the lateral and vertical forces, respectively due to the tire j on the axle i. Among the terms on the right hand side of equation (2.6), the only unknown is the acceleration $\vec{a}_{mui}$ of the unsprung mass. Since the position of the axle is defined relative to the sprung mass to which it is attached, the acceleration of the unsprung mass is derived from:

$$\vec{a}_{mui} = \vec{a}_{msk} + \vec{a}_{Ri/msk} + \vec{a}_{mui/Ri} \tag{2.7}$$

where $\vec{a}_{msk}$, $\vec{a}_{mui/Ri}$ and $\vec{a}_{Ri/msk}$ are the accelerations of the sprung mass k, the unsprung mass i with respect to the sprung mass k and the sprung mass k with respect to the roll center and the roll center with respect to the sprung mass k, respectively. The sprung mass acceleration along the body fixed coordinates

$(\vec{i}_s, \vec{j}_s, \vec{k}_s)_k$ in turn is given by:

$$\begin{aligned}\vec{a}_{msk} = {} & (\dot{u}_s + q_s w_s - r_s v_s)_k \vec{i}_{sk} + (\dot{v}_s + u_s r_s - p_s w_s)_k \vec{j}_{sk} \\ & + (\dot{w}_s + p_s v_s - q_s u_s)_k \vec{k}_{sk}\end{aligned} \tag{2.8}$$

Since the roll center is assumed to be located at a fixed distance from the sprung mass center of gravity (c.g.), the position of the roll center with respect to the sprung mass center of gravity can be expressed in the following manner:

$$\vec{r}_{Ri/msk} = X_{Ri} \vec{i}_{sk} + Z_{Ri} \vec{k}_{sk} \tag{2.9}$$

where, X_{Ri} and Z_{Ri} are the longitudinal and vertical distances from the sprung mass c.g. to the roll center of the axle i. The corresponding velocity and acceleration of the roll center are derived as follows:

$$\vec{w}_{Ri/msk} = (Z_{Ri} q_s)_k \vec{i}_{sk} + (-p_s Z_{Ri} + X_{Ri} r_s)_k \vec{j}_{sk} - X_{Ri} q_{sk} \vec{k}_{sk} \tag{2.10}$$

$$\begin{aligned}\vec{a}_{Ri/msk} = {} & (\dot{q}_s Z_{Ri} - X_{Ri} q_s^2 + p_s r_s Z_{Ri} - X_{Ri} r_s^2)_k \vec{i}_{sk} \\ & + (-\dot{p}_s Z_{Ri} + X_{Ri} \dot{r}_s + Z_{Ri} q_s r_s + X_{Ri} q_s p_s)_k \vec{j}_{sk}\end{aligned}$$

$$+(-p_s^2 Z_{Ri} + X_{Ri} r_s p_s - Z_{Ri} q_s^2 - X_{Ri}\dot{q}_s)_k \vec{k}_{sk} \tag{2.11}$$

Similarly, the unsprung mass acceleration with respect to the roll center is described as:

$$\vec{a}_{mui/Ri} = p_{ui} r_{ui} z_{ui} \vec{i}_{ui} - (\dot{p}_{ui} z_{ui} + 2 p_{ui} \dot{z}_{ui}) \vec{j}_{ui} - (p_{ui}^2 z_{ui} - \ddot{z}_{ui}) \vec{k}_{ui} \tag{2.12}$$

Combining (2.8), (2.11) and (2.12) and transforming the acceleration defined in the sprung mass coordinate system to the unsprung mass coordinate system, yields:

$$\begin{aligned}
\vec{a}_{mui} \vec{j}_{ui} = &-(\dot{u}_s + q_s w_s - r_s v_s + \dot{q}_s Z_{Ri} - X_{Ri} q_s^2 + p_s r_s Z_{Ri} - X_{Ri} r_s^2)_k \theta_{sk} \sin\phi_{ui} \\
&+(\dot{v}_s + u_s r_s - p_s w_s - \dot{p}_s Z_{Ri} + X_{Ri} \dot{r}_s + Z_{Ri} q_s r_s + X_{Ri} q_s p_s)_k \cos(\phi_{sk} - \phi_{ui}) \\
&-(\dot{w}_s + p_s v_s - q_s u_s - p_s^2 Z_{Ri} + X_{Ri} r_s p_s - Z_{Ri} q_s^2 - X_{Ri}\dot{q}_s)_k \sin(\phi_{sk} - \phi_{ui}) \\
&- \dot{p}_{ui} z_{ui} - 2 p_{ui} \dot{z}_{ui}
\end{aligned} \tag{2.13}$$

From (2.6) and (2.13), the roll center force is obtained as:

$$\begin{aligned}
F_{Ri} = &-m_{ui}[-(\dot{u}_s + q_s w_s - r_s v_s + \dot{q}_s Z_{Ri} - X_{Ri} q_s^2 + p_s r_s Z_{Ri} - X_{Ri} r_s^2)_k \theta_{sk} \sin\phi_{ui} \\
&+(\dot{v}_s + u_s r_s - p_s w_s - \dot{p}_s Z_{Ri} + X_{Ri} \dot{r}_s + Z_{Ri} q_s r_s + X_{Ri} q_s p_s)_k \cos(\phi_{sk} - \phi_{ui}) \\
&-(\dot{w}_s + p_s v_s - q_s u_s - p_s^2 Z_{Ri} + X_{Ri} r_s p_s - Z_{Ri} q_s^2 - X_{Ri} q_s^2)_k \sin(\phi_{sk} - \phi_{ui}) \\
&- \dot{p}_{ui} z_{ui} - 2 p_{ui} \dot{z}_{ui}] + (F_{yi1} + F_{yi2} + F_{yi3} + F_{yi4}) \cos\phi_{ui} \\
&- (F_{Zi1} + F_{Zi2} + F_{zi3} + F_{Zi4}) \sin\phi_{ui} + m_{ui} g \sin\phi_{ui}
\end{aligned} \tag{2.14}$$

Equations of Motion of the Sprung Masses

For the vehicle model presented in Figure 2.1 each sprung mass is assumed to posses five DOF, namely: Lateral, Vertical, Roll, Yaw and Pitch. Five second-order differential equations, derived to describe the motion of each sprung mass, are presented in the following manner.

Equations of Lateral Motion:

$$m_{sk}\dot{v}_{sk} - m_{sk}(p_s w_s - u_s r_s)_k = \sum \bar{j}_{sk} \text{ component of the constraint forces}$$

$$+ \sum_{i=j1}^{j2} [F_{Ri}\cos(\phi_{sk} - \phi_{ui}) - (F_{i1} + F_{i2})\sin(\phi_{sk} - \phi_{ui})]$$

$$+ m_{sk} g \sin\phi_{sk} \; ; \; k = 1, 2 \text{ and } i = 1,....5 \qquad (2.15)$$

where j1 and j2 designate the axles attached to the sprung mass: j1 = 1 and j2 = 3 for k = 1; and j1= 4 and j2 = 5, for k = 2.

Equations of Vertical Motion:

$$m_{sk}\dot{w}_{sk} - m_{sk}(q_s u_s - p_s v_s)_k = \sum \bar{k}_{sk} \text{ component of the constraint forces}$$

$$+ \sum_{i=j1}^{j2} [F_{Ri}\sin(\phi_{sk} - \phi_{ui}) + (F_{i1} + F_{i2})\cos(\phi_{sk} - \phi_{ui})]$$

$$+ m_{sk} g \cos\phi_{sk} \qquad (2.16)$$

Equation of Roll Motion:

$$I_{xxsk}\dot{p}_{sk} - (I_{yys} - I_{zzs})_k q_{sk} r_{sk} = \sum \text{roll moments from the constraints}$$

$$-\sum_{i=j1}^{j2} F_{Ri}\cos(\phi_{sk}-\phi_{ui})\,Z_{Ri}+\sum_{i=j1}^{j2}(F_{i1}+F_{i2})s_i$$

$$+\sum_{i=j1}^{j2}(F_{i1}+F_{i2})\sin(\phi_{sk}-\phi_{ui})\,Z_{Ri}$$

$$+\sum_{i=j1}^{j2}\mathrm{KRS}_i(\phi_{sk}-\phi_{ui}) \qquad (2.17)$$

where KRS_i is the auxiliary roll stiffness of the suspension springs on axle i.

Equations of Pitch Motion:

$$I_{yysk}\dot{q}_{sk}-(I_{zzs}-I_{xxs})_k\,p_{sk}r_{sk} = \Sigma \text{ pitching moments from the constraints}$$

$$+\sum_{i=j1}^{j2}[F_{Ri}\sin(\phi_{sk}-\phi_{ui})$$

$$+(F_{i1}+F_{i2})\cos(\phi_{sk}-\phi_{ui})]\,X_{ui} \qquad (2.18)$$

where X_{ui} is the longitudinal distance of axle i from the c.g. of the sprung mass to which it is attached.

Equations of the Yaw Motion:

Since, the axles experience the yaw motion together with the sprung mass, the yaw moments of inertia of the axles are combined with the yaw moment of inertia of the sprung mass to obtain an equation applicable to the combined rigid body:

$$\left[\sum_{i=j1}^{j2} I_{zzui}+I_{zzsk}\right]\dot{r}_{sk}-(I_{xxs}-I_{yys})_k\,p_{sk}q_{sk}$$

$$= \Sigma \text{ yaw moments due to the constraints}$$

$$+\sum_{i=j1}^{j2} [\,[F_{Ri}\cos(\phi_{sk}-\phi_{ui})-(F_{i1}+F_{i2})\sin(\phi_{sk}-\phi_{ui})]\,X_{ui}$$

$$+(AT_{i1}+AT_{i2}+AT_{i3}+AT_{i4})\cos\phi_{sk}\,] \qquad (2.19)$$

Equations (2.15) to (2.19) constitute the governing differential equations of motion of the sprung masses. The equation needed to evaluate the unknown constraint forces and tire forces are developed in the subsequent sections.

Equations of Motion of the Unsprung Masses

Each of the five unsprung masses shown in Figure 2.1 is assigned roll and bounce DOF. The equations of roll and bounce motions of each of the unsprung masses are derived as follows.

Equation of Roll Motion:

$$I_{xxui}\dot{p}_{ui} = -(F_{i1}+F_{i2})\,s_i - F_{Ri}\,Z_{ui} - [(F_{yi1}+F_{yi2}+F_{yi3}+F_{yi4})\cos\phi_{ui}$$

$$+(F_{Zi1}+F_{Zi2}+F_{Zi3}+F_{Zi4})\sin\phi_{ui}\,](HR_i\cos\phi_{ui}-Z_{ui})$$

$$+(F_{Zi1}-F_{Zi4})(T_i+A_i)\cos\phi_{ui}+(F_{Zi2}-F_{zi3})T_i\cos\phi_{ui}+KRS_i(\phi_{sk}-\phi_{ui}) \qquad (2.20)$$

Equations of Vertical Motion:

$$m_{ui}\bar{a}_{mui}\bar{k}_{ui} = m_{ui}g\cos\phi_{ui} + F_{i1}+F_{i2}-(F_{Zi1}+F_{Zi2}+F_{Zi3}+F_{Zi4})\cos\phi_{ui}$$

$$-(F_{yi1}+F_{yi2}+F_{yi3}+F_{yi4})\sin\phi_{ui} \qquad (2.21)$$

where F_{Zij}, the vertical force developed by the tire j (j = 1,..,4) on axle i (i = 1,...,5). The acceleration $\vec{a}_{mui}\vec{k}_{ui}$ is evaluated in a manner similar to the one employed for evaluation of $\vec{a}_{mui}\vec{j}_{ui}$ in equation (2.13)

$$\begin{aligned}\vec{a}_{mui}\vec{k}_{ui} = &-(\dot{u}_s + q_s w_s - r_s v_s + \dot{q}_s Z_{Ri} - X_{Ri} q_s^2 + p_s r_s Z_{Ri} - X_{Ri} r_s^2)_k \theta_{sk} \cos\phi_{ui} \\ &+(\dot{v}_s + u_s r_s - p_s w_s - \dot{p}_s Z_{Ri} + X_{Ri} \dot{r}_s + Z_{Ri} q_s r_s + X_{Ri} q_s p_s)_k \sin(\phi_{sk} - \phi_{ui}) \\ &+(\dot{w}_s + p_s v_s - q_s u_s - p_s^2 Z_{Ri} + X_{Ri} r_s p_s + Z_{Ri} q_s^2 - X_{Ri} \dot{q}_s)_k \cos(\phi_{sk} - \phi_{ui}) \\ &+(\ddot{Z}_{ui} - p_{ui}^2 Z_{ui}) \end{aligned} \tag{2.22}$$

The differential equations governing the motion of the sprung masses contain terms related to the constraint forces and moments. These constraint forces and moments, arising at the fifth wheel coupling, are derived from the kinematic constraint equations. The fifth wheel is a single point constraint, where the articulation between the two units takes place. The constraint acceleration equations, needed to solve for the lateral and vertical forces, are derived upon equating accelerations of the constraint point on the tractor to that of the same point on the semitrailer [35]. The roll moments due to the torsional compliance of the articulation mechanism are evaluated from the relative angular displacement between the sprung weights of the tractor and the semitrailer. The roll moment acting on the tractor sprung weight, M_{x1}, is computed from the product of the fifth wheel constraint stiffness K_5 and relative angular displacement resolved about the $\vec{i}_{s1}$ coordinate. The roll and pitch moments acting on the sprung weight of the

semitrailer, M_{x2} and M_{y2} respectively, are determined M_{x1} using the coordinate transformation:

$$M_{x1} = K_5 [\phi_{s2} \cos(\psi_{s2} - \psi_{s1}) - \theta_{s2} \sin(\psi_{s2} - \psi_{s1}) - \phi_{s1}] \quad (2.23)$$

$$M_{x2} = -M_{x1} [\cos(\psi_{s2} - \psi_{s1}) + \theta_{s1}\theta_{s2}] \quad (2.24)$$

$$M_{y2} = -M_{x1} [\theta_{s2} \cos(\psi_{s2} - \psi_{s1}) \sin\phi_{s2} - \theta_{s1} \sin\theta_{s2} - \sin(\psi_{s2} - \psi_{s1}) \cos\phi_{s2}] \quad (2.35)$$

2.3 Forces and Moments at the Tire-Road Interface

The forces and moments developed at the tire-road interface are formulated using the tire properties and road roughness. The measured cornering properties of radial truck tires [36] are used to compute the lateral forces and aligning moments generated at the tire-road interface. The cornering properties of tires are influenced by many design and operating factors in a highly complex manner. The vertical load and slip-angles most significantly affect the cornering forces and aligning moment characteristics of pneumatic tires. Figure 2.5 illustrates the cornering force F_{yij} of 11R22.5 tires, as a function of normal load and side-slip angles. The figure illustrates the nonlinear dependency of cornering force on both normal load and side slip angles. The lateral forces and moments due to tires are thus derived using a look-up table in conjunction with linear interpolation, based upon the instantaneous normal load and side-slip angle developed. The instantaneous side slip angle developed at a tire-road interface is derived from the instantaneous forward and lateral velocity at the tire-road interface, as shown in

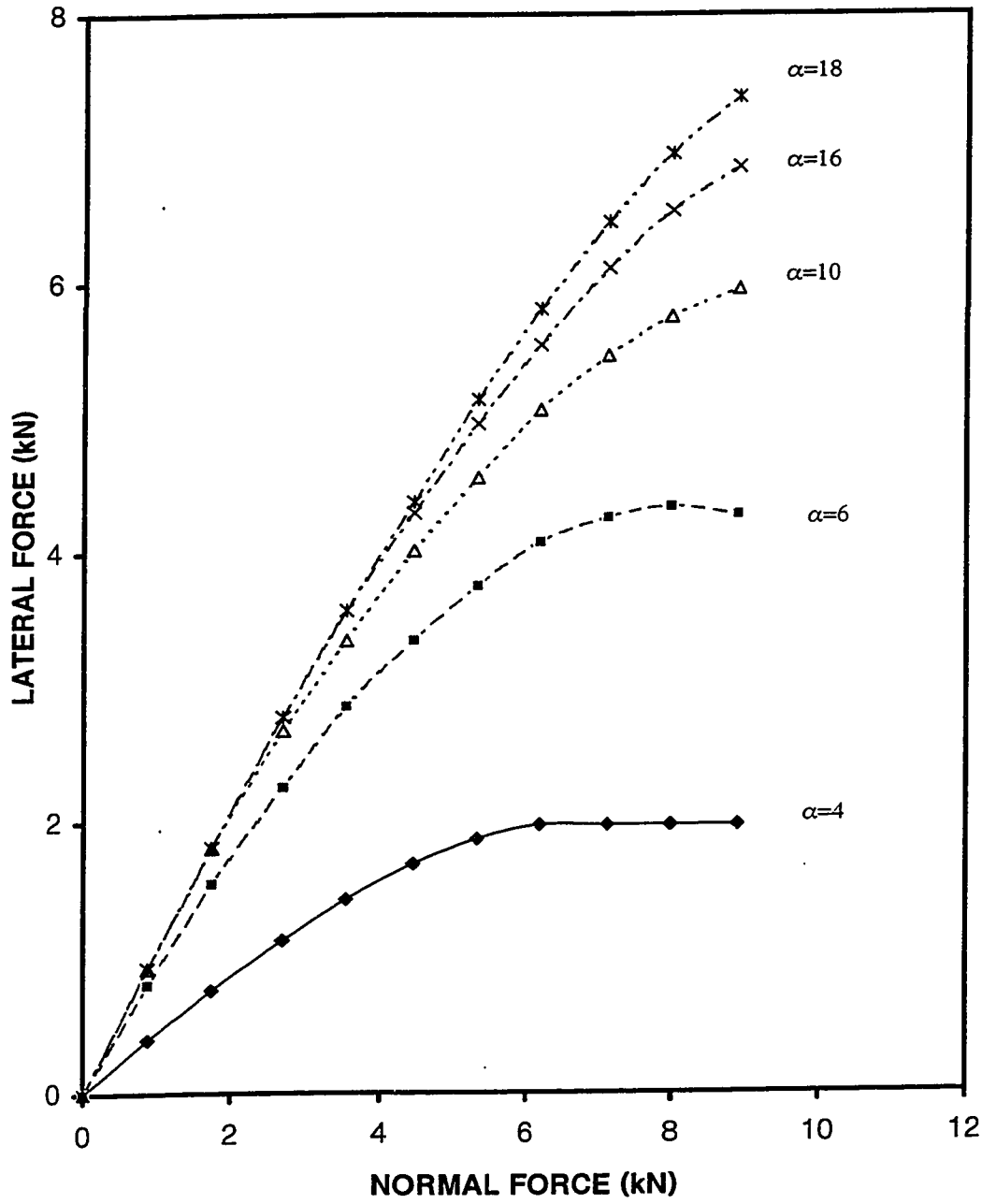

Figure 2.5: Lateral force characteristics of a tire as function of normal for various slip angles.

Figure 2.5. The side slip angle at the tire-road interface is expressed in terms of the body-fixed velocities of the sprung masses and the axles. The side slip angle of the tire j on the axle i, α_{ij} is expressed as:

$$\alpha_{ij} = \tan^{-1}\left[\frac{V_{axle_i}}{U_{tire_{ij}}}\right] - \delta_i \; ; \; i = 1,..5 \text{ and } j = 1,..4 \tag{2.26}$$

where $V_{axle\ i}$ is the lateral velocity at the tire-road interface, which is related to the velocities and displacements of the sprung and unsprung masses:

$$V_{axle_i} = (v_s - Z_{Ri} p_s) \cos\phi_s + \frac{x_{ui} r_s}{\cos\phi_s} - p_{ui} HR_i \cos\phi_{ui}$$

U_{tireij} is the longitudinal velocity of tire j on axle i, and is given by:

$$U_{tire_{i1}} = u_s + (T_i + A_i) r_s$$

$$U_{tire_{i2}} = u_s + T_i r_s$$

$$U_{tire_{i3}} = u_s - T_i r_s$$

$$U_{tire_{i4}} = u_s - (T_i + A_i) r_s \tag{2.27}$$

where T_i is the half tire inner track width of axle i, and A_i is the dual tire spacing and δ_i is the front wheel steer angle and $\delta_i = 0$, for i = 2,..5.

The instantaneous vertical load acting on the tire j of axle i, F_{zij}, is a function of tire deformation and compliance of the tire KT_{ij}. The instantaneous tire deformation, however, is a complex function of road roughness and the displacement response of

sprung and unsprung masses. Assuming linear vertical stiffness of the tire and nearly point contact with the road, the vertical tire force can be expressed as:

$$F_{zij} = KT_{ij}\,\Delta_{ij} \tag{2.28}$$

where Δ_{ij} is the vertical deflection of the tire, which is related to the deflections of the sprung and unsprung masses, and the road roughness. The deflection of the outer left tire (j = 1) on axle i can be expressed as:

$$\Delta_{i1} = \Delta_{0i} + \Delta z_s - Z_{Ri}(1 - \cos\phi_s) + z_{ui}\cos\phi_{ui} - z_{u0i} - (T_i + A_i)\sin\phi_{ui}$$
$$- x_{ui}\theta_s - \mathrm{LRD};\ i = 1,..,3 \text{ for } k = 1, \text{ and } i = 4, 5 \text{ for } k = 2. \tag{2.29}$$

where Δz_s and the vertical deflections of the c.g.'s of the sprung and unsprung masses along the inertial axis $\vec{k}_n$ ($\Delta z_s = 0$ at time t = 0). Z_{u0i} is the vertical distance between the roll center and the c.g. of axle i corresponding to static equilibrium (t = 0). Δ_{0i} is the static deflection of the tire, and LRD describes the elevation of the road at the left-tire contact point. It is further assumed that the two tires are subjected to identical road elevation. The two right tires are subject to another identical road elevation, which is different from that encountered by the left tires.

The vertical deflections of remaining tires on axle i are derived from:

$$\begin{aligned}
\Delta_{i2} &= \Delta_{i1} + A_i \sin\phi_{ui} - \mathrm{LRD} \\
\Delta_{i3} &= \Delta_{i2} + 2T_i \sin\phi_{ui} + \mathrm{LRD} - \mathrm{RRD} \\
\Delta_{i4} &= \Delta_{i3} + A_i \sin\phi_{ui} - \mathrm{RRD}
\end{aligned} \tag{2.30}$$

where RRD is the elevation of the road at the contact point with right tires. Equations (2.29) and (2.30) are solved using specific road profiles to determine the instantaneous normal loads, which are further utilized to determine the effective cornering forces and aligning moments from the look-up tables.

2.4 Method of Solution and Performance measures

The coupled differential equations of motion, (2.15) to (2.19), describe the motions of the sprung and unsprung masses of the tractor and semitrailer. The directional dynamics of the tractor-semitrailer configuration is thus represented by a 20 DOF system, which is subjected to two different and simultaneous inputs arising from the road roughness and the steering maneuvers. The cornering and vertical forces developed by the tires are computed using the look-up table and Equations (2.26) to (2.30). The yaw/roll software developed by UMTRI is modified to incorporate the roughness of the road at the two tracks of the vehicle, vertical and nonlinear damping forces. The equations of motion are solved using numerical integration technique based upon a predictor-corrector method. The response characteristics of the vehicle are evaluated to assess the influence of road roughness on the directional performance and that of the steering maneuver on the dynamic wheel loads. A number of performance measures are formulated to assess the directional and dynamic load performance of the vehicle. These performance measures, are grouped in two different sets, referred to as: (i) directional performance measures and (ii) road damage potentials. The different performance indices from these two sets of measures are described in the following subsections.

2.4.1 Performance Measures

Based on the response of the 20 DOF vehicle system, it is possible to evaluate a very wide range of performance measures. The selection of the performance measures depends on the objective of the study. The present investigation focuses the influence of road roughness on the directional performance and the influence of directional maneuver on the dynamic wheel load. Then primary performance measures considered are therefore, (i) directional performance measures (ii) road damage potentials. Then performance indices from these two measures are described in the following subsections.

2.4.2 Directional Performance Measures

The roll and yaw directional stability of a vehicle is directly related to its response to steering inputs. The highway safety associated with rollover potential and handling of the vehicle is thus directly related to its directional response to a steering input. Although a large number of performance measures have been proposed [21], the performance measures related to handling and dynamic rollover of the vehicle are considered in this study. An articulated vehicle subject to a steering input imposes lateral forces on the sprung and unsprung masses, which in turn develop side-slip angles at each tire road contact. The difference in the slip angles between different axle tires of a vehicle is referred to as the understeer coefficient K_{us}. The understeer coefficient of a vehicle

describes its handling behavior and stability limits [22]. The vehicle may approach certain instabilities when K_{us} is below its critical value given by:

$$K_{uscr} = gL/U^2 \tag{2.31}$$

where L is the effective wheelbase and U is the forward speed. The K_{us} of a vehicle is strongly affected by the vertical tire loads, cornering properties of tires, and motion of the sprung and unsprung masses. The value and sign of K_{us} is an effective performance indicator for handling behavior of the vehicle, and is represented by a handling diagram.

Heavy vehicles, subject to steering input experience considerable load transfer from inner to outer tires due to vehicle roll and lateral acceleration. This load transfer has been considered as an effective measure for the dynamic rollover stability performance of the vehicle. The roll and yaw stability of articulated vehicles can be further measured in terms of lateral acceleration experienced by the rearmost unit for a given acceleration of the tractor unit. This measure, referred as rearward amplification factor, is an effective tool for evaluating the safety performance of the vehicle under dynamic steering inputs. For a given vehicle configuration, the rollover and jackknife tendencies of articulated vehicles may be expressed in terms of their roll and yaw rates, respectively. The various measures considered in this study are discussed below.

Handling Diagram:

The handling diagram provides important information related to the stability and control characteristics of a vehicle over the entire operational rage of lateral acceleration. The

steady-state handling characteristics of the tractor and the semitrailer are derived from the simple yaw plane model. The respective equations for steady-state handling are expressed as:

$$\delta = \frac{L_1}{R_1} + K_{ust}\frac{U^2}{gR_1}$$

$$\gamma = \frac{L_2}{R_2} + K_{uss}\frac{U^2}{gR_2} \tag{2.32}$$

where δ is the front axle steer angle and γ is the articulation angle, L_1 and L_2 are the wheelbases of the tractor and semitrailer, respectively. R_1 and R_2 are the radii traced by tractor and semitrailer, respectively. K_{ust} and K_{uss} are the coefficients of understeer of tractor and semitrailer, respectively. U is the forward speed of the vehicle and g is the acceleration due to gravity. Substituting for the lateral accelerations, $a_1 = (U^2/R_1)$ and $a_2 = (U^2/R_2)$, and (U/r_1) for the turning radius R_1, where r_1 is the yaw velocity of the tractor, Equation (2.32) yields:

$$K_{ust}\, a_1 = -\left(\frac{L_1 r_1}{U} - \delta\right)$$

$$K_{uss}\, a_2 = -\left(\frac{L_2 r_2}{U} - \gamma\right) \tag{2.33}$$

where a_1 and a_2 are the lateral acceleration of tractor and semitrailer units. The handling characteristics of the vehicle are directly related to magnitude and sign of K_{uss}

and K_{ust}. An understeer vehicle (K_{uss}>0; K_{ust}>0) can be shown to be unconditionally stable. An oversteer tractor (K_{ust}<0) may lead to a directional instability, while oversteer semitrailer (K_{uss} < 0)may yield poor turning abilities. The handling diagrams of the tractor and semitrailer, a plot of lateral acceleration against the handling parameters $\left(\frac{L_1 r_1}{U}-\delta \text{ or } \frac{L_2 r_2}{U}-\gamma\right)$, are obtained from the steady-state response of the vehicle for different forward speeds under the influence of smooth, medium and rough roads. The slope of the handling curve is related to the understeer coefficient in the following manner:

$$\frac{d(a_1)}{d(\frac{L_1 r_1}{U}-\delta)} = - \frac{1}{K_{us}}$$

Method of Evaluation:

A three-point measure is used to characterize the handling diagram of a vehicle over the entire operating range as suggested by M. EI-Gindy [21]. The diagram is constructed using the {(L/R - δ), a_1} coordinate system, where δ is the front axle steer angle. The first point is designed to place upper and lower limits on the understeer coefficient, K_{us}, at a lateral acceleration level of 0.1 g, in order to ensure reasonable controllability. Without such limits, the driver either will have difficulty steering the vehicle or will have trouble coping with its (hyper)sensitivity. The understeer coefficient is held in the range from 0.0 degrees/g (sensitivity boundary) to 2.0 degrees/g (steerability boundry). The second point in the diagram addresses the level of lateral acceleration at which the

vehicle transforms from understeer to oversteer. The lateral acceleration at which the transition takes place should not be less than 0.18g to ensure that a reasonable level of lateral acceleration can be reached before the onset of oversteer. The final third point in the diagram addresses the understeer coefficient, K_{us}, at a lateral acceleration of 0.3 g. The coefficient within this acceleration should be higher than a critical understeer coefficient, K_{uscr}, by a certain margin of safety in order to prevent loss of directional stability in the presence of external perturbation. The critical understeer coefficient is defined as $-Lg/U^2$, where the vehicle speed U is taken as 100 km/h. The handling performance is evaluated from the steady state response of the vehicle subject to a ramp-steer input at a rate of 0.02 degrees/sec at the front axle.

Dynamic Rollover Stability Measures

Load Transfer Ratio (LTR):

Under dynamic maneuvers, a load shift takes place from inner to outer wheels, due to lateral acceleration and roll displacement of the sprung masses. The magnitude of the load shift provides a direct indication of dynamic rollover stability of the vehicle. This indicator is measured in terms of load transfer ratio (LTR), is defined as [21]:

$$\text{LTR} = \left| \frac{F_{zl} - F_{zr}}{F_z} \right| \tag{2.33}$$

Where F_{zl} is the sum of all the left wheel loads, F_{zr} is the sum of the right wheel loads and F_z is the sum of all the wheel loads. Above equation reveals that LTR approaches

Unity value, when all the wheels on a single track lose contact with the road indicating definite rollover. It is recommended that the LTR of a vehicle must not exceed 0.6 [21].

Rearward Amplification Factor (RWA):

The rearward amplification ratio is a frequency dependent measure, defined as the ratio of the peak (positive or negative) lateral acceleration at the center of gravity of the rearmost trailer to the amplitude controlled lateral acceleration of 0.15g at the center of the front axle of the lead unit (tractor). This measure defines the amplification of lateral acceleration from the tractor to the trailer unit during a maneuver.

$$\text{RWA} = \frac{a_2}{a_1} \tag{2.34}$$

where a_2 is the lateral acceleration at the trailer c.g. and a_1 is the lateral acceleration at the front axle c.g. of the tractor

Method of Evaluation:

This measure is obtained during a rapid high-speed path change maneuver conducted at 100 km/h, such that a lateral acceleration of 0.15g at the center of the front axle is produced within a time period constraint of 3.0 seconds. The recommended target value of the rearward amplification is 2.2 [21].

Roll, Yaw and Pitch Rates:

The rollover and jackknife potentials of a vehicle are related to the rates of sprung mass roll and yaw angles, respectively. The roll and yaw rates are also frequently used as measures of handling performance under steady-state condition. The relative yaw rate of

articulated unit is further used as an effective indicator of jackknife potential of an articulated vehicle. The present investigation further examines the pitch rate, which may provide interesting insight on the influence of road roughness on the handling performance.

2.4.3 Performance Measures to Assess Road Damage Potentials

The assessment of road damage potentials of heavy vehicles is highly complex due to lack of definite failure mechanism of the pavements. As discussed in the literature review, extensive work has been done on this aspect and several performance measures have been proposed [3,26,27]. Among all the measures, dynamic load coefficient has received a wide application since it permits the relative road damaging potentials of different vehicles without consideration of pavement failure mechanism. Road damage potential can be further be examined in terms of peak dynamic loads and road stress factor. These measures along with new measures such as peak cornering force and peak resultant force are presented below.

Dynamic Load Coefficient (DLC):

DLC is a convenient measure of variation in the tire force over a period of time. It is a statistical measure reflecting tire force deviation from a mean value. The 'Dynamic Load Coefficient' (DLC) , is defined as [3, 26, 27];

DLC = RMS dynamic tire force / Mean tire force

The average force for each tire evaluated during a simulation, which is taken as static tire force and can be expressed as:

$$\bar{F}_{ij} = \frac{\sum_{i=1}^{N} F_{ij}}{N} \qquad \text{where j = 1,..5;}$$

The time history can further be used to establish the standard deviation (s_{ij}) of the force experience by the tire around its mean. The DLC for a tire on j^{th} tire on the axle i can now be expressed in terms of variation over the mean as:

$$DLC_{ij} = \frac{s_{ij}}{\bar{F}_{ij}} \tag{2.35}$$

where DLC_{ij} = Dynamic load coefficient of left tires.

$\bar{F}_{ij}$ = Mean tire force of the left tires.

s_{ij} = Standard deviation of the left tire forces.

Here the mean force represents the time average of tire force in the entire simulation period, which is similar in magnitude to the static tire force. The RMS dynamic tire force is equal to the square root of the area under the tire force spectral density graph. The magnitude of dynamic tire forces depends on roughness of the road surface, speed, vehicle configuration, mass distribution, and properties of the suspension and tires. The DLC, as defined in Equation (2.35), is a measure of variation in dynamic wheel load rather than the instantaneous peak, which may be considerably large. The peak tire force is thus considered as a measure of the dynamic loads.

Peak Tire Force:

The peak force is the maximum force transmitted to the pavement during the entire simulation time history, and is given by:

$$F_{max} = \text{Max } \{F_{zij}, i = 1, N\} \tag{2.36}$$

where F_{zij} is the instantaneous tire vertical and N is the number of simulation points.

Road Stress Factor:

The Road Stress Factor, is calculated under the assumption that road damage depends on the fourth power of the instantaneous (dynamic) wheel force at a point on the road. Assuming that dynamic wheel forces follow a Gaussian distribution, the expected road stress factor is defined as [3]:

$$\Phi = E (1+ 6S^2 + 3S^4) P^4_{stat} \tag{2.37}$$

where S is the coefficient of variation of the dynamic tire force and P_{stat} is the static tire force. Although, S is not equal to the Dynamic load Coefficient(DLC), it has been proposed to replace S by DLC in order to assess the relative performance characteristics of different suspension. The dynamic road stress factor is thus defined as:

$$v = 1 + 6DLC^2 + 3DLC^4 \tag{2.38}$$

The dynamic road stress factor given in (2.38) may be considered as a lower estimate since it assumes that the distribution of loading at a specific point of the pavement is normal. The dynamic component of the tire force arising from interactions between

vehicle and the pavement, however, may yield higher loads, which tend to occur at a specific point in the pavement. Assuming that the dynamic tire force distributions are normal, the 95^{th} percentile impact factor may be estimated as follows [3, 26]:

$$IF_{95^{th}} = 1 + 1.645\ DLC \tag{2.39}$$

The dynamic road stress factor corresponding to the 95^{th} percentile impact factor force is given by [3, 26]:

$$v = (IF_{95^{th}})^4 \tag{2.40}$$

Peak Cornering Force:

The cornering forces developed by tires during a steering maneuver further impose lateral forces at the tire-road interface, which may lead to further degradation of the pavement surface. It is thus proposed to investigate the peak lateral forces transmitted to the pavement during a steering maneuver.

Peak Resultant Force:

The peak resultant force is evaluated in order to examine the influence of the lateral and the vertical forces at tire-road contact when the vehicle undergoes a directional maneuver. The resultant force is computed from:

$$F_{resultant} = \sqrt{F_z^{\,2} + F_y^{\,2}} \tag{2.41}$$

where F_z and F_y are the tire vertical and lateral forces. This force is further used in the calculation of DLC and road stress factor to determine the contribution of the lateral forces transmitted to the pavement. The measures described in this section are used to

evaluate the dynamic performance of the vehicle. The influence of road roughness on the directional dynamics performance is discussed in chapter 4, while the influence of steering maneuvers on the dynamic tire loads is examined in chapter 5.

2.5 Candidate Vehicle Parameters

The directional and dynamic load performance characteristics are analyzed for a five-axle tractor-semitrailer configuration, presented in Figure 2.1. The GVW of the candidate vehicle is 41814 kg, which represents most commonly employed freight vehicles in Canada [35]. The weight and dimensional parameters of the candidate are presented in Table 2.1 [36]. The tractor front axle comprises a leaf spring suspension, while the tractor rear and trailer axles are considered to employ modern air suspension. The force-deflection properties of the suspension springs are presented in Figure 2.3 and 2.4 The vehicle is considered to employ radial tires with vertical stiffness (KT_{ij}) of 869.5 kN/m.

TABLE 2.1

CANDIDATE VEHICLE PARAMETERS [36]

PARAMETERS	TRACTOR			TRAILER	
Sprung Mass (kg)	6259.57			32205.06	
Roll Mass Moment of Inertia (kg-m^2)	296.37			3540.97	
Pitch Mass Moment of Inertia (kg-m^2)	3665.22			55688.31	
Yaw Mass Moment of Inertia (kg-m^2)	3665.22			55688.31	
Center of Gravity Height (m)	1.40			2.23	
Unsprung Mass Parameters	Axle-1	Axle-2	Axle-3	Axle-4	Axle-5
Axle Load (kN)	53.44	89.07	89.07	89.07	89.07
Longitudinal Position from c.g.(m)	1.42	-2.54	-4.06	-4.99	-6.82
Axle Center of Gravity Height (m)	0.5	0.5	0.5	0.5	0.5
Dual Tire Spacing (m)	0	0.33	0.33	0.33	0.33
Roll Center Height (m)	0.46	0.74	0.74	0.73	0.73
Fifth Wheel Parameters					
Longitudinal Position from Tractor c.g. (m)				-2.94	
Longitudinal Position from Semitrailer c.g. (m)				6.33	
Roll Stiffness (kg-m / deg)				11500	

Chapter 3

Characterization of Road Roughness and Steering Inputs

3.1 General

The performance measures defined to assess both the directional response and the dynamic wheel loads are strongly influenced by the excitations arising from road roughness and steering inputs. The vehicle performance is further influenced by various design and operating factors, such as vehicle speeds and load distribution. In order to study the influence of road roughness on the directional performance of the vehicle, it is necessary to identify respective maneuvers to be performed at highway speeds, and the roughness characteristics of the typical roads. For this study, standard maneuvers such as: turning, typical lane change and evasive maneuver are considered to evaluate the vehicle performance. Since the primary focus of the study is to assess the influence of road roughness on the directional behavior of the vehicle, a number of measured road profiles are therefore, analyzed to identify three groups of roads, namely: Smooth, Medium and Rough roads based on a Roughness Index (RI) value. The roughness characteristics of the

roads in the vicinity of two tracks of the vehicle are considered to incorporate the influence of cross-slope of the road. The roughness characteristics of the two tracks are analyzed to study the correlation between the road inputs on the left and right wheels. The roll excitations due to road roughness are further derived.

3.2 Characterization of Road Roughness

One of the primary operating characteristics of a road, whether paved or unpaved, is the level of service that it provides to its users. In turn, the variation of this level of service or serviceability with time provides one measure of road performance. The measurement of roughness is important in terms of evaluating road surfaces and their performance. Road serviceability, or ride quality, is largely a function of road roughness. Road test studies performed by the American Association of State Highway Officials (AASHO) have shown that about 95 percent of the road user's perception of the serviceability of a road result from the roughness of its surface profile [33]. A rough pavement can reduce friction between the tire and the road, and cause uneven lateral and vertical forces, and physical damage to a vehicle. Furthermore, the driver may or may not be able to maintain control of the vehicle under highway speed maneuvers. The severity of road roughness may be assessed in term of the magnitude of roughness and its frequency components. The ride quality, traction, braking, and handling performance of a vehicle are strongly related to the magnitude and frequency components of the road.

The road profiles are frequently measured using a profilometer along left and right wheel tracks in equal intervals. When using measured road profile data, the assumption is made that phase shift is the only difference between the profiles at the front and rear tires. Since measured road profile data are in discrete form (0.3m spacing), interpolation of this data between consecutive measured points is necessary. Furthermore, the effects of occasional large irregularities, such as potholes, are incorporated within the data. In this study, the measured roughness profiles of different highways are analyzed in terms of their roughness. The road profiles are expressed in three types of roughness based upon a roughness index, and referred as 'smooth', 'medium-rough' and 'rough'. The correlation between the profiles on the left and right tracks of different roads is further investigated.

3.2.1 Classification of Road Profiles

Different road profiles may be classified based on their roughness and spectral components. The roughness profiles of various roads in Canada have been measured and reported [40]. The measured profiles describe the elevation in the vicinity of both left- and right wheel tracks including local grades and abrupt variations, such as potholes and cracks. The elevations of roads are reported over a length of approximately 500 m at intervals of 0.3 m. and represent a wide range of roughness conditions. The road profiles considered in this study are thus classified under smooth, medium and rough roads using a Roughness Index (RI). The roughness index is defined as the sum of absolute values of vertical heights of all the bumps, large or small, that occur over 1 km length of the

highway, and is expressed as m/km or in/mile. The roughness index (RI) values are computed from:

$$RI = \sum_{i=1}^{n} |LRD(X_i)| ; 0 < X_i < 1 \text{ km} \tag{3.1}$$

Where LRD is the deviation of the left road profile from the mean value at every 0.3m interval, n is the total number of measured data points available over 1 km length, and X is the longitudinal coordinate of the road profile data. Gordan [37] analyzed the profiles of various roads and classified them in various categories, ranging from exceptionally smooth to extremely rough, based upon the RI values. Table 3.1 summarizes the classification of road profiles and the range of RI values.

Table 3.1: Roughness Rating of roads based upon RI values [37]

m/ km	Ratings
0 – 0.79	Exceptionally smooth
0.8 – 1.19	Very Good
1.2 – 1.5	Good
1.6 – 1.9	Fair
2.0 – 2.3	Acceptable
2.4 – 2.7	Poor
2.8 – 3.1	Very Poor
3.2 and Above	Extremely Rough

The roughness data acquired for three different roads was smoothened to eliminate the contributions due to localized gradients. Figure 3.1 to 3.3 illustrate the roughness profiles of three different roads, referred to as 'Road A', 'Road B', 'Road C' .The peak elevations of the roads A, B, C are observed to be approximately 0.2 cm, 0.5 cm, 1.5 cm, respectively. While the road A appears to be smoothest one, the road C can be considered the most rough. The RI values of left- and right- track profiles of the roads are computed using Equation (3.1) and summarized in Table 3.2.

Table 3.2: Roughness Index of roads

Road	RI (m/km)	
	Left-Track	Right-Track
A	1.48	1.59
B	3.52	4.78
C	5.82	5.15

A comparison of the RI values with those presented by Gordan [37] reveals that the road A may be classified as a good road, while the RI values of the road B fall within the range of very poor to extremely rough road. The RI values of road C fall in the range for extremely rough roads. Based upon the relative RI values, the road A is considered as a smooth road in this study. The roads B and C are considered as medium rough and rough roads.

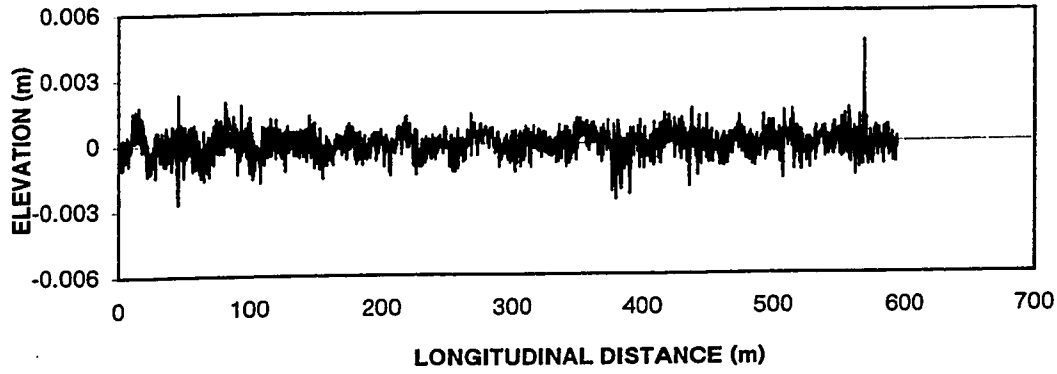

Figure 3.1: Road profile of smooth road (Road A).

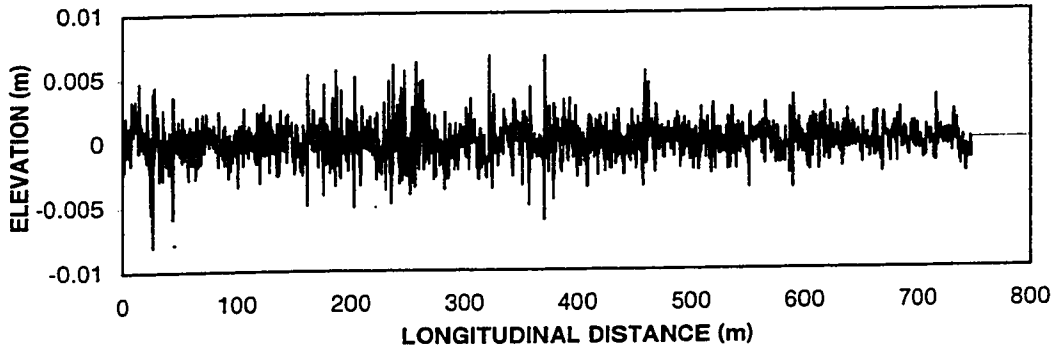

Figure 3.2: Road profile of medium-rough road (Road B).

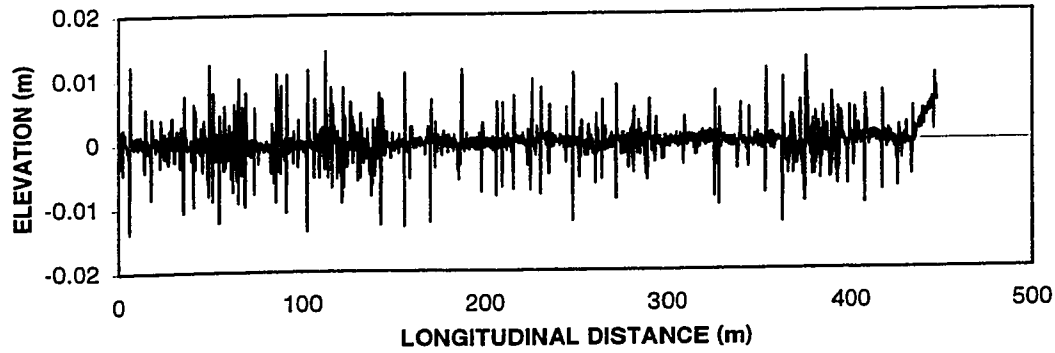

Figure 3.3: Road profile of a rough road (Road C).

The roughness of road in the vicinity of tracks of vehicles is further examined to determine the correlation between the two tracks. The correlation coefficient 'r', can be used as a measure to indicates the event by which the left and right road profiles are related. Pearson's coefficient of correlation for ungrouped data has theoretical limits of ± 1 [38]. A value of 'r' approaching +1 indicates a direct relationship between the variates, whereas a value approaching –1 indicates an inverse relationship. A value of r tending toward 0 indicates that no relationship exists between the variates. The correlation coefficient r is defined as [38]:

$$r = \frac{\frac{\sum (LRD)(RRD)}{N} - \frac{\sum (LRD)\sum (RRD)}{N^2}}{\sigma_{LRD}\sigma_{RRD}} \qquad (3.2)$$

where LRD and RRD are the deviations of the road profile at the left and right tracks, respectively, from localized mean, and N is the number of measured data points. σ_{LRD} and σ_{RRD} are the standard deviations of the two data sets, given by given by:

$$\sigma_{LRD} = \sqrt{\frac{\sum (LRD)^2}{N} - \frac{(\sum LRD)^2}{N^2}};$$

$$\sigma_{RRD} = \sqrt{\frac{\sum (RRD)^2}{N} - \frac{(\sum RRD)^2}{N^2}};$$

The correlation coefficient for the selected smooth, medium and rough roads are computed for the left and right tracks and are summarized in Table 3.3. From the results, it may be concluded that the elevations of right and left tracks of all these roads are more

or less independent. The vehicle response to excitations arising from the two tracks may thus be evaluated assuming uncorrelated inputs.

Table 3.3: Correlation Coefficient of the selected Roads

Roads	Coefficient of Correlation 'r'
Road A (Smooth)	.118
Road B (Medium)	.174
Road C (Rough)	.014

3.3 Directional Maneuvers

Directional response and handling performance of a vehicle are strongly related to the steering inputs. The directional dynamics of the articulated heavy vehicles are frequently investigated using steady steering inputs to determine steady state response behavior, and transient steering inputs to study the transient roll and yaw directional response of the vehicle [19, 21]. In this study, the influence of road roughness on the directional behavior of the vehicle is investigated using two types of steering inputs, open-loop constant steering and closed-loop path change maneuvers. The specific steering maneuvers used are discussed below.

Open-Loop Constant Steer Maneuver:

A steady or constant steer input is utilized to study the steady-state handling behavior of the vehicle. The steer angle of the front wheels is gradually increased as a ramp function until it approaches the specified angle. The steer angle is then held constant for the remaining simulation time. Alternatively, a ramp-steer input is employed to study the stability limits of the vehicle. A ramp-steer maneuver consisting of a ramp-steer rate of 0.02 deg/sec at the front axle at a constant forward speed of 100 km/h, is used in the study, as recommended by El-Gindy [21].

Closed-Loop Lane Change and Evasive Maneuvers:

The articulated vehicle combinations experience high rearward amplification and lateral acceleration response during lane change and evasive maneuvers. The directional dynamics are thus investigated using a closed-loop path-follower model developed to compute the front wheel angle required to follow the prescribed path. Typical path followed by the vehicle during lane-change and evasive maneuver are shown in Figure 3.4. For a given path, the front wheel steer angle δ is computed in the following manner:

$$\delta = \theta_2 - \theta_1 \tag{3.3}$$

where, θ_2 is the slope of the line joining the center of the front axle and the coordinates of the specified path and θ_1 is the slope of the line joining center of front axle and the future position of the center of the front axle after a small preview time interval of T. A number of studies have proposed the use of standardized maneuvers in order to evaluate the relative stability and performance characteristics of heavy vehicles [19,21]. Figure 3.5

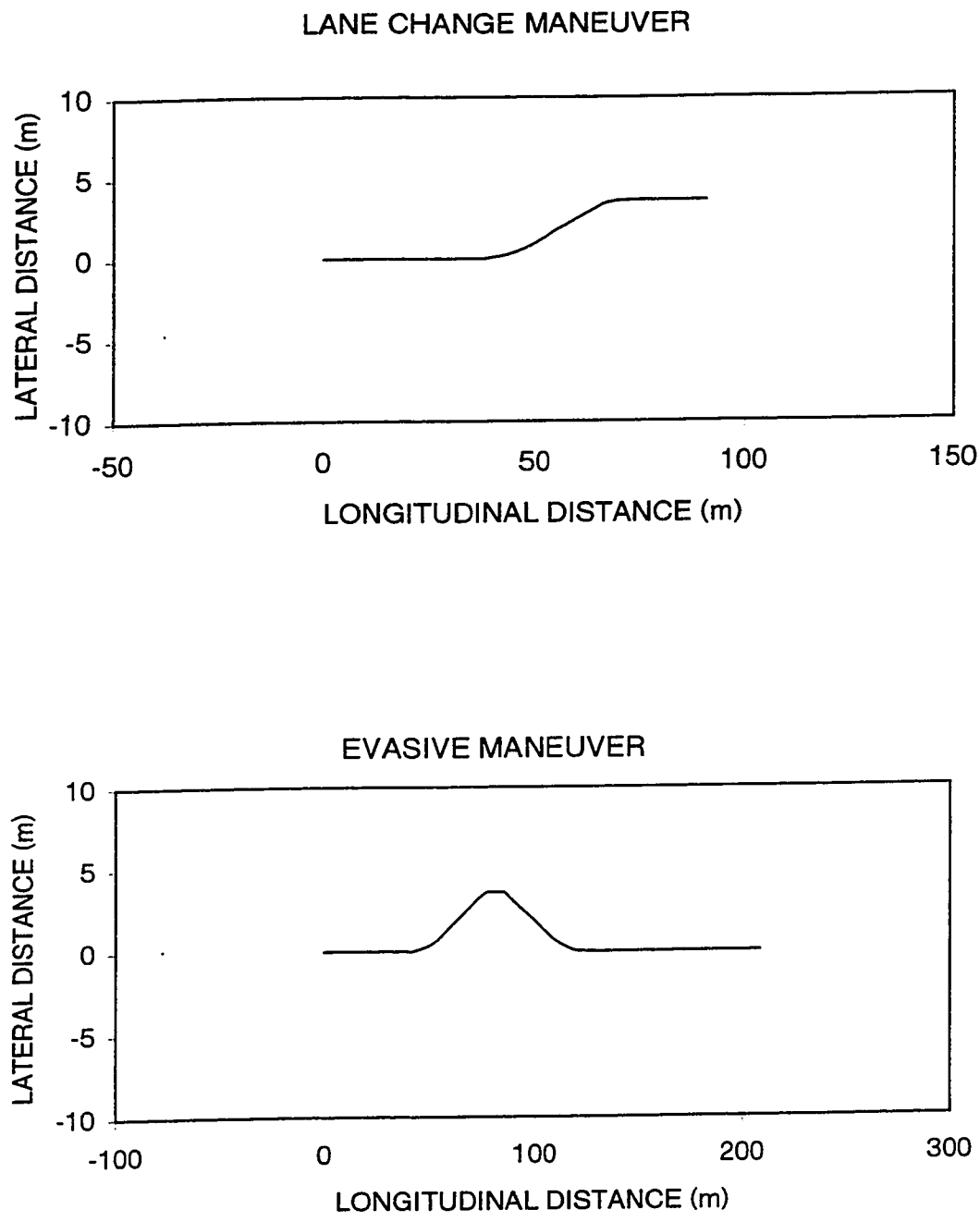

Figure 3.4: Trajectories of typical lane-change and evasive maneuvers.

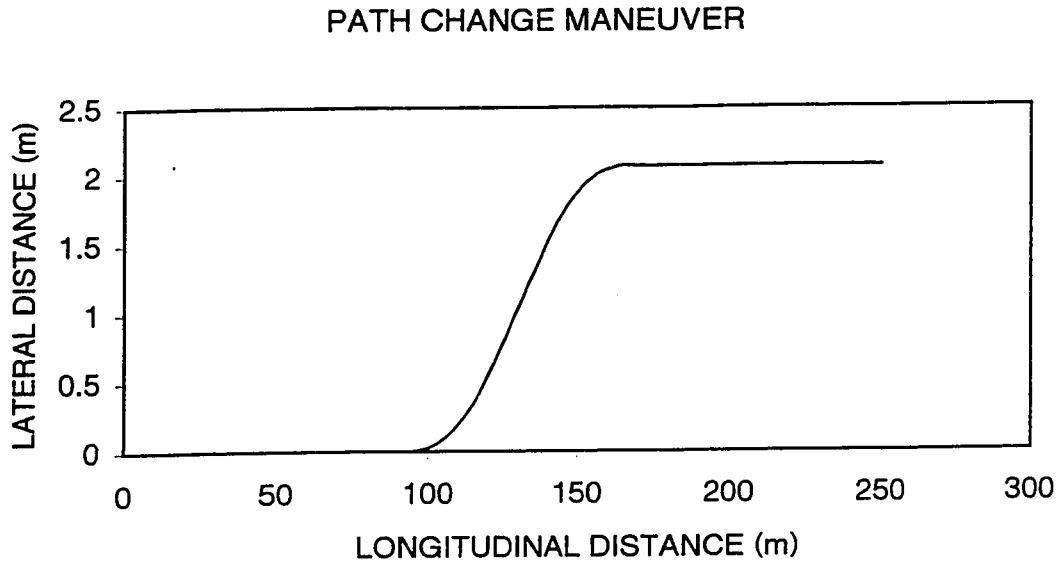

Figure 3.5: Trajectory of a path-change maneuver.

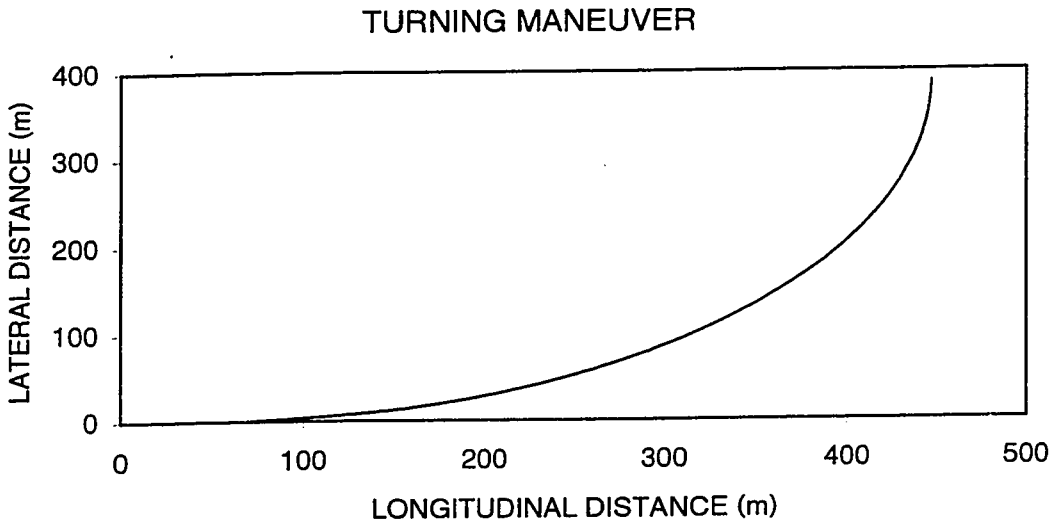

Figure 3.6: Trajectory of a high-speed turning maneuver.

illustrates the recommended path change maneuver, which is used to compute the performance measures in terms of the rearward amplification factor and lateral load transfer ratio. The difference between the path-change and the lane-change is the lateral distance taken by the vehicle to enter into a new path. For a path-change the lateral distance is 2.06 m, while that for a lane-change the lateral distance is 3.59 m.

Steady-State High-speed Turning Maneuver:

The directional performance of vehicle undergoing a steady turn is investigated using a closed-loop path following maneuver. The vehicle is required to follow a turn of radius 393 m at a speed of 50 km/h [21]. The trajectory of the turn maneuver is illustrated in Figure 3.6. The steady turning directional stability performance of the vehicle subject to this maneuver is evaluated in terms of LTR and RWA.

Using various road roughnesses and turning maneuvers presented in this section, a methodology is developed for the simulations of the tractor-semitrailer combination as presented in the following section.

3.4 Methodology

The directional dynamic response of a vehicle is known to be strongly dependent upon the directional maneuvers performed, specifically, the rate of change of lateral path coordinate and the vehicle speed. The response analysis may thus be performed for a wide range of maneuvers and speeds in order to derive the total response behavior of the

vehicle. The directional response under the influence of road roughness however, can be effectively investigated using a set of representative maneuvers, such as steady-turning, lane-change, evasive and path change maneuvers. In this study, the response analyses are carried out using the above maneuvers performed at respective speeds, illustrated in Table 3.4.

Table 3.4: Simulation Matrix

Vehicle Speed (km/h)	50	70	100	120
Road Roughness	Maneuver			
None	Steady-Turning	Lane Change Evasive	Lane Change Evasive Path-change	Lane Change Evasive
Smooth	Steady-Turning	Lane Change Evasive	Lane Change Evasive Path-change	Lane Change Evasive
Medium Rough	Steady-Turning	Lane Change Evasive	Lane Change Evasive Path-change	Lane Change Evasive
Rough	Steady-Turning	Lane Change Evasive	Lane Change Evasive Path-change	Lane Change Evasive

Chapter 4

Influence of Road Roughness on Directional Response

4.1 General

As discussed in the literature review, steady-state and dynamic directional response of articulated vehicles have been extensively investigated [19,21]. All the reported studies, however, employ the assumption of perfectly smooth road. Depending on the forward speed, road roughness may significantly influence the tire-road contact characteristics, which in turn may adversely affect the vehicle control and directional performance. It is expected that beside ride quality, the road roughness will influence vehicle performance when subjected to steering and on braking. The present investigation focuses on the influence of road roughness on the dynamic directional response of articulated vehicles.

In order to systematically study the influence of road roughness it is necessary to apply various combinations of road roughness, vehicle speed and typical steering maneuvers. All these inputs, considered for the vehicle model developed in chapter 2, are discussed in chapter 3. As discussed in chapter 3, the measured road profiles are selected

to represent, smooth, medium and rough roads. For vehicle forward speeds in the range of 70 to 120 km/h, the directional response characteristics are evaluated for the three road conditions under different steering maneuvers. The steering inputs represent a single and double lane change maneuvers as well as a path change maneuver discussed in chapter 3. Results of simulation are used to obtain various measures of directional performance, which are also discussed in chapter 2. The various performance measures include rearward amplification factors, load transfer ratio, handling diagram, as well as roll, yaw and pitch rates. In all cases results are compared with those obtained from perfectly smooth road in order to demonstrate the influence of road roughness. Vehicle parameters used for the simulation are those presented in Table 2.1.

4.2 Effects of Road Roughness on Steering

Steering and handling characteristics of road vehicle are concerned with its response to steering commands that affect its direction of motion. Depending on tire characteristics, a steering input introduces lateral or cornering forces at the tire-road interface. The cornering force characteristics are strongly influenced by the normal force at the contact patch. On the other hand, the roughness of a pavement directly influences the normal forces that act at the tire-pavement interface. The roughness can further alter the surface friction, which in turn will change the cornering force characteristics of the tire. Road roughness can therefore, has a complex influence on the overall steering performance of the vehicle.

A driver guides the vehicle down the road by a series of understeer and oversteer inputs. This allows the driver to maintain the vehicle in the desired position on the roadway and to make adequate turns, lane changes, and other maneuvers necessary to traverse the roadway safely. As a result of steering inputs and corrections, lateral forces are generated between the tire and pavement. These are the forces that act parallel to the road and at right angles to the axis of the wheel plane. As a result of this side force, and tire deflection there exists an angle between the wheel plane and direction of motion. The angle α usually referred to, as slip-angle is a phenomenon of side slip primarily associated with lateral elasticity of the tire. The magnitude of the lateral force that acts at the tire-road interface is dependent on the normal force exerted by the tire and slip angle. This is usually not a linear relation, and thus changes in loading can have notable effects on the steering input necessary for a particular maneuver. Figure 2.5 shows typical relationship among slip angle, normal force, and lateral forces. The relationship shown is for reasonable level of friction and is strongly influenced by the available friction. Slippery pavement would greatly reduce the values of the lateral force that can be generated for a given slip angle. The characteristics shown in Figure 2.5 demonstrate highly nonlinear relationship between the normal load and lateral forces for commonly encountered ranges of slip angles (4 to 10 degrees). For slip angle of 6 degrees, if the normal force is increased by 1500 N from a nominal force of 4500 N, the lateral force will only be increased by 700 N from 3500 N. This is extremely important to note in evaluating the influence of roughness since pavement roughness can easily cause the normal force to fluctuate. On relatively smooth pavements, the variation in normal force may be very small, these variations can be quite significant on rough pavements, which

may lead to considerable variation in lateral force available to control the vehicle. In situations where high lateral forces are necessary or where vehicle requires a particular lateral friction level to under take a maneuver, this loss of force could lead to loss of control of the vehicle.

A lot of research has been done in this area. Quinn and Hildebrand [39] reported on the various factors that can affect the lateral force developed by a tire. The study presented the side slip and steer angle necessary to make a 90 degrees turn on smooth and rough pavements. It has been shown that the steering inputs required for this maneuver on a smooth surface is significantly different than that required on a rough surface. During turning operation, the driver is required to conduct greater steering angles to compensate for the loss of lateral force. The non-uniformities in the road roughness, however, pose excessive demands on the steering performance of the driver. As the driver progresses down the highway and encounters a smoother section of the pavement, the driver often oversteers in order to make appropriate corrections. If this happens too frequently, the driver cannot respond rapidly enough and may lose control of the vehicle. Possible influences of road roughness on the directional response measures of an articulated vehicle are examined in the following sections through simulations carried out in this investigation. The influence of road roughness on the front wheel steer angle of the tractor is shown in Figure 4.1.

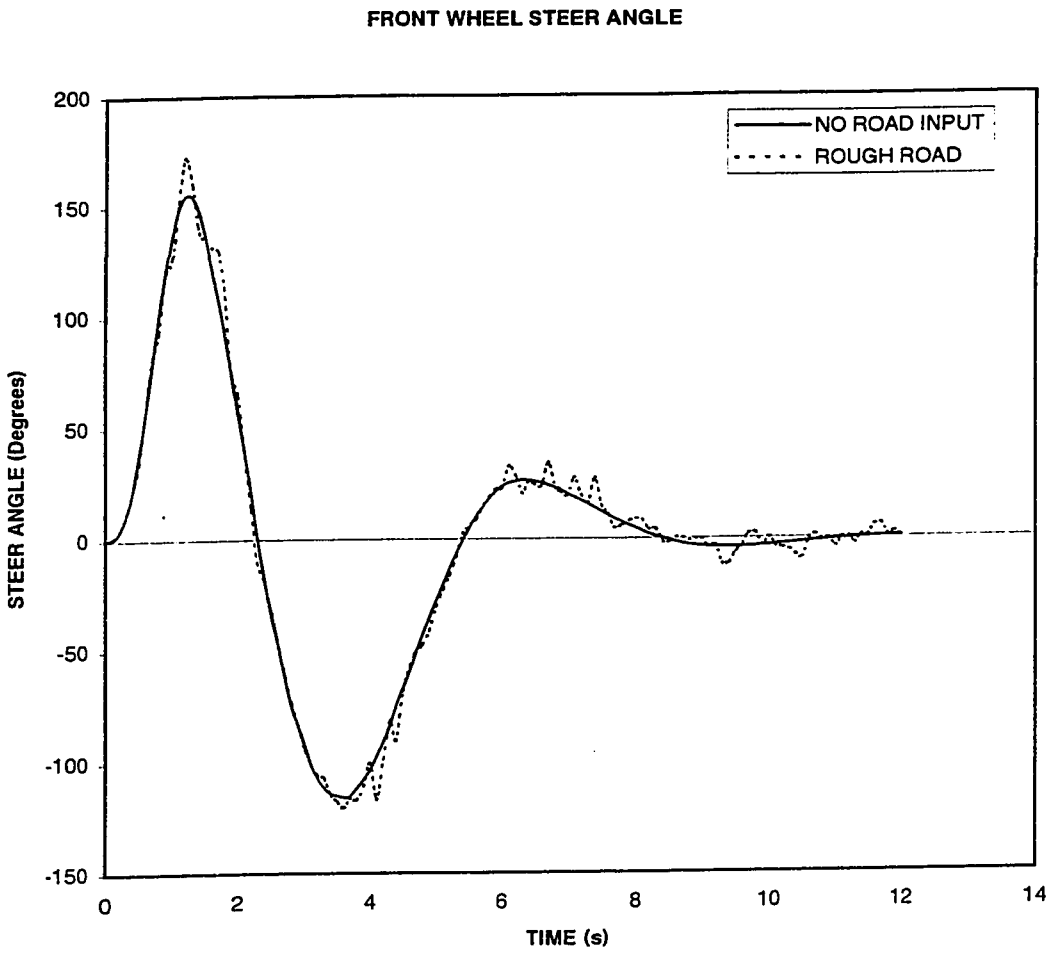

Figure 4.1: Tractor front wheel steer angle during single lane change maneuver at 100 km/h.

4.3 Influence of Road Roughness on Directional Performance

Simulation results are obtained at the different speeds namely: 70, 100 and 120 km/h. Under single and double lane change, turning and path change maneuvers. The simulations are carried out for these different road roughnesses and in the absence of road roughness. The various simulations are presented in a simulation matrix discussed in section 3.4. The most prominent factor that can be easily visualized during the single and double lane change maneuvers is the lateral acceleration of the tractor and the trailer.

The roll and yaw stability limits of heavy vehicles have been related to its lateral acceleration response. The rollover limits of heavy vehicles undergoing steady-turns and highway maneuvers are of invariably expressed in terms of static and dynamic rollover thresholds, respectively. The rollover threshold is the limiting value of lateral acceleration encountered in a steady turn, which the vehicle can withstand. The dynamic rollover threshold has been related to effective lateral acceleration of the vehicle under a transient directional maneuver [35]. The first sets of results are thus obtained to examine the levels of lateral acceleration experienced by the tractor and trailer under single and double lane change maneuvers. Figures 4.2 and 4.3 illustrates the time history of lateral acceleration response of tractor and semitrailer, respectively, when the vehicle is subject

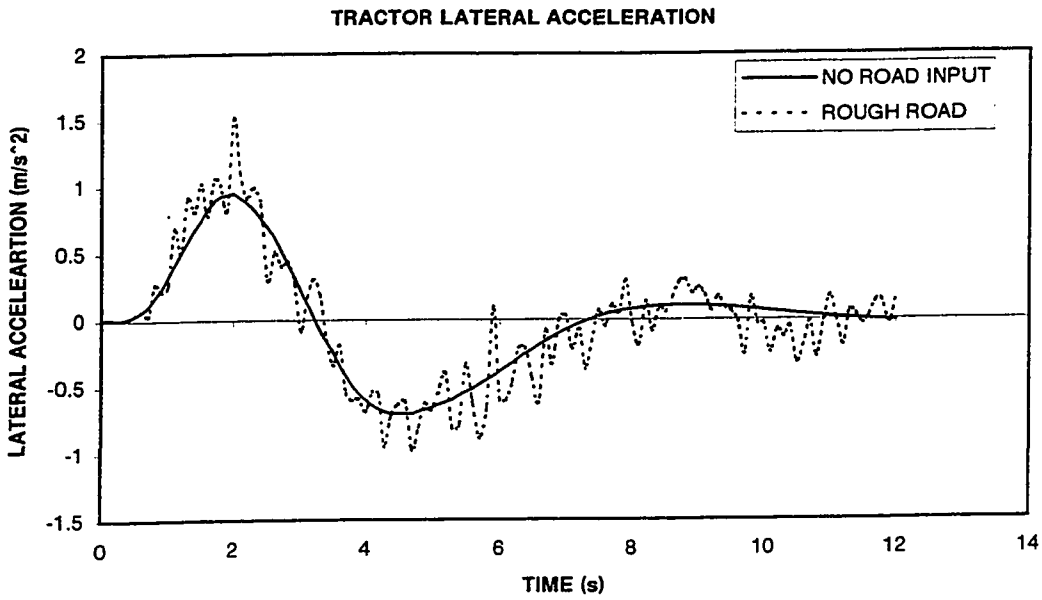

Figure 4.2: Lateral acceleration of tractor during single lane change maneuver at 70 km/h.

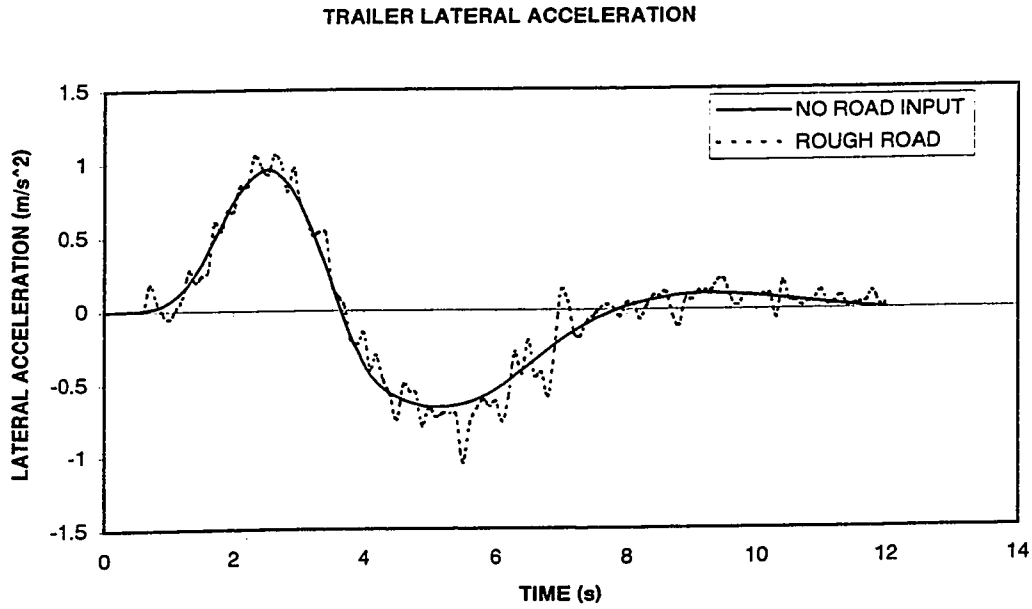

Figure 4.3: Lateral acceleration of trailer during single lane change maneuver at 70 km/h.

to a lane change maneuver at a speed of 70 km/h. The figures illustrate the comparison of lateral acceleration response obtained under rough and perfectly smooth road. It is observed that the peak lateral acceleration of the tractor increases by 50% due to the rough road roughness. However, the trailer peak lateral acceleration increases by 30%, which clearly indicates the influence of road roughness on the lateral acceleration of both tractor and trailer. The peak lateral acceleration response obtained under different maneuvers, speeds and road roughness conditions are derived and summarized in Table 4.1. The results clearly show considerable influence of road roughness on the peak lateral acceleration. The results, however, do not exhibit a definite trend, which may be attributed to random vibrations in the local elevations of the road. Based on the lateral acceleration response of the two units, certain inferences described below are made:

Under any given road condition, the peak lateral acceleration of the tractor and trailer increase with increase in vehicle speed during single and double lane change maneuvers, irrespective of road roughness. The peak lateral acceleration increases by 60% - 100%, when the speed is increased from 70 to 100 km/h. The relative increase in peak lateral acceleration is not as significant, when the speed is further increased to 120 km/h. At any given speed, the lateral acceleration level of both tractor and trailer, in general increase with deterioration of the road. During a single lane-change performed at 70 km/h, the peak lateral accelerations of tractor and semitrailer encountered on a rough road by over 50% and 5 % respectively. The increase in lateral acceleration due to road roughness at high speeds and under evasive maneuvers is not as significant. The results shown in Table 4.1 show one variation from the above observation. It shows that at very

high speed (120 km/h) the road roughness has the least influence on the lateral acceleration and that the lateral acceleration at this speed may be less on rough road than those on smooth road. This discrepancy may be attributed to the cross-slope or roll deflection caused by the roughness at two tracks, and the spectral components of roll excitations.

Table 4.1: Comparison of peak lateral acceleration of tractor and semitrailer subject to single and double lane change maneuvers at different speeds and road conditions.

SPEED (km/h)	ROAD INPUT	SINGLE LANE CHANGE MANEUVER		DOUBLE LANE CHANGE MANEUVER	
		TRACTOR a_{y1} (m/s^2)	TRAILER a_{y2} (m/s^2)	TRACTOR a_{y1} (m/s^2)	TRAILER a_{y2} (m/s^2)
70	NONE	0.946	0.934	1.1	1.06
	SMOOTH	0.943	0.924	1.1	1.09
	MEDIUM	1.01	0.959	1.14	1.07
	ROUGH	1.47	0.967	1.33	1.14
100	NONE	1.62	1.67	1.83	2.23
	SMOOTH	1.61	1.64	1.89	2.241
	MEDIUM	1.69	1.691	1.89	2.24
	ROUGH	1.87	1.77	1.9	2.23
120	NONE	1.671	1.732	1.91	2.33
	SMOOTH	1.692	1.74	1.92	2.32
	MEDIUM	1.73	1.832	1.935	2.316
	ROUGH	1.645	1.829	1.948	2.311

4.3.1 Rearward Amplification Factor

The rearward amplification factor (RWA) is a frequency dependent measure, defined as the ratio of the peak (positive or negative) lateral acceleration at the center of gravity of the rearmost trailer to the amplitude of controlled lateral acceleration of 0.15g at the center of the front axle of the lead unit (tractor). In this investigation, a given path is followed by the vehicle at different speeds and the RWA is defined as the ratio of the peak lateral acceleration at the c.g. of tractor and trailer. Further to RWA, results are obtained in terms of roll angle experienced by tractor and trailer and their ratio. Results are obtained for single and double lane change maneuvers as well as for turning and path change maneuvers.

It should be noted that the path followed by the vehicle is not exactly as it is defined by the maneuvers shown in chapter 3. Then path followed by a vehicle is a complex function of the speed, vehicle configuration, driver preview interval and transport lag and severity of the path. Many studies have concluded that the driver preview interval varies significantly with vehicle speed, a definite pattern however is not yet identified due to lack of knowledge on the complex driver- vehicle interactions. In this study, the preview interval was varied from 0.3 to 2.0 s in order to achieve minimal path error at different speeds. Figure 4.4 illustrates a comparison of the desired path with the vehicle under different speeds.

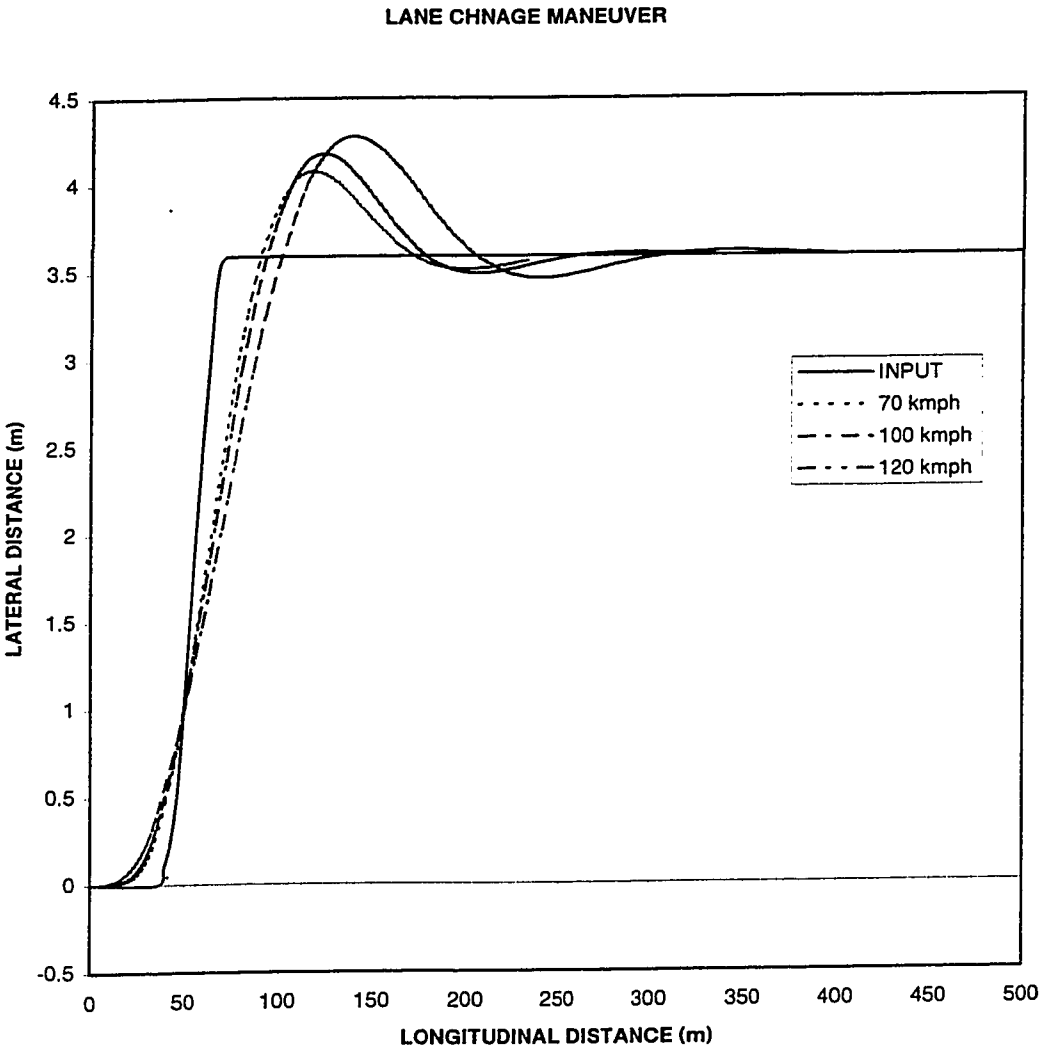

Figure 4.4: Comparison of path followed by the vehicle at different speeds with the input trajectory.

Case I: Single lane change maneuver

The vehicle is subjected to single lane change maneuvers at 70, 100 and 120 km/h under the influence of no road, smooth, medium and rough road inputs. The results are analyzed to derive the peak lateral accelerations and roll angles of the sprung masses. The lateral acceleration and roll angle rearward amplification factors are computed and presented in Figure 4.5. It is observed that at low speeds the influence of road input on rearward amplification of lateral acceleration is pronounced especially under medium and rough roads. In comparison to no road input, the road roughness reduces the amplification factor by 10% and 40% under medium and rough roads, respectively, which in turn enhances stability of the vehicle. But at higher speeds, the influence of road roughness diminishes as the speed of the vehicle gains importance in dictating the level of lateral acceleration. Under single lane change maneuver, as it is shown in Table 4.1, the influence of road roughness reduces considerably at higher speeds. At high speeds, the trailer acceleration grows at relatively higher rate than that of the tractor resulting in amplification of lateral acceleration. The results presented as roll angle amplification factor in Figure 4.5, on the other hand, show negligible influence of both road roughness and forward velocity. This can be partly attributed to the cross slope of the road and the roll flexibility of the articulation mechanism. The roll angle rearward amplification response of the vehicle subject to single lane-change at 70 km/h and rough road condition is considerably lower than that encountered under perfectly smooth road. This discrepancy is most likely attributed to the cross-slope of the road, which tends to counter the roll deflection of the dominant trailer sprung mass. The rearward amplification, however, tends to exceed the value for perfectly smooth road at higher speeds.

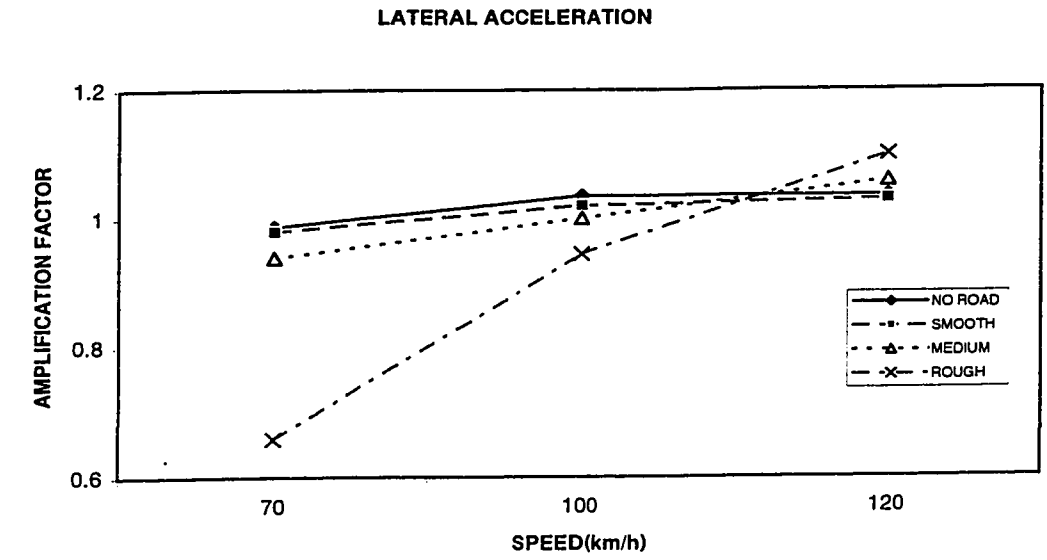

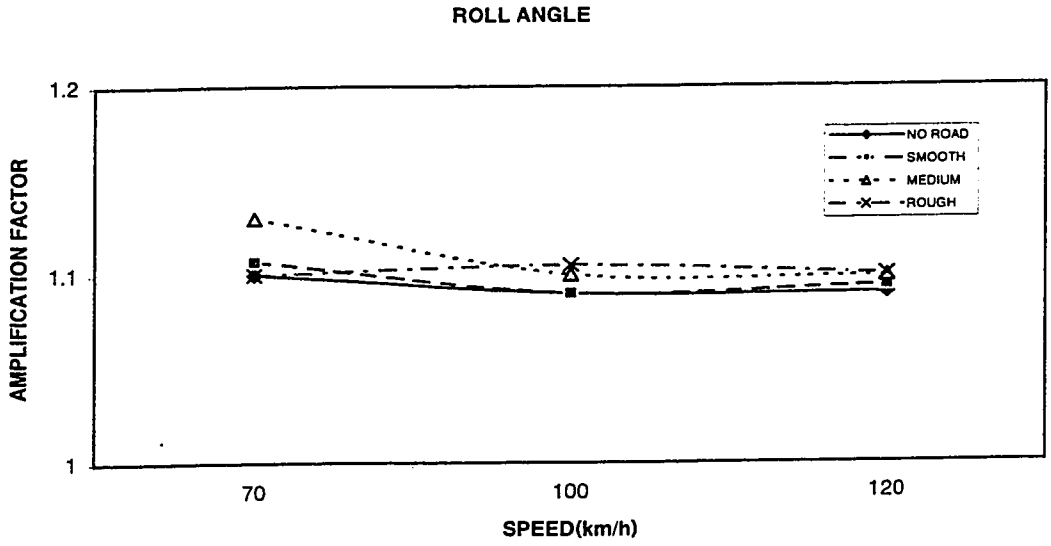

Figure 4.5: Lateral acceleration and roll angle rearward amplification factors during a single lane change maneuver.

Case II: Double lane change maneuver

The vehicle is subjected to undergo double lane change maneuvers at the specified three speeds and road conditions. The results in terms of lateral acceleration and roll angle amplification factors are presented in Figure 4.6. In case of double lane change, the lateral acceleration attained by both the tractor and the semitrailer are relatively higher than those experienced during the single lane change maneuver. It is evident that the influence of road roughness in this case is more evident through out the speed range. The results show that in comparison to no road input, rough road reduces the lateral acceleration amplification factors by 30% at 70 km/h and by 10% at 120 km/h. The peak lateral acceleration encountered on a rough road, however, tends to be higher, as evident from Table 4.1. The roll angle amplification factor under double lane change maneuver, shown in Figure 4.6, indicate greater sensitivity to speed in comparison to single lane change response. In general the roll amplification factor reduces slightly as speed is increased, where influence of road roughness is not very significant.

Case III: Path-change maneuver

The results obtained from the vehicle subjected to path change maneuver presented in Figure 4.7. These results in terms of lateral acceleration and roll angle amplification factors are obtained for 100 km/h. This maneuver is simulated in order to verify the performance measures suggested by M.El-Gindy [21]. The results clearly show that the influence of road roughness on the amplification factors for lateral acceleration and the roll angle is relatively small.

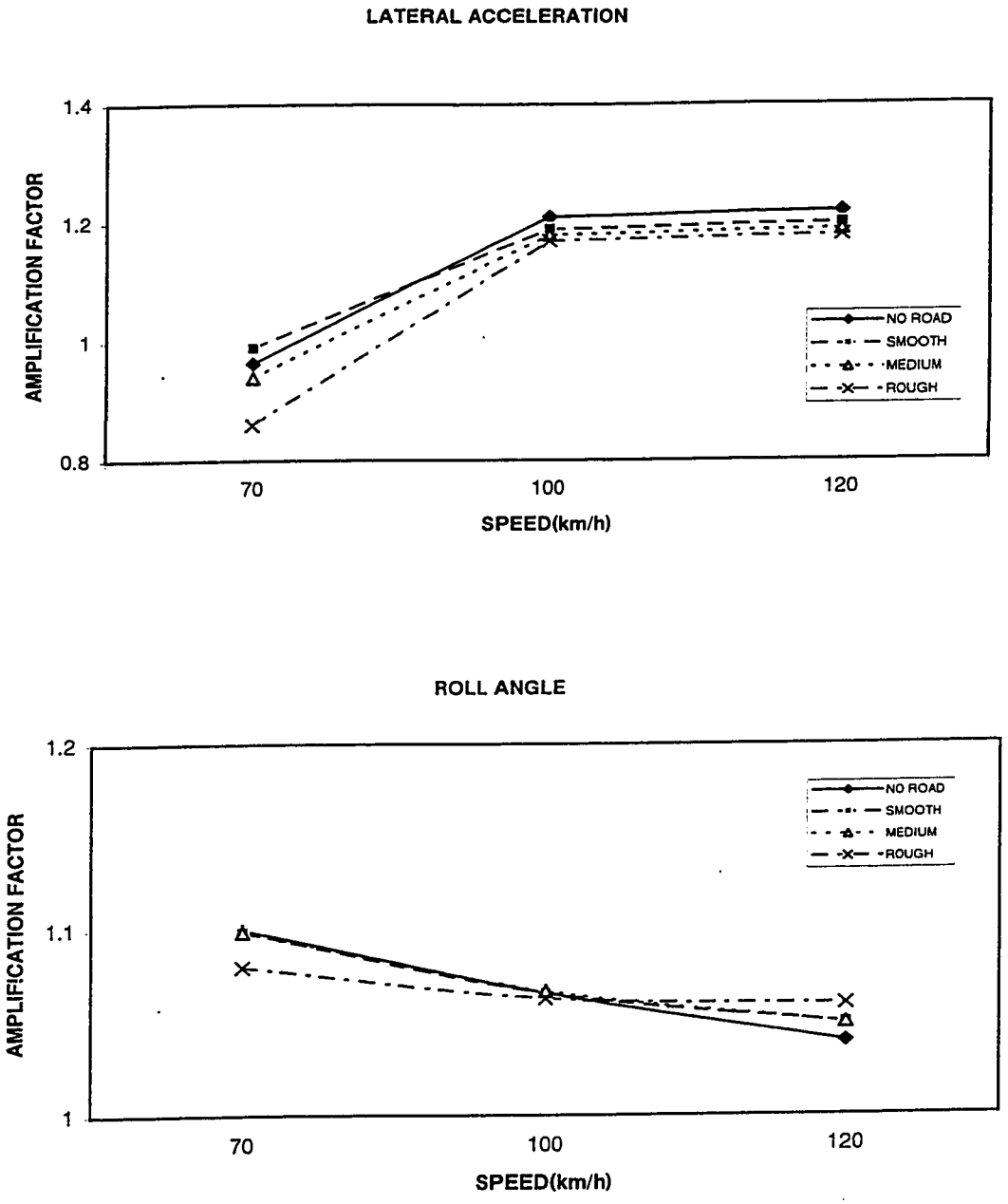

Figure 4.6: Lateral acceleration and roll angle rearward amplification factors during a double lane change maneuver.

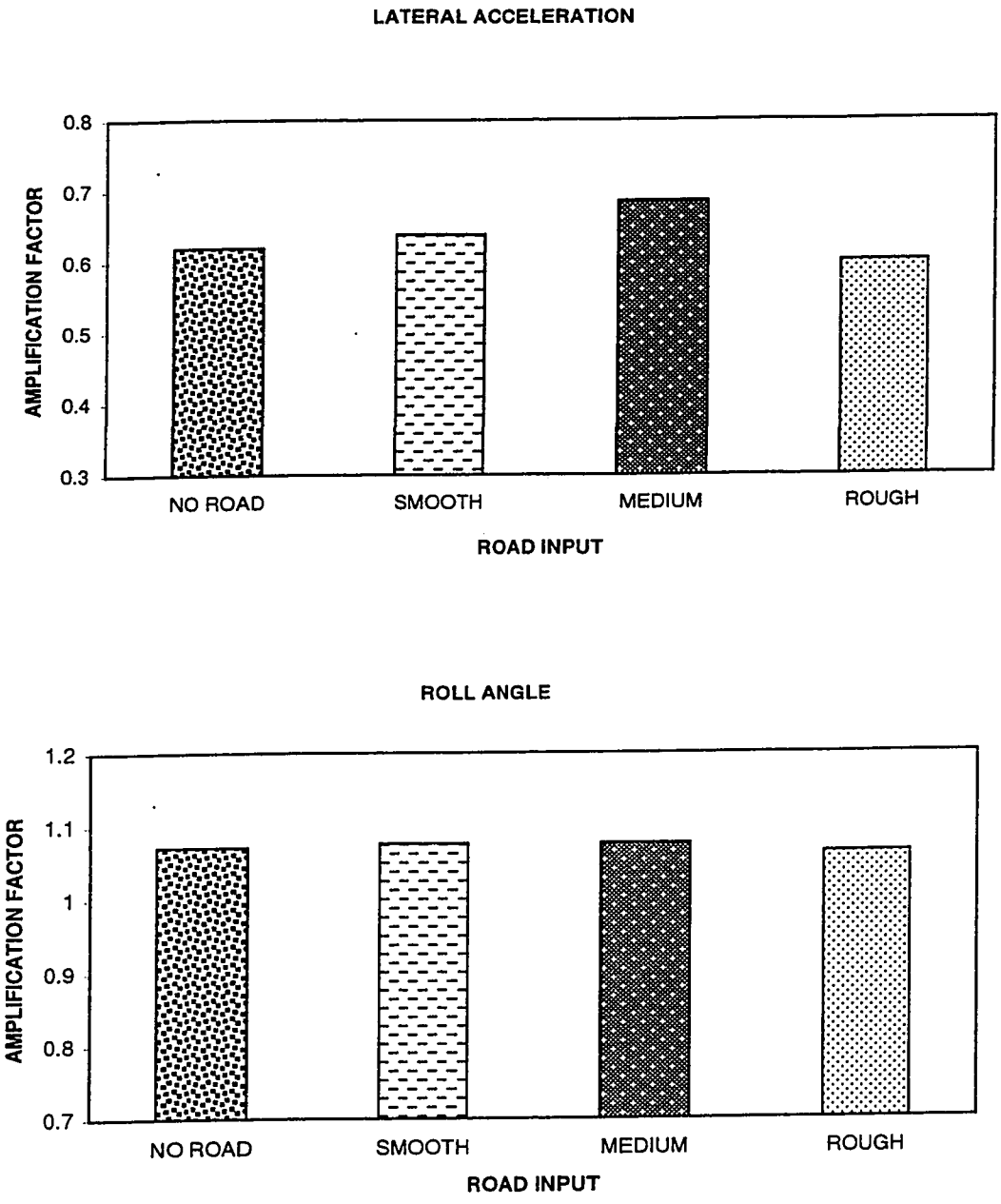

Figure 4.7: Lateral acceleration and roll angle rearward amplification during a path-change maneuver.

Case IV : Turning maneuver

Turning is a maneuver required to negotiate a shallow turn and is typically performed at relatively slow speeds. Simulation results are computed in terms of lateral acceleration and roll angle amplification factors under different road inputs at a speed of 50 km/h. Because of slow speed and shallow turn, the lateral acceleration amplification ratio is less than 1.0 for all road inputs. As the results show, there is no definite trend with respect to the level of road roughness, and there is a 10 % reduction in the lateral acceleration amplification factor for rough road in comparison to no road input. The results Figure 4.8 further show no influence of road roughness on the roll angle amplification factor which varies between 1.0 and 1.07. The results show trends similar to those observed under transient single- and double- lane change maneuvers.

4.3.2. Load Transfer Ratio

The load transfer ratio (LTR) is defined as the ratio of the absolute value of the difference between the sum of the right wheel loads and sum of the left wheel loads, to the sum of the wheel loads. The LTR is frequently used as a measure for the dynamic roll stability of the vehicle. The LTR value of 1.0 corresponds to loss of wheel/road contact in one side of the vehicle. Depending on the speed and maneuver, the LTR value may vary between 0 and 1.

It is recommended that the peak LTR value in a given maneuver remains below 0.6 [21]. The articulated heavy vehicle is considered to undergo different maneuvers at

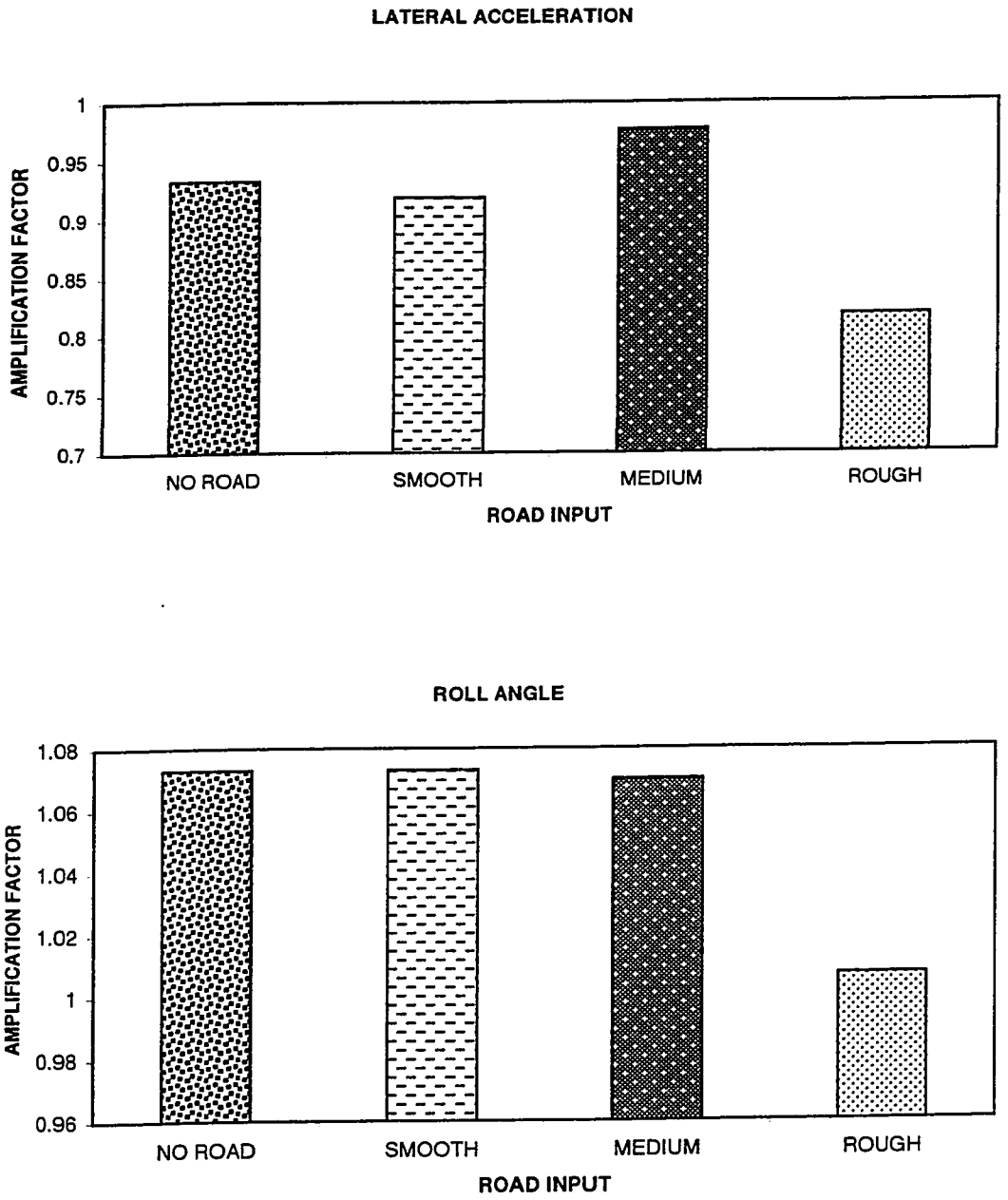

Figure 4.8: Lateral acceleration and roll angle rearward amplification factors during a turning maneuver.

different speeds under different road conditions. The simulated results are analyzed to derive the load transfer ratio under different maneuvers, which are discussed below.

Case I : Single lane change maneuver

The LTR values are obtained for each axle under single lane change maneuver and four different road inputs. The results at 70, 100 and 120 km/h for axle no. 2 to 5 are presented in Figure 4.9. It is evident from the results, that LTR and thus the roll stability of vehicle is strongly influenced by the road roughness for range of roads and speeds considered. These results show that the LTR remains within the prescribed limit of 0.6 for all axles of the vehicle traversing smooth and medium roads only at 70 km/h. For speeds of 100 and 120 km/h axles 3, 4 and 5 rapidly approach instability (LTR = 1.0). The results for all axles show a profound effect of very rough road on the level of LTR. For the vehicle configuration under single lane change maneuver, it can be considered notable at 70 km/h and beyond when operated on rough road. A vehicle considered to exhibit an acceptable value of LTR (< 0.6) under a perfectly smooth road may reveal unstable behavior on rough roads. It is thus vital to examine the roll stability measures under representative road roughness conditions. It has been established that the roll instability, in-general, is initiated at the trailer axles. The instability propagates towards the tractor drive axles due to large inertia associated with the trailer. An examination of the LTR response of the axle 5 reveals that the LTR under rough roads exceeds that under perfectly smooth roads by over 20% to 100%, depending upon the vehicle speed.

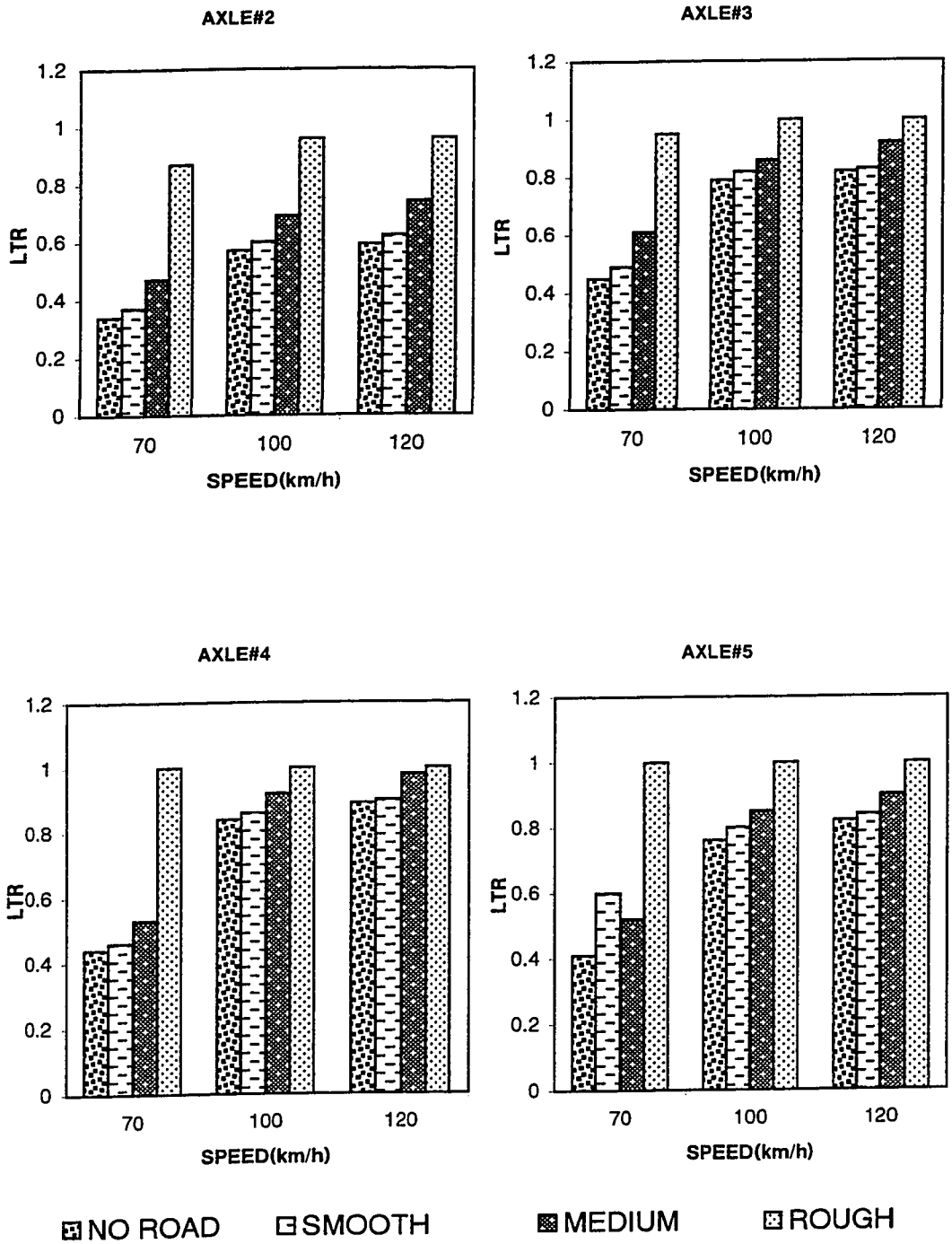

Figure 4.9: Load transfer ratio of different axles during a lane change maneuver.

Case II : Double lane change maneuver

Similar to the single lane change, the LTR values are next obtained under a double lane change maneuver. The LTR response of axle 2 to 5 in the speed range is shown in Figure 4.10. The results at 70 km/h reveal significant influence of road roughness similar to that observed for a single lane change. The vehicle approaches rollover condition (LTR = 1.0) at higher speeds, irrespective of the road roughness. Again the vehicle is found to be stable for up to medium road where LTR value is within 0.6 for all axles. Then vehicle is clearly unstable for rough road even at 70 km/h the influence of rough road on the values of LTR at higher speed cannot be evaluated since the vehicle is not stable even on smooth under no road inputs.

Case III : Path-change maneuver

Unlike turning maneuver, the path change maneuver is very severe as it is performed at 100 km/h. During the path change maneuver the load transfer ratio is also found to be quite severe, as shown in Figure 4.11. The LTR values in this case are more than those obtained from single lane change maneuver at 100 km/h. This can be attributed to the fact that is path change maneuver, the vehicle follows exactly the path given as input. In this case the driver transport lag and preview interval are selected as .05 and 0.3 respectively.

Case IV: Turning maneuver

Under low speed turning maneuver the lateral acceleration and resulting LTR values are considerably lower. The LTR values at speed of 50 km/h for axles 2 to 5 are shown in Figure 4.12. It is evident that at this speed, the drive axles experience very meager

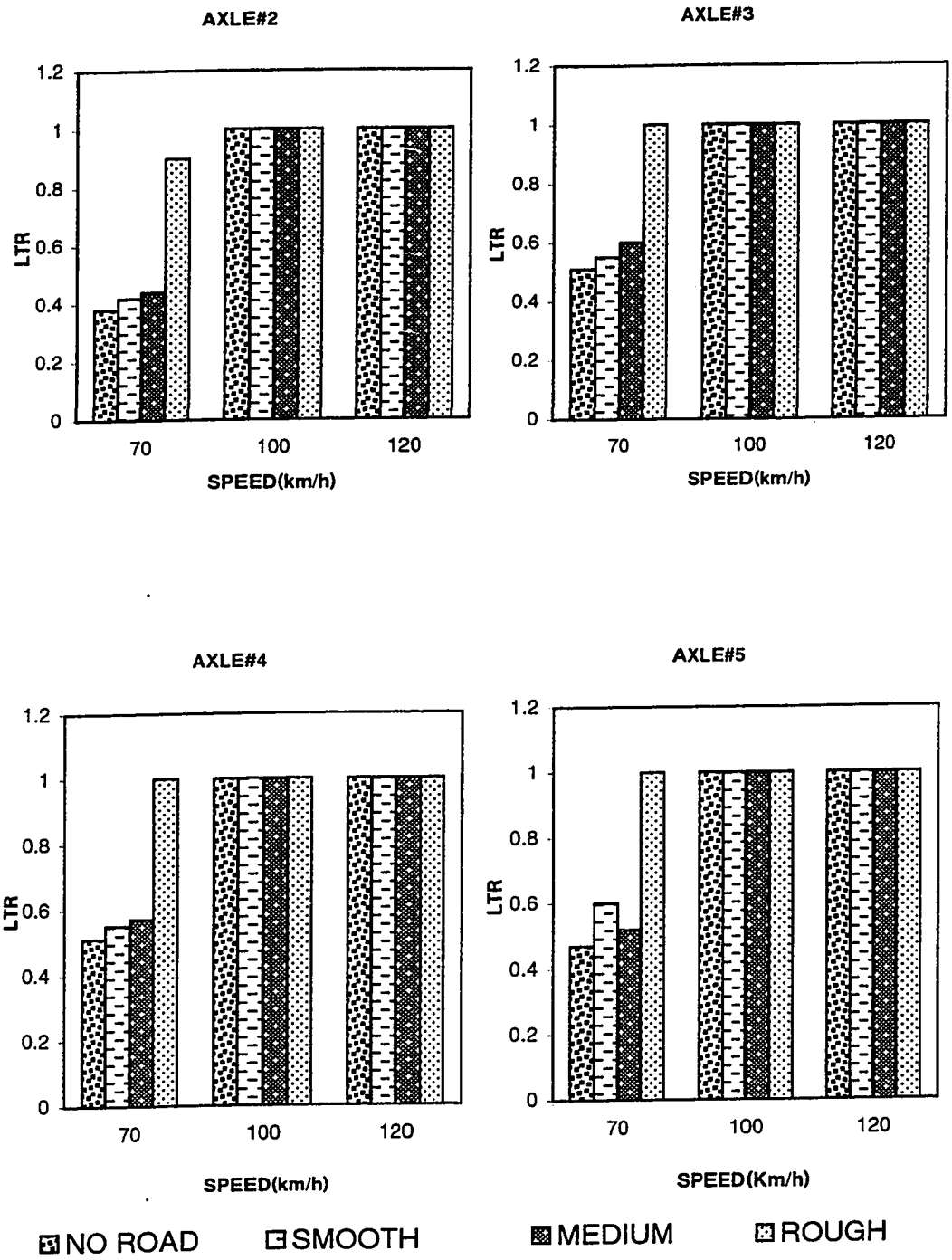

Figure 4.10: Load transfer ratio of different axles during a double lane change maneuver.

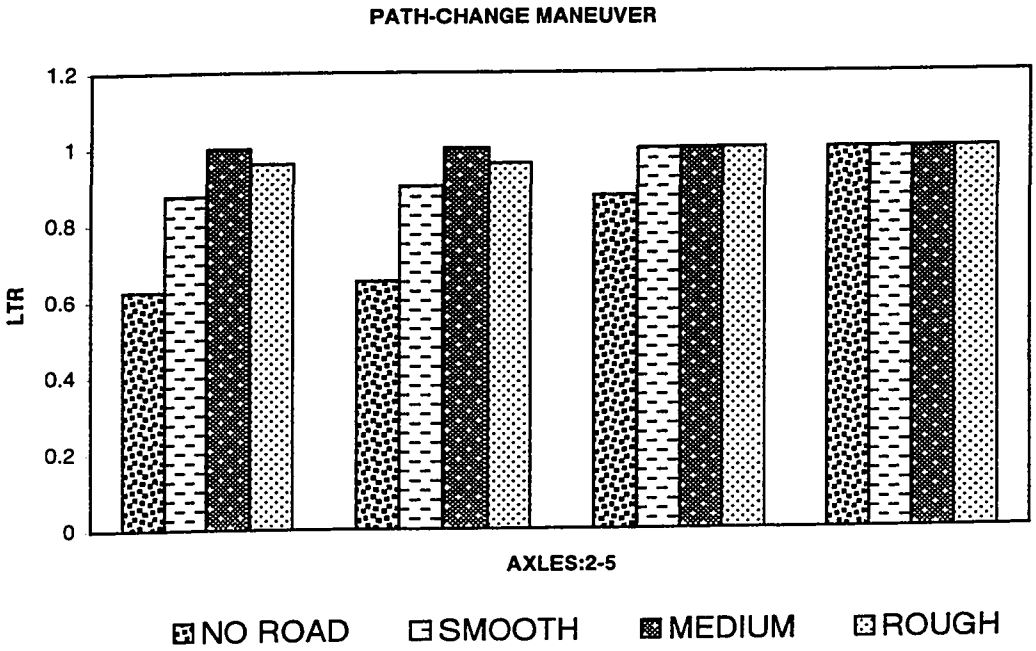

Figure 4.11: Load transfer ratio of different axles during a path-change maneuver.

transfer of load, whereas the trailer axles experience considerable load transfer which, however, remain within the limiting value of 0.6. The effect of road roughness under such maneuver, as shown in the Figure 4.12, is not highly significant. The LTR of trailer axles may increase in the order of 16% under rough roads.

4.3.3 Handling Diagram

Handling diagram is an effective measure to examine the influence of vehicle and operating parameters on the steering characteristics and handling performance. In this section, the handling diagrams are obtained from the tractor semitrailer under various road inputs. In a diagram, the vehicle lateral acceleration in g-units, a_y /g which is same as (U^2/gR), is plotted as function of the steering parameter (L/R - δ), where L is the wheelbase, R is the turning radius, and δ is the average front wheel steer angle. During a turning maneuver, the turning radius R may be difficult to measure directly. However, it can be readily determined from the yaw velocity (r_1) and the forward speed U of the vehicle ($R = U/r_1$). The handling diagram, therefore can be expressed as a plot of lateral acceleration in g-units, a_y/g Vs a parameter based on ($r_1 L/U - \delta$). The slope of the curve in the handling diagram describes the understeer coefficient of the vehicle:

$$\frac{d(a_y/g)}{d(r_1 L/U - \delta)} = -\frac{1}{K_{us}} \tag{4.1}$$

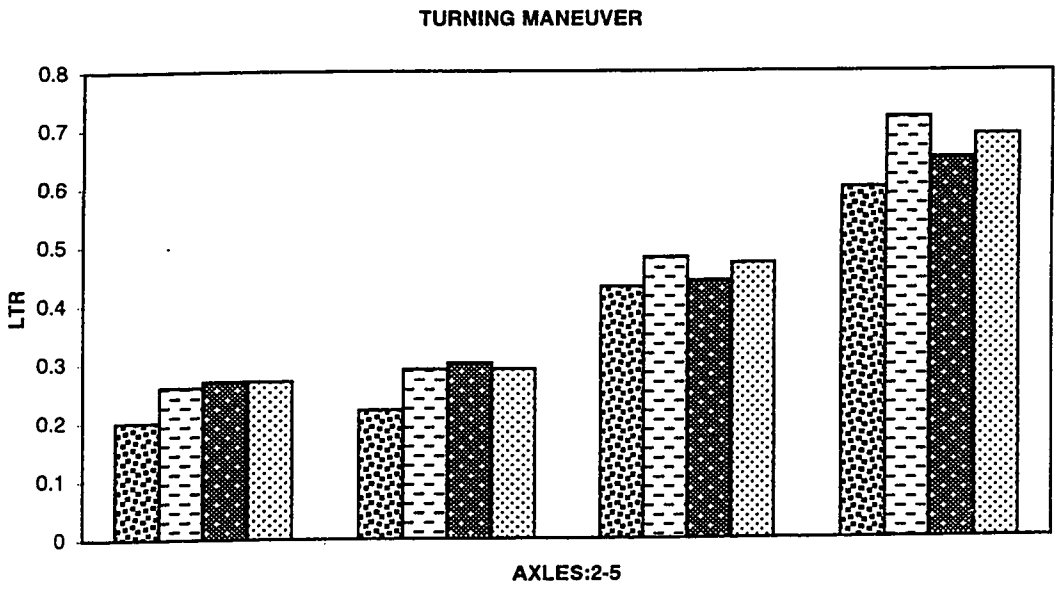

Figure 4.12: Load transfer ratio during a turning maneuver.

A negative slope of the curve implies a positive value of the K_{us} and thus understeer behavior of the vehicle. While an infinite slope refers to neutral steer, the positive slope reveals oversteer vehicle response. The road vehicles are known to be unconditionally stable for $K_{us} > 0$, and may exhibit instabilities for $K_{us} < 0$ at speeds above the critical speed. The handling performance of the combination may be examined using the equations of steady-state handling of the tractor and semitrailer [22]. The equation of steady-state handling for the tractor may be expressed as:

$$\delta = \frac{L_t}{R} + K_{ust}\frac{U^2}{gR} \tag{4.2}$$

where L_t is the wheelbase of the tractor and K_{ust} is the understeer coefficient of the tractor. For most of the tractor-semitrailers, the fifth wheel is located slightly ahead of the center of the tractor rear axle. With this assumption, the tractor rear tire may be considered as the 'steered tire' for the semitrailer, and the articulation angle γ between the tractor and the semitrailer may be expressed by:

$$\gamma = \frac{L_s}{R} + K_{uss}\frac{U^2}{gR} \tag{4.3}$$

where L_s is the wheelbase of the semitrailer and K_{uss} is the understeer coefficient for the semitrailer. The ratio of the articulation angle and the steer angle of the tractor, often referred to as the articulation gain, is frequently used to examine the handling behavior of articulated vehicles:

$$G_z = \frac{\gamma}{\delta} = \frac{L_s / R + K_{uss}(U^2 / gR)}{L_t / R + K_{ust}(U^2 / gR)} \tag{4.4}$$

the yaw divergence of the trailer with respect to the tractor is directly obtained from the articulation gain G_z, which is strongly dependent upon the understeer coefficients, K_{ust} and K_{uss}. The articulation gain remains finite over the entire range of speeds, when both $K_{ust} > 0$ and $K_{uss} > 0$. An oversteer trailer ($K_{uss} < 0$) coupled with understeer tractor ($K_{ust} > 0$) also yields finite value of G_z. The articulation gain, however, approaches negative values, when forward speed exceeds the critical speed of the trailer, given by:

$$U_{cr} = \sqrt{\frac{gL_s}{|-K_{uss}|}} \tag{4.5}$$

Where U_{cr} is the critical speed of the trailer. The vehicle approaches definite instability, when tractor is oversteer ($K_{ust} < 0$) and the vehicle speed approaches its critical speed, given by:

$$U_{cr} = \sqrt{\frac{gL_t}{|-K_{ust}|}} \tag{4.6}$$

Where U_{cr} is the critical speed of the tractor. An examination of Equation (4.6) reveals that the articulation gain approaches infinite at speeds approaching the critical speeds leading to vehicle jackknife. The jackknife potential of the vehicle can be further observed for both units being oversteer ($K_{uss} < 0$ and $K_{ust} < 0$), specifically when

$$\frac{K_{uss}}{K_{ust}} < \frac{L_s}{L_t} \tag{4.7}$$

the results of the above analysis indicate that for any form of directional instability (jackknifing or trailer swing) to occur, the tractor must be oversteer. Jackknifing can occur when the semitrailer is either understeer or oversteer. However, for trailer swing to occur, in addition to the condition that the semitrailer must be oversteer, it is required that the ratio of the understeer coefficient of the semitrailer to that of a tractor be greater than the ratio of the semitrailer wheelbase to the tractor wheelbase.

Using the above criteria, the stability of tractor semitrailer can now be examined under different levels of road inputs. The results are analyzed using three-point measure discussed in chapter 3.

Case I : No road input (perfectly smooth surface)

The vehicle response is evaluated under a ramp steer input and the results are utilized to determine the slope of the handling curves in the presence of varying road roughness. In the absence of road input, the handling diagram of the tractor and details are presented in Figure 4.13. The figure further presents the understeer coefficients of tractor and trailer as a function of lateral acceleration. The results clearly show that the vehicle satisfies the 'first point' in the three-point measure discussed earlier. The understeer coefficient value stays above 2.0 degrees corresponding to a lateral acceleration level of 0.15 g. This indicates hypersensitivity condition experienced by the driver [21]. The recommendation given in the first point is for a particular vehicle configuration. The need for second and

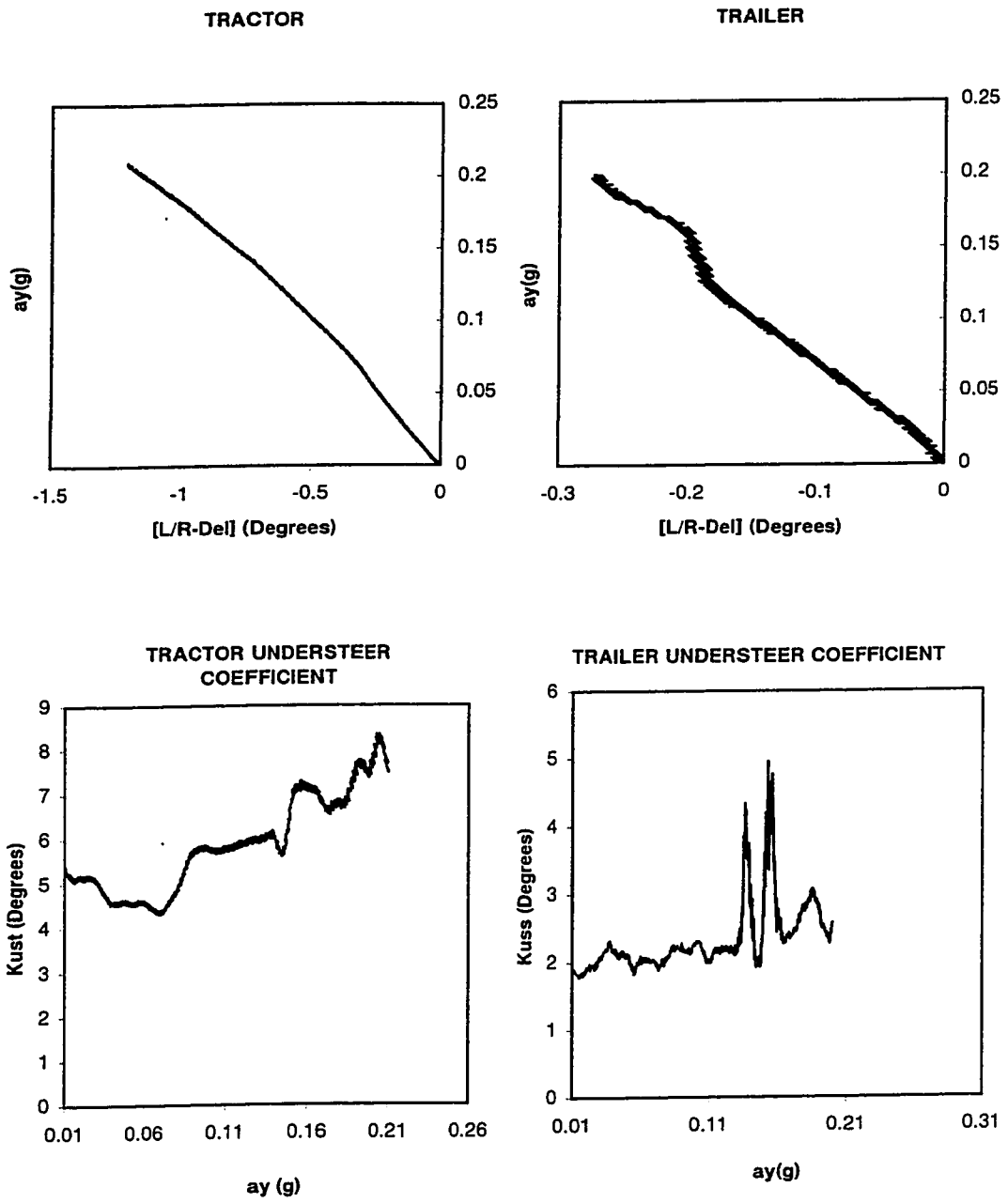

Figure 4.13: Handling diagram and understeer coefficient of tractor and semitrailer under no road input.

third point does not arise since the vehicle stays understeer through out the range of measures. The vehicle is also considered to be stable in terms of jackknife and trailer swing, since both units exhibit understeer behavior ($K_{uss} > 0$; $K_{ust} > 0$).

Case II : Smooth road

Tractor and trailer handling diagrams along with variation in understeer coefficients under smooth road inputs are shown in Figure 4.14. The vehicle exhibits understeer characteristics throughout the range of maneuvers and is hence stable and thus stable behavior. The understeer coefficient of the trailer, however, reduces to 0.5 degrees corresponding to 0.14g lateral acceleration.

Case III : Under Medium rough road

The handling diagram of the vehicle subject to a medium rough road is shown in Figure 4.15. Under the influence of medium rough road, the tractor behaves as an understeer vehicle through out the simulation, the trailer characteristics change to oversteer corresponding to a lateral acceleration level of 0.2 g. Further examination of results revealed that the trailer characteristics shifts back to understeer from oversteer in less than a second. An examination of the yaw rates of tractor and trailer further revealed that the trailer yaw rate remains well below the tractors preventing from trailer swing or jackknife.

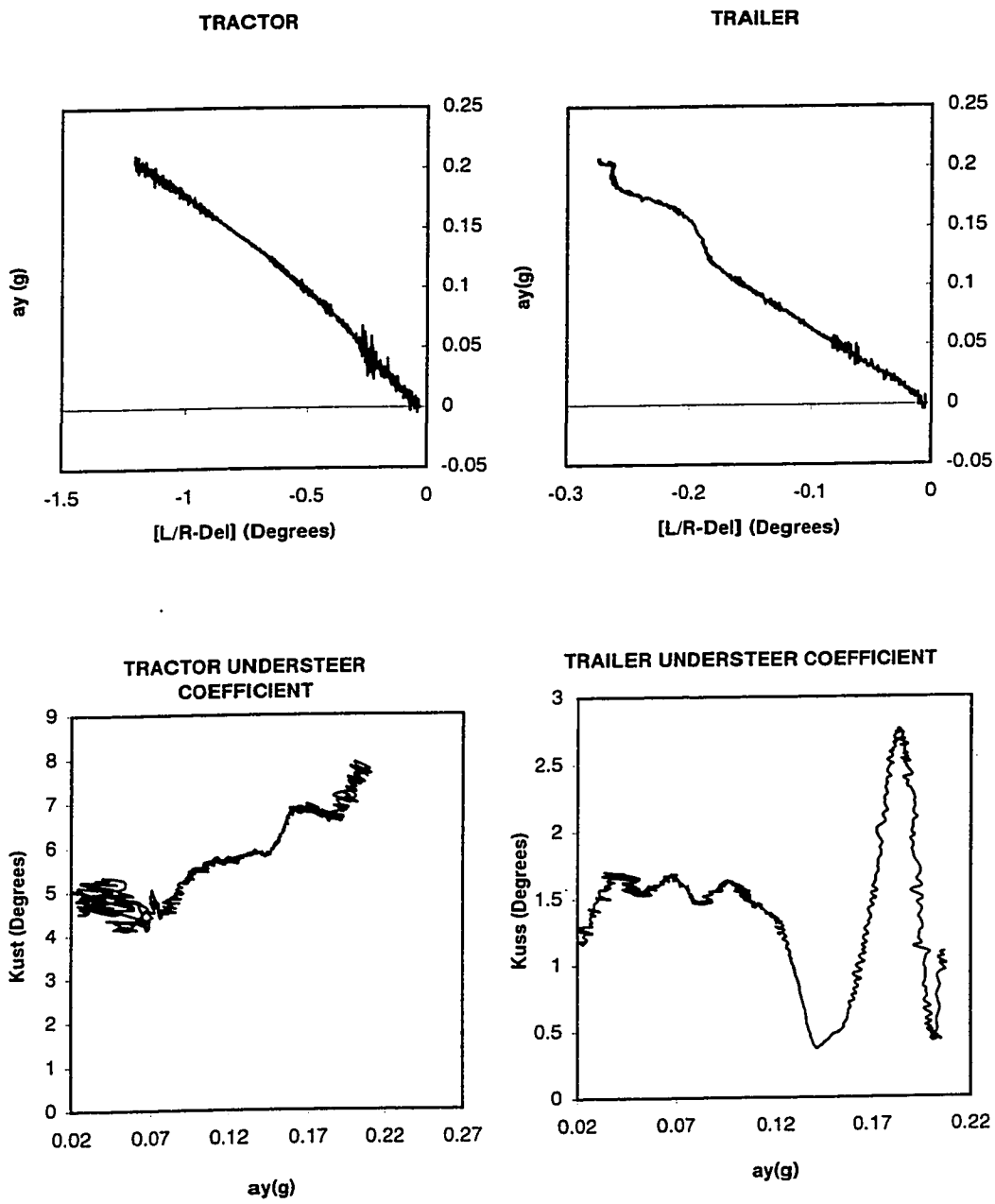

Figure 4.14: Handling diagram and understeer coefficient of tractor and semitrailer under smooth road input.

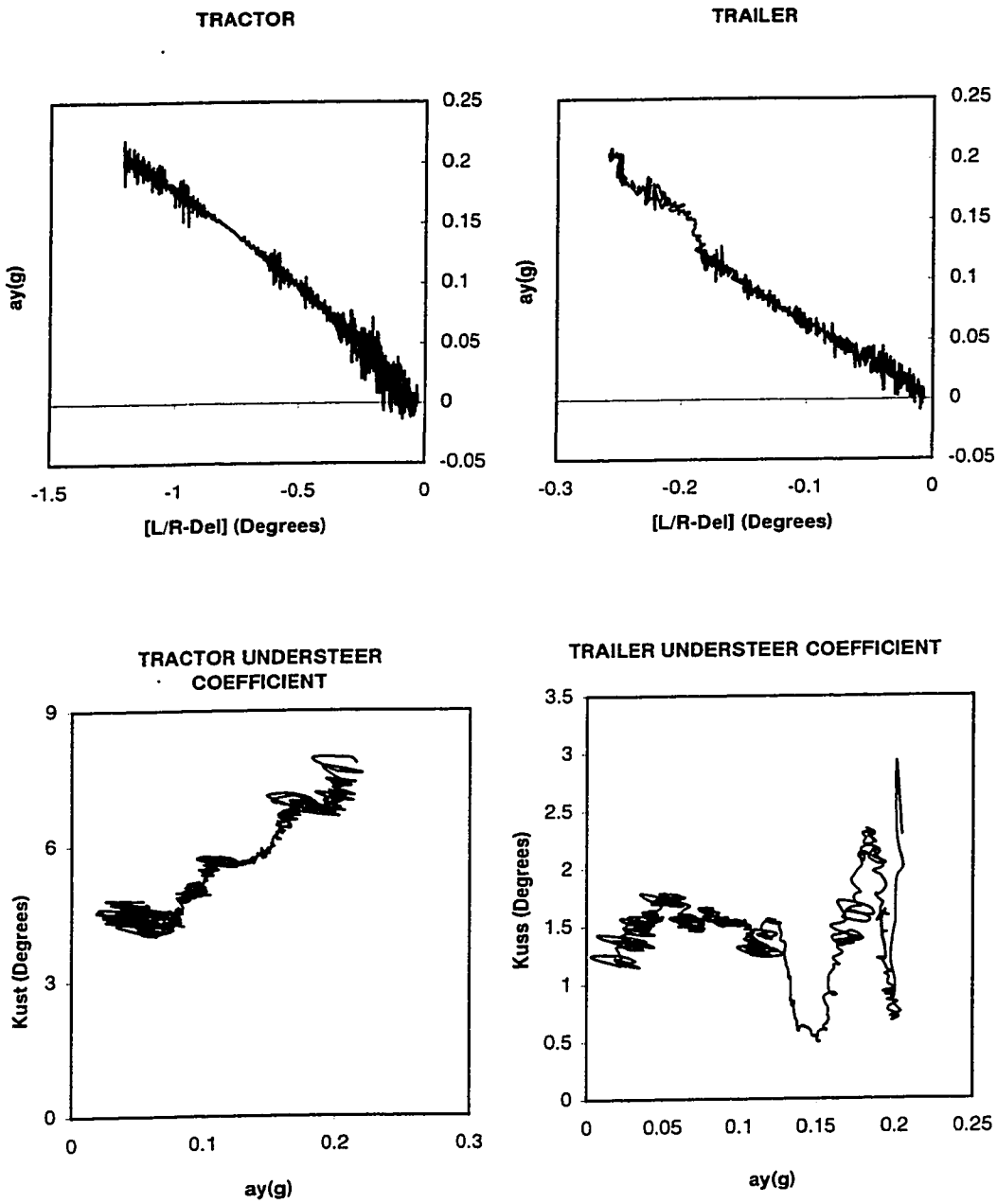

Figure 4.15: Handling diagram and understeer coefficient of tractor and semitrailer under medium rough road.

Case IV : Rough road

Similar results are obtained from the rough road as shown in Figure 4.16. The vehicle behaves in a similar fashion as observed under medium rough road inputs. In this case, the trailer characteristic changes to oversteer for a short period at a relatively lower level of lateral acceleration of 0.14g. The yaw rates also revealed that the trailer yaw rate remains less than the tractor's yaw rate.

The simulation results reveal that the vehicle remains stable under all the three road conditions considered. The rough roads, however, has definite influence on the steering characteristics of the trailer. The values of the understeer coefficients decrease considerably at relatively lower levels of lateral acceleration under the influence of road roughness.

4.3.4 Roll, Yaw and Pitch Rates

Roll, yaw and pitch rates as a measure of directional performance are discussed in chapter 3. In this section, the time history of these maneuvers from different maneuvers and road inputs are presented and discussed.

Roll Rate:

The roll rates of the tractor and trailer sprung weights are evaluates under different operating conditions to identify the influence of road inputs. The roll rate response characteristics of the tractor and trailer are evaluated under turning (at 50 km/h), path-

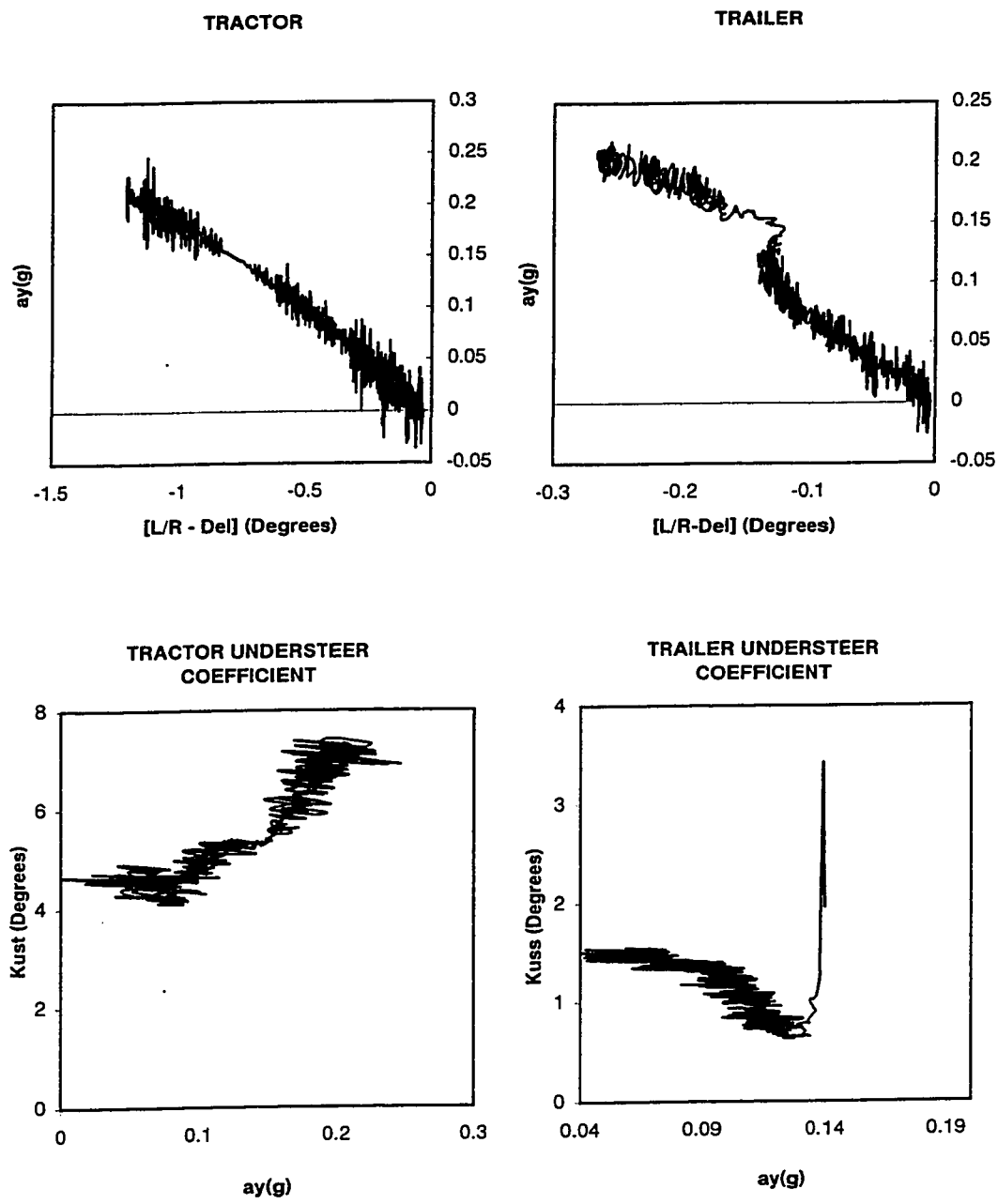

Figure 4.16: Handling diagram and understeer coefficient of tractor and semitrailer under rough road inputs.

change (at 100 km/h), lane change and evasive maneuvers (70, 100 and 120 km/h). From the results, it is concluded that the tractor and trailer increase with increase in vehicle speed. The influence of road roughness on the roll rates is very prominent at low speeds, as shown in the Figures 4.17 to 4.20. The roll rates response of both unity subject to a turning maneuver at 50 km/h increase considerably with the road roughness, as shown in Figure 4.17. The peak roll rate of the tractor and trailer are obtained as 1.15 and 1.12 deg/s, respectively under no road roughness. The peak values of the roll rate of the tractor increase to nearly 1.3 deg/s, 2.5 deg/s and 6.5 deg/s, under the influence of smooth, medium rough and rough roads respectively. The results show that a vehicle under road roughness will exhibit considerable oscillations in roll and may lead to a roll instability under the presence of additional disturbances, such as abrupt irregularity, cross-wind etc. The influence of road roughness on the roll rates of the vehicle subject to a path change maneuver at 100 km/h, however, is relatively insignificant, as shown in Figure 4.18. The results show that roll rate of the tractor increases by approximately 10% under the influence of rough roads, while that of the trailer may decrease slightly.

The vehicle jackknife and trailer swing potentials are strongly related to the yaw rates of the tractor and trailer. The yaw rates of the two sprung weights are thus evaluated under different directional maneuvers and roughness, and results are presented in Figures 4.21 to 4.24. The results show that the influence of road roughness on the yaw rate response of the vehicle is insignificant, irrespective of the maneuver, and the road roughness affects the vertical tire-road interactions in a highly significant manner its effect on the yaw behavior of the vehicle is small.

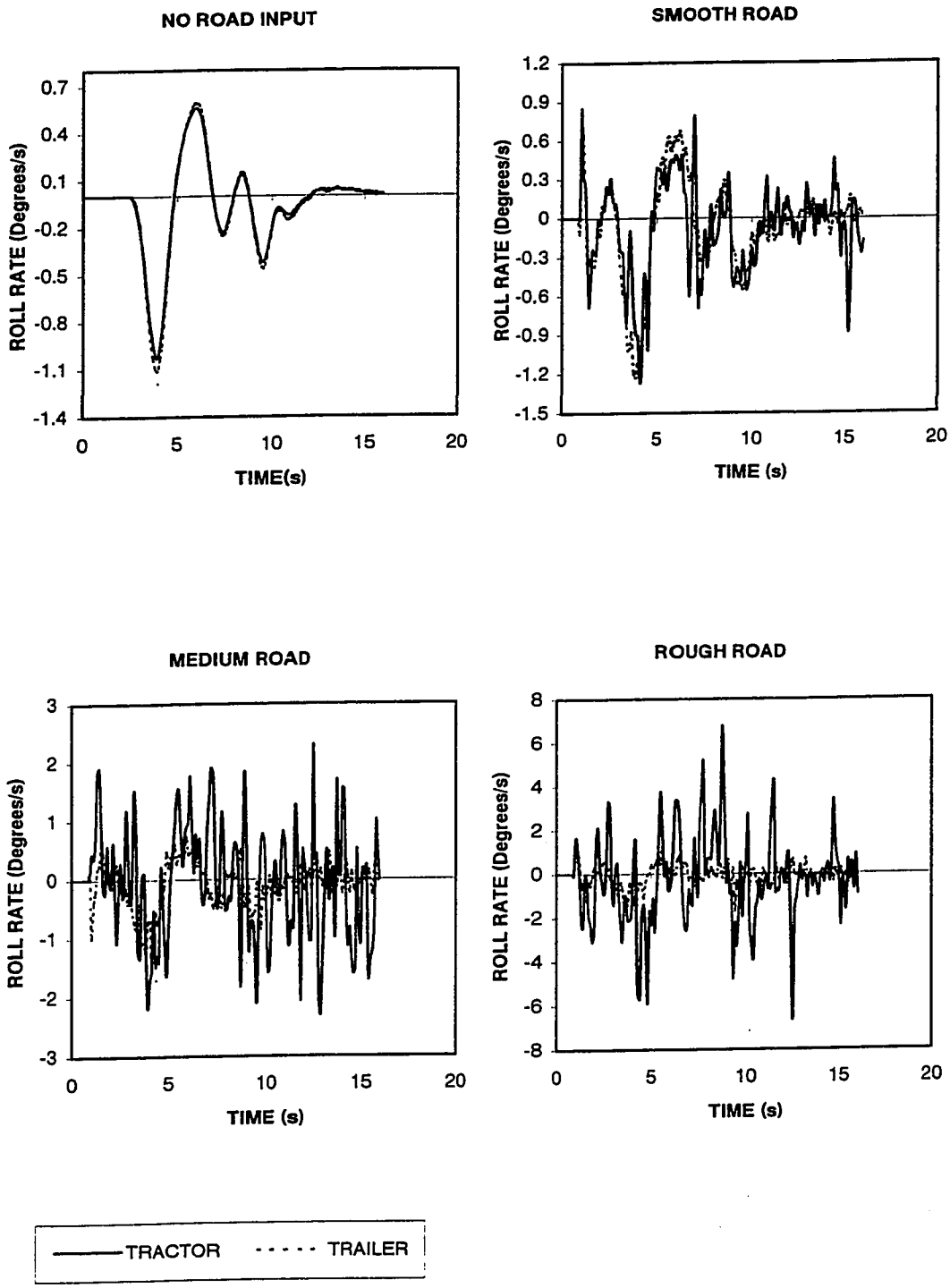

Figure 4.17: Roll rate response of the vehice subject to turning maneuver at 50 km/h.

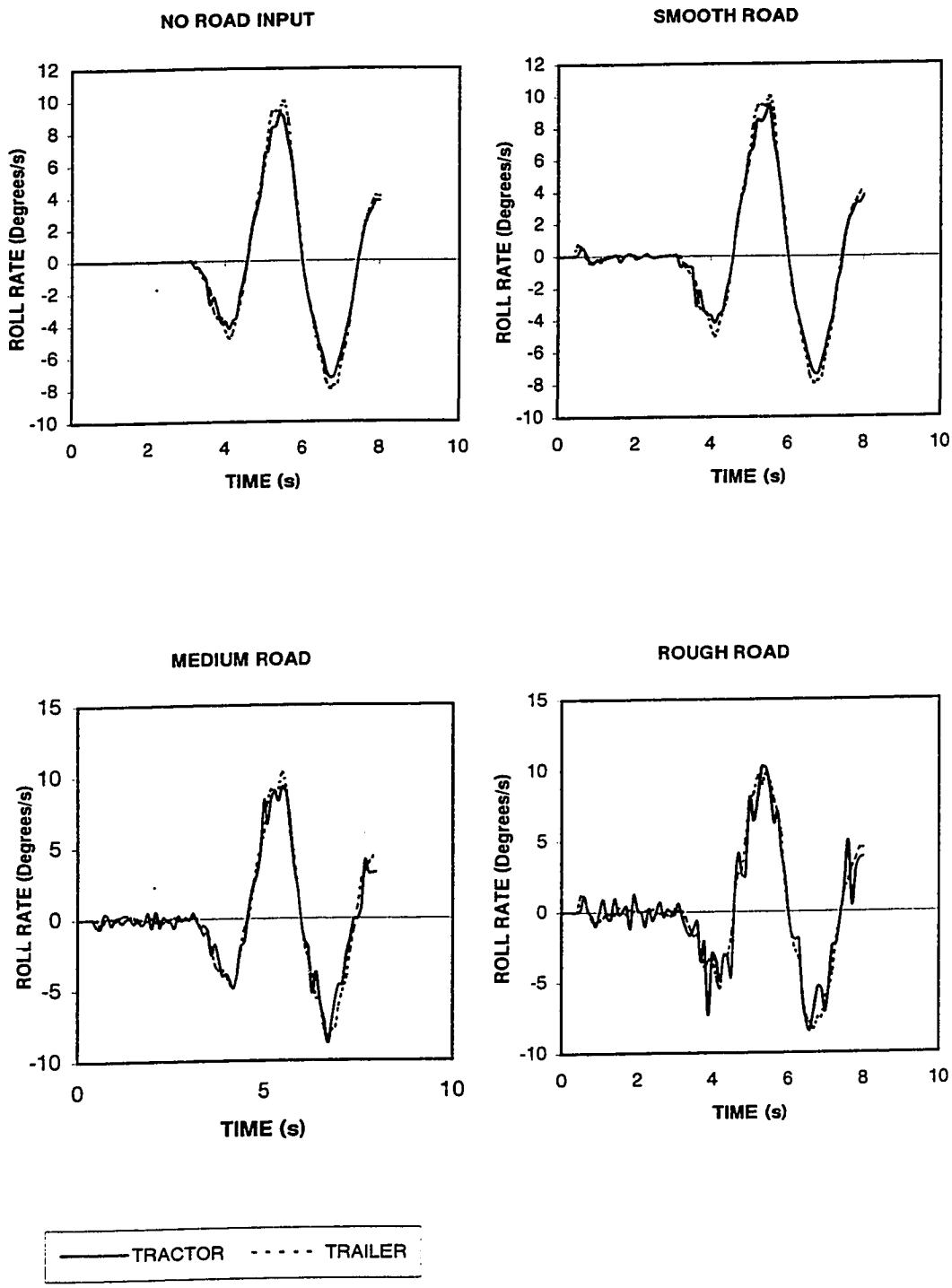

Figure 4.18: Roll rate response of the vehicle subject to path-change maneuver at 100 km/h.

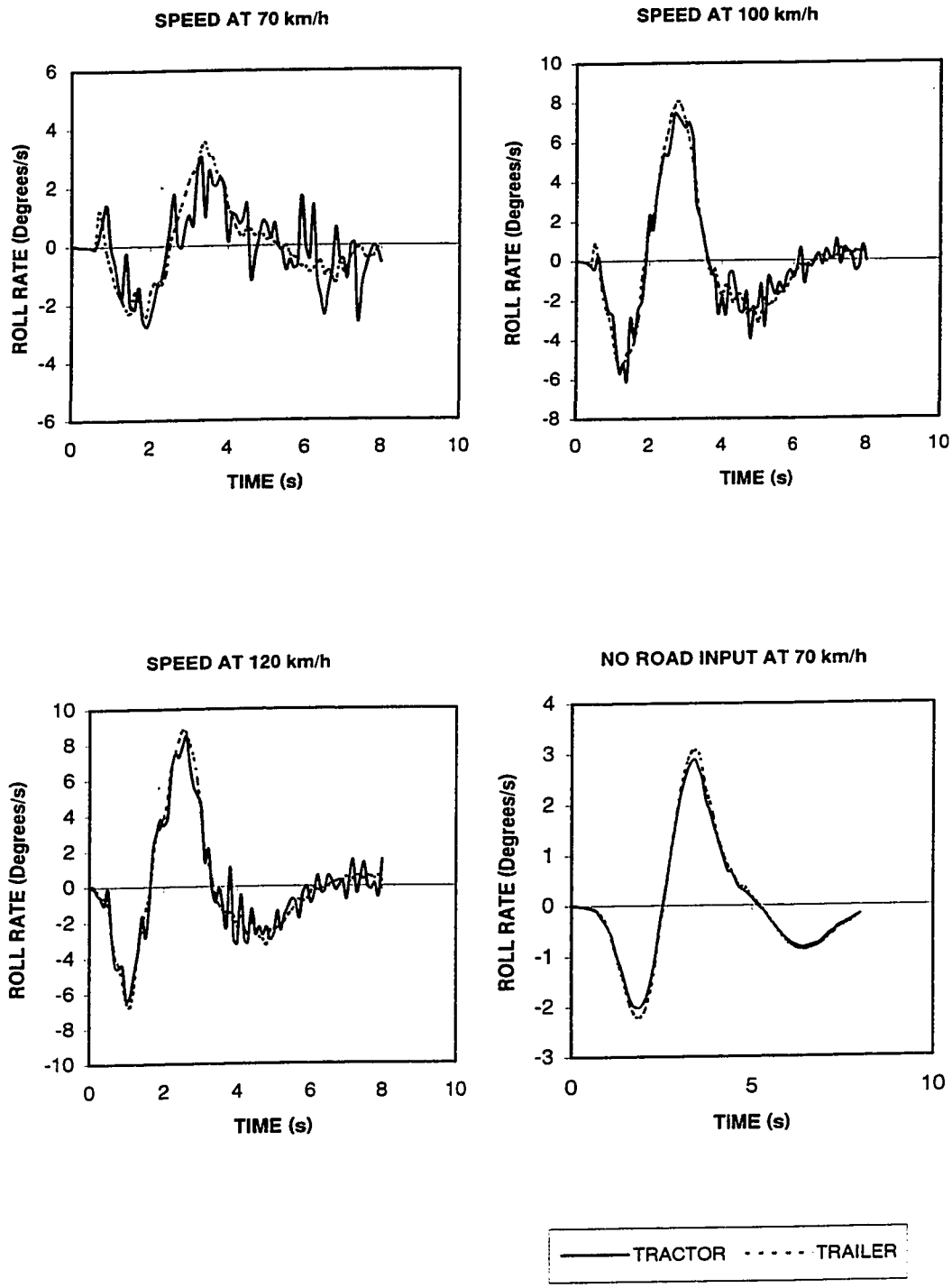

Figure 4.19: Roll rate response of the vehicle subject to lane change maneuver under rough road.

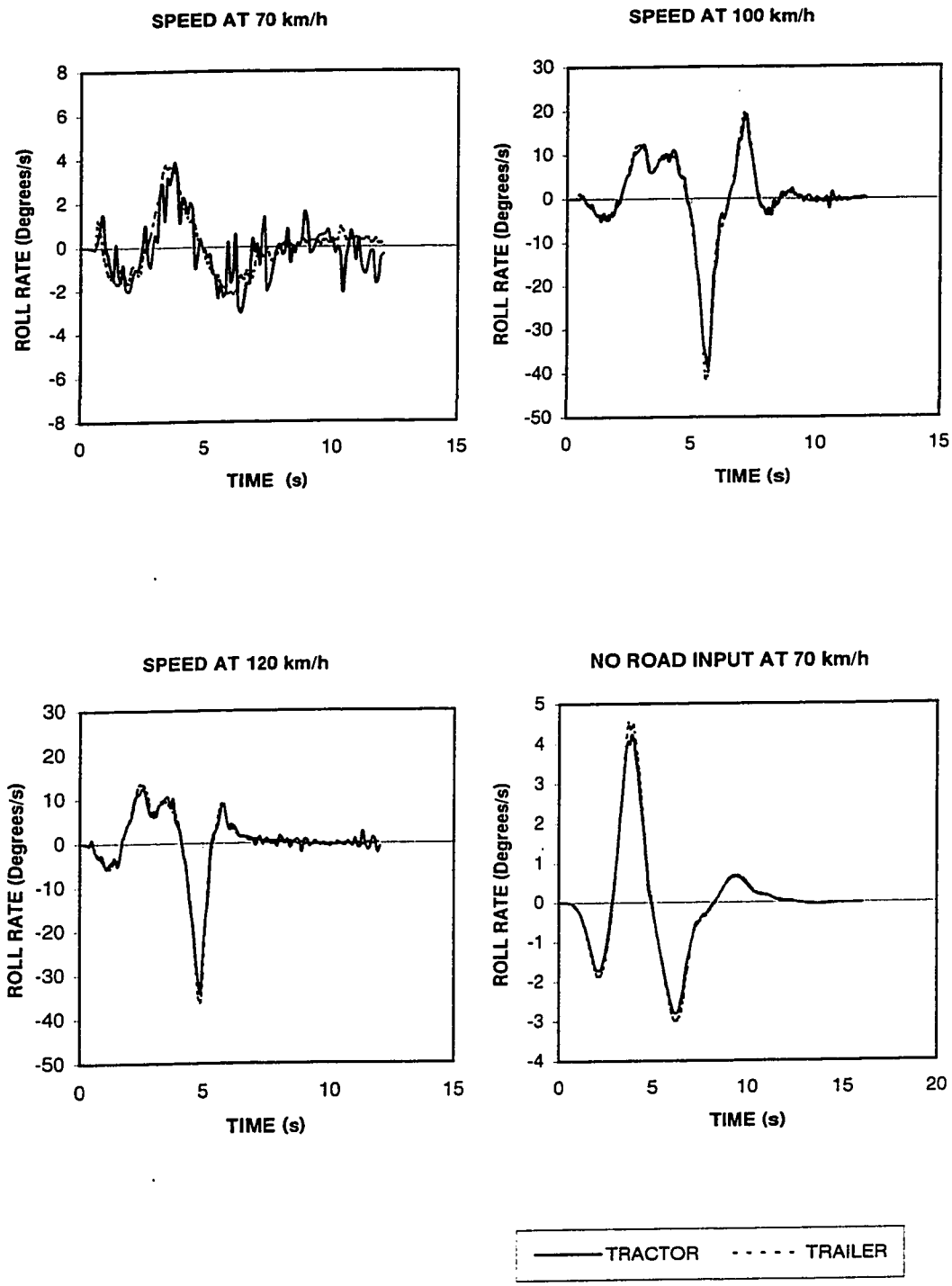

Figure 4.20: Roll rate response of the vehicle subject to double lane change maneuver under rough road.

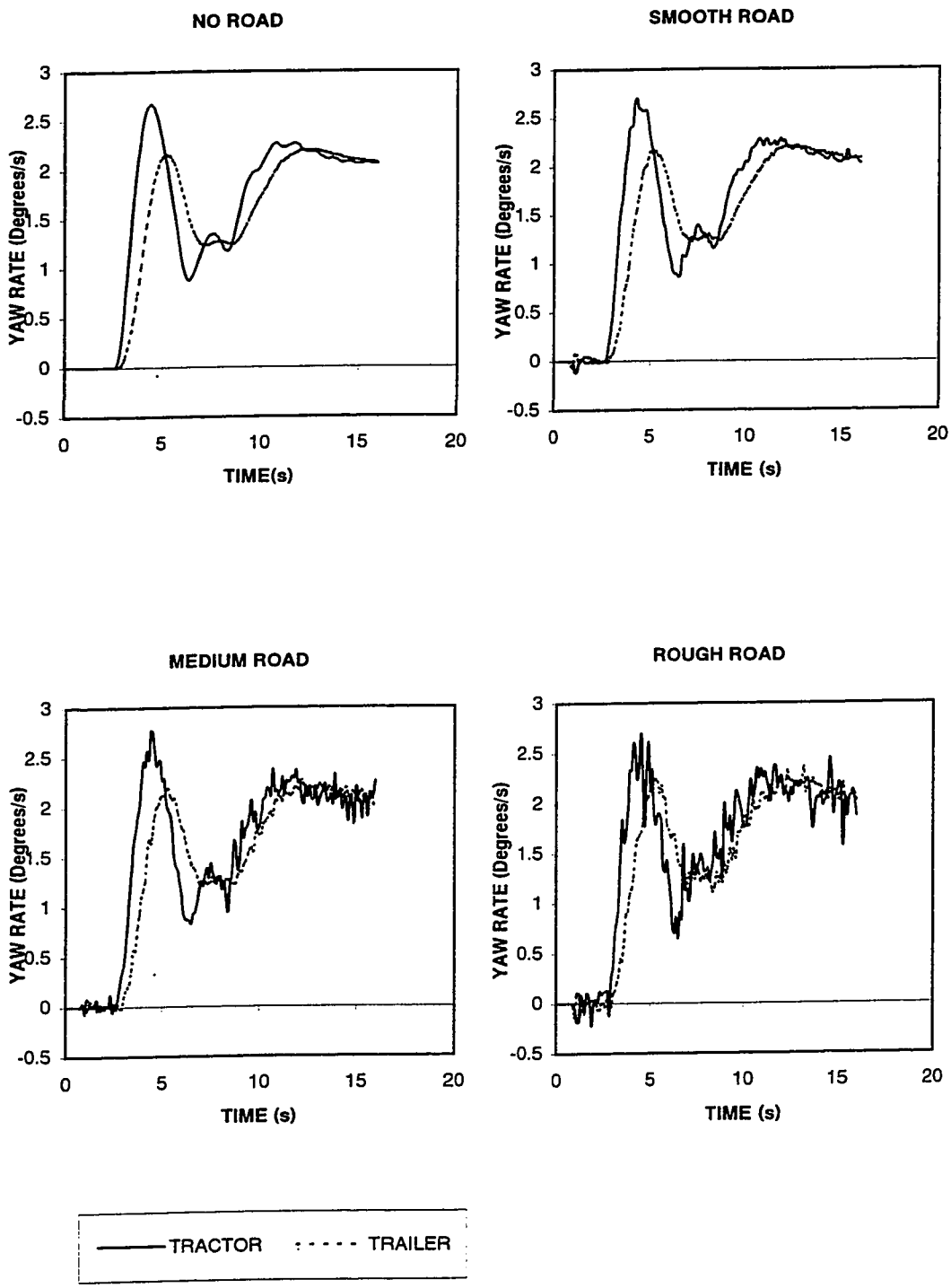

Figure 4.21: Yaw rate response of the vehicle subject to turning maneuver at 50 km/h.

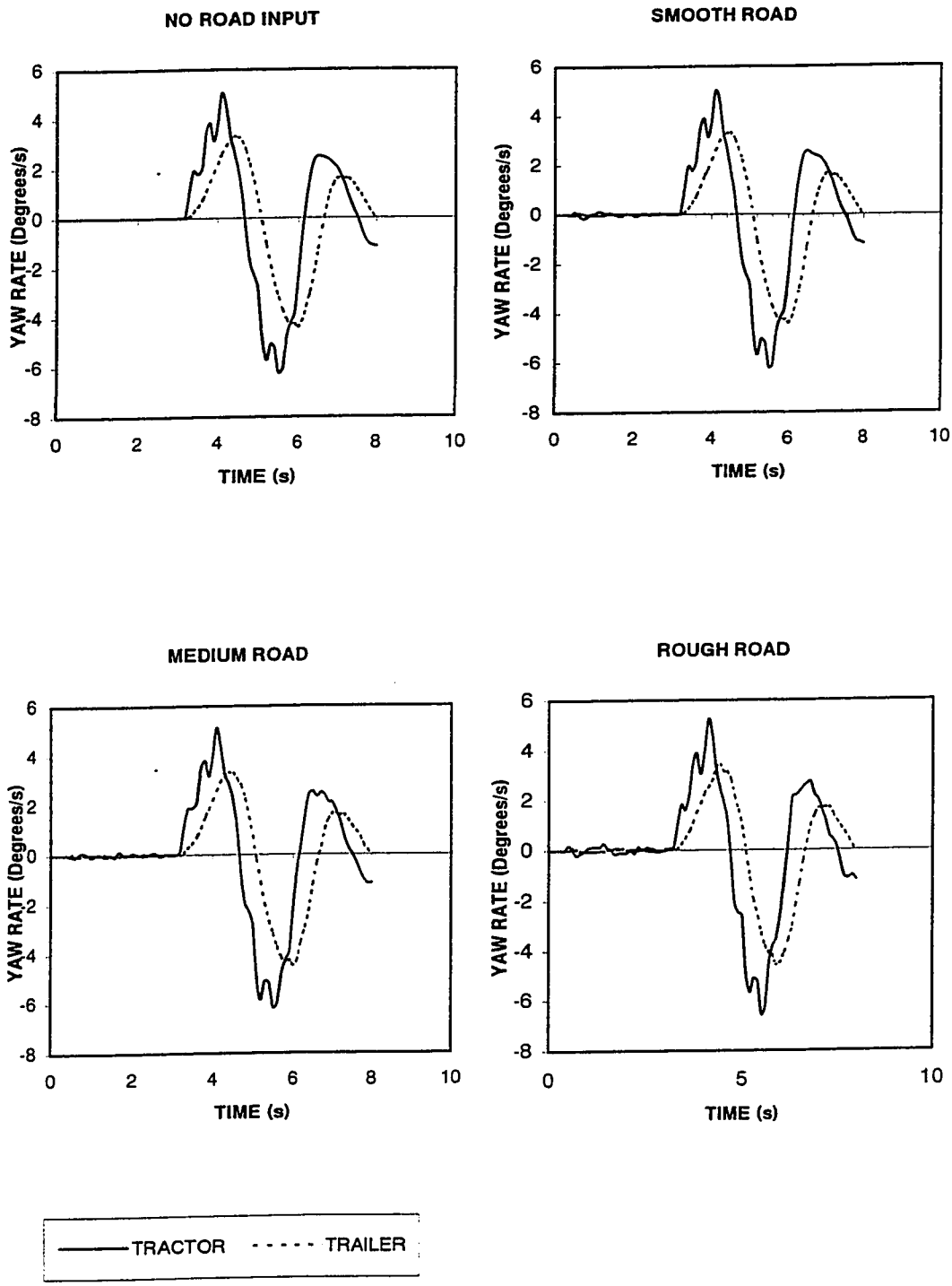

Figure 4.22: Yaw rate response of the vehicle subject to path-change maneuver at 100 km/h.

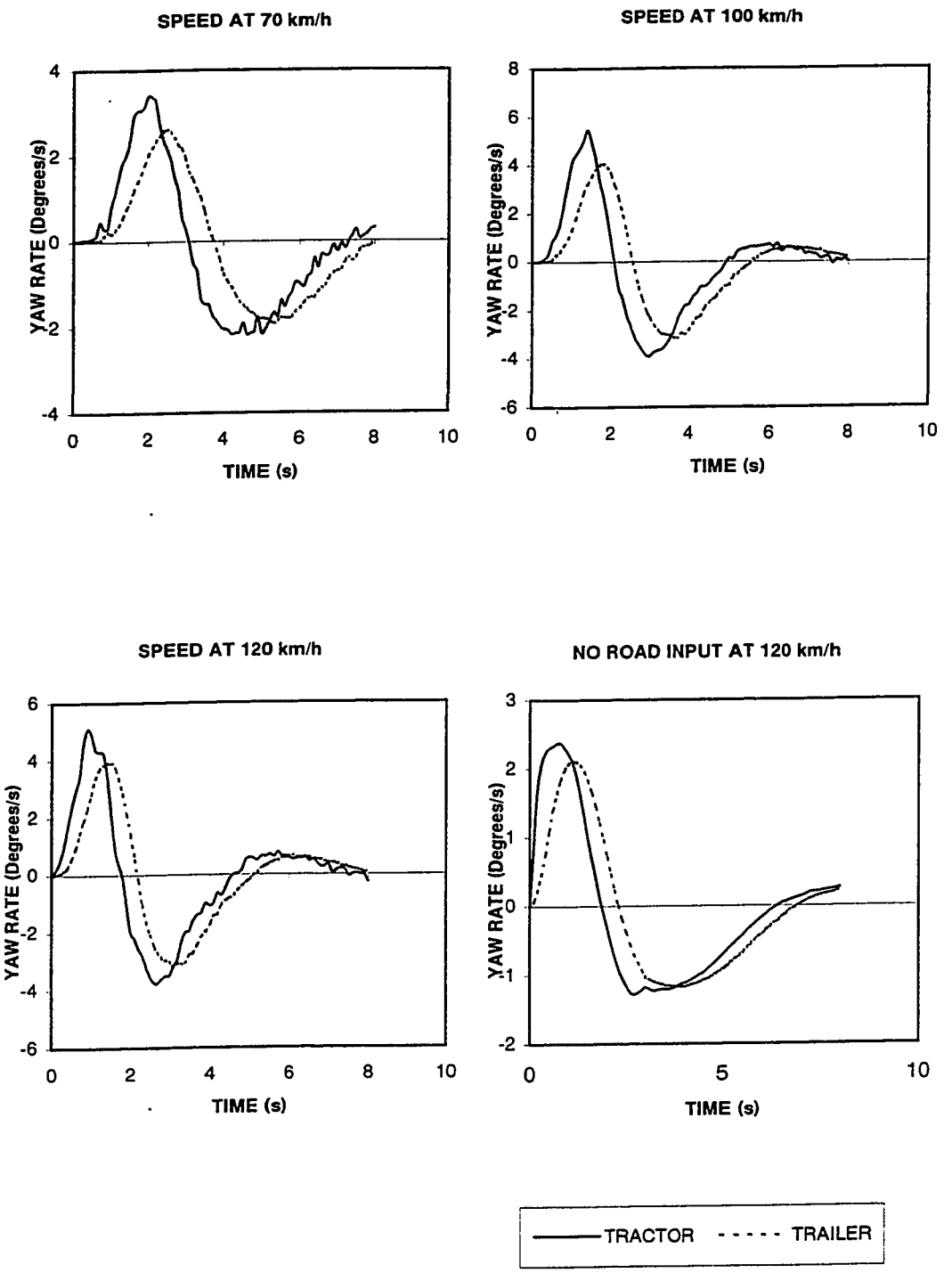

Figure 4.23: Yaw rate response of the vehicle subject to lane change maneuver under rough road.

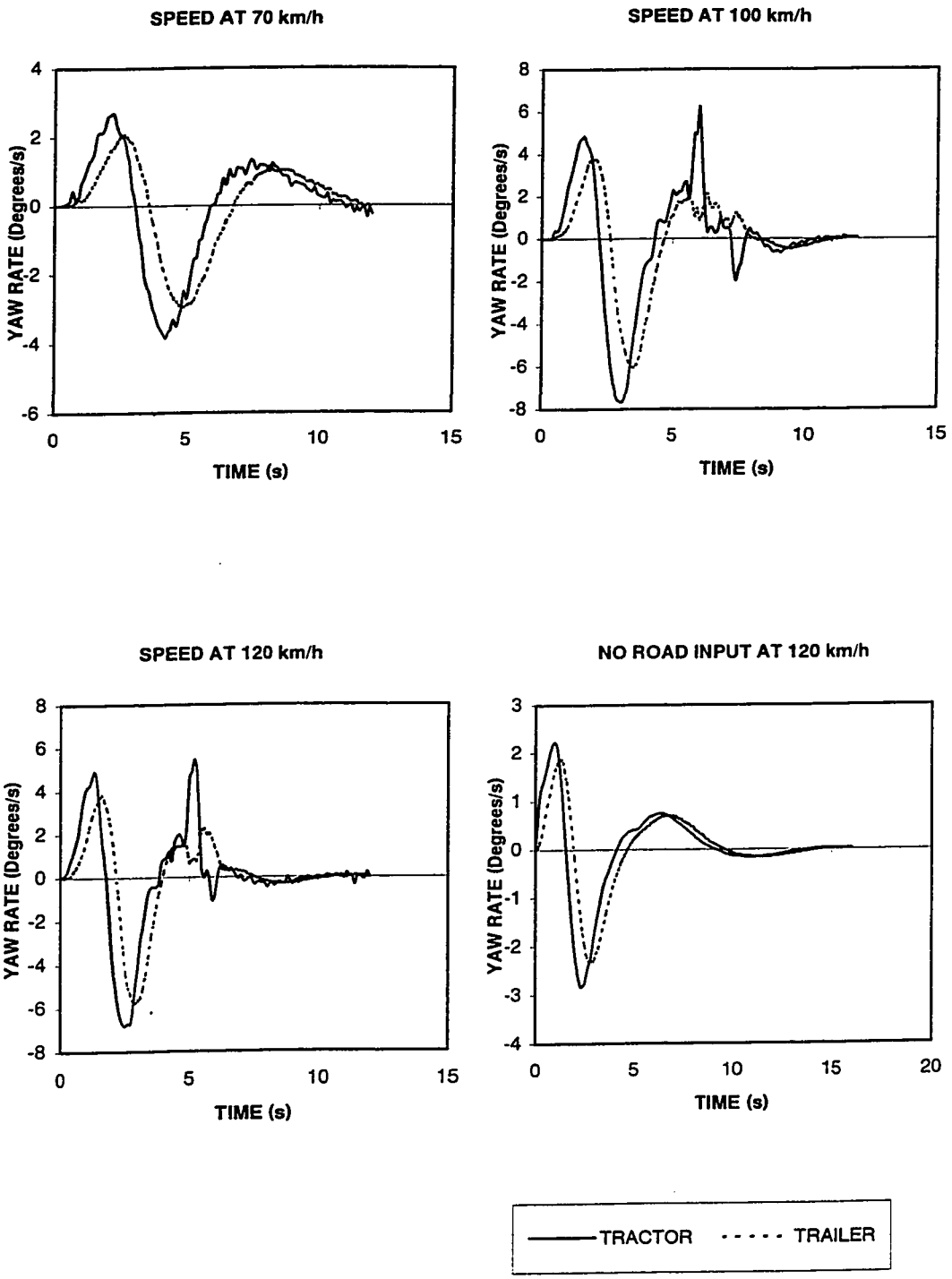

Figure 4.24: Yaw rate response of the vehicle subject to double lane change maneuver under rough road.

The dynamic load transfer from/to trailer axles, is strongly related to the vehicle pitch and pitch rates. The high vehicle pitch and pitch rate may thus affect the braking and acceleration performance of the vehicle. Although, the dissertation research focuses on the vehicle response under constant forward speed, the pitch rates are examined to illustrate the extent of possible load shift under the influence of road roughness. Figures 4.25 to 4.28 illustrate the pitch rates of tractor and semitrailer subject to different steering and road inputs. It should be noted that the pitch response of the vehicle is strongly coupled with the vertical dynamics of the vehicle. The strong influence of road roughness on the vertical tire-road interactions thus affects the pitch rates of the vehicle in a significant manner. The results show that during a lane change maneuver the influence the influence of rough road inputs is quite insignificant upon different forward speeds. However during double lane change the there is an increase of 2.0 deg/s when the forward speed is increased from 70 km/h to 100 km/h. During path change and turning maneuver the change is significant from 1.5 deg/s to 4.0 deg/s when the vehicle travels from smooth road to rough road.

4.4 Summary

The influence of road roughness on the directional dynamics of the articulated heavy vehicle is investigated by comparing the vehicle response under road roughness with those under no road input. The performance measures of the articulated heavy vehicle are evaluated under different road inputs and different speeds. The results of the study

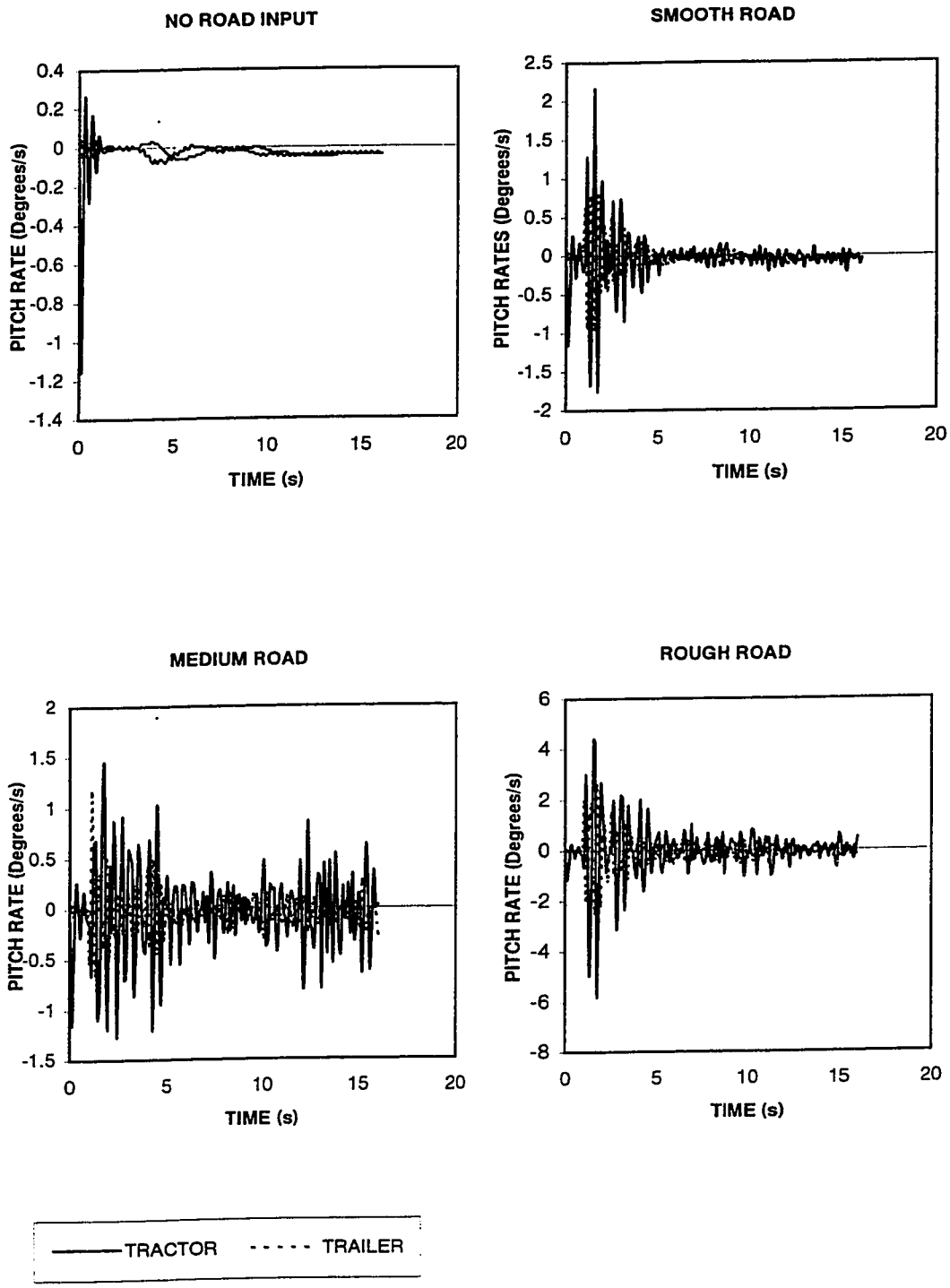

Figure 4.25: Pitch rate response of the vehicle subject to turning maneuver at 50 km/h.

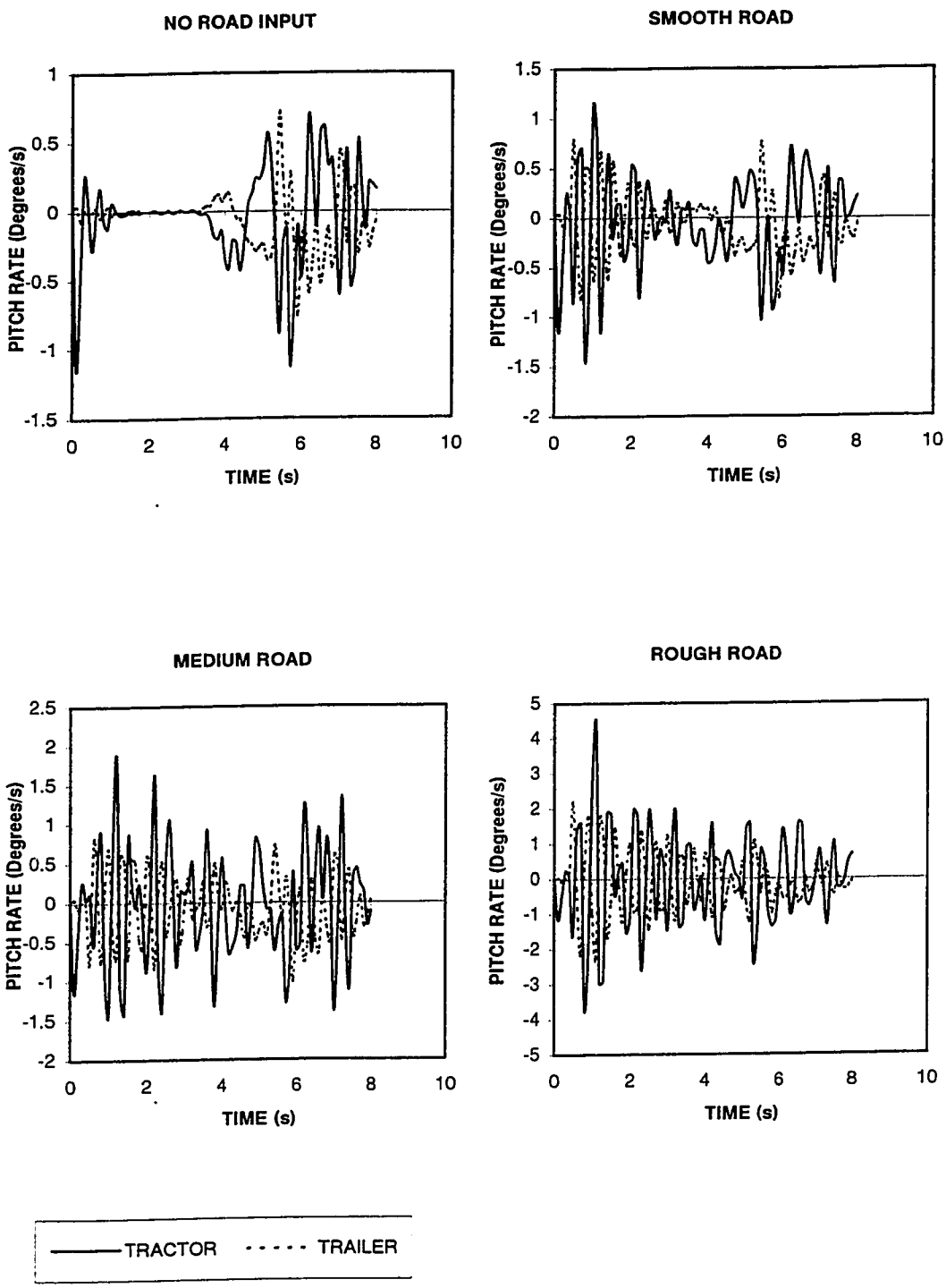

Figure 4.26: Pitch rate response of the vehicle subject to path-change maneuver at 100 kmph.

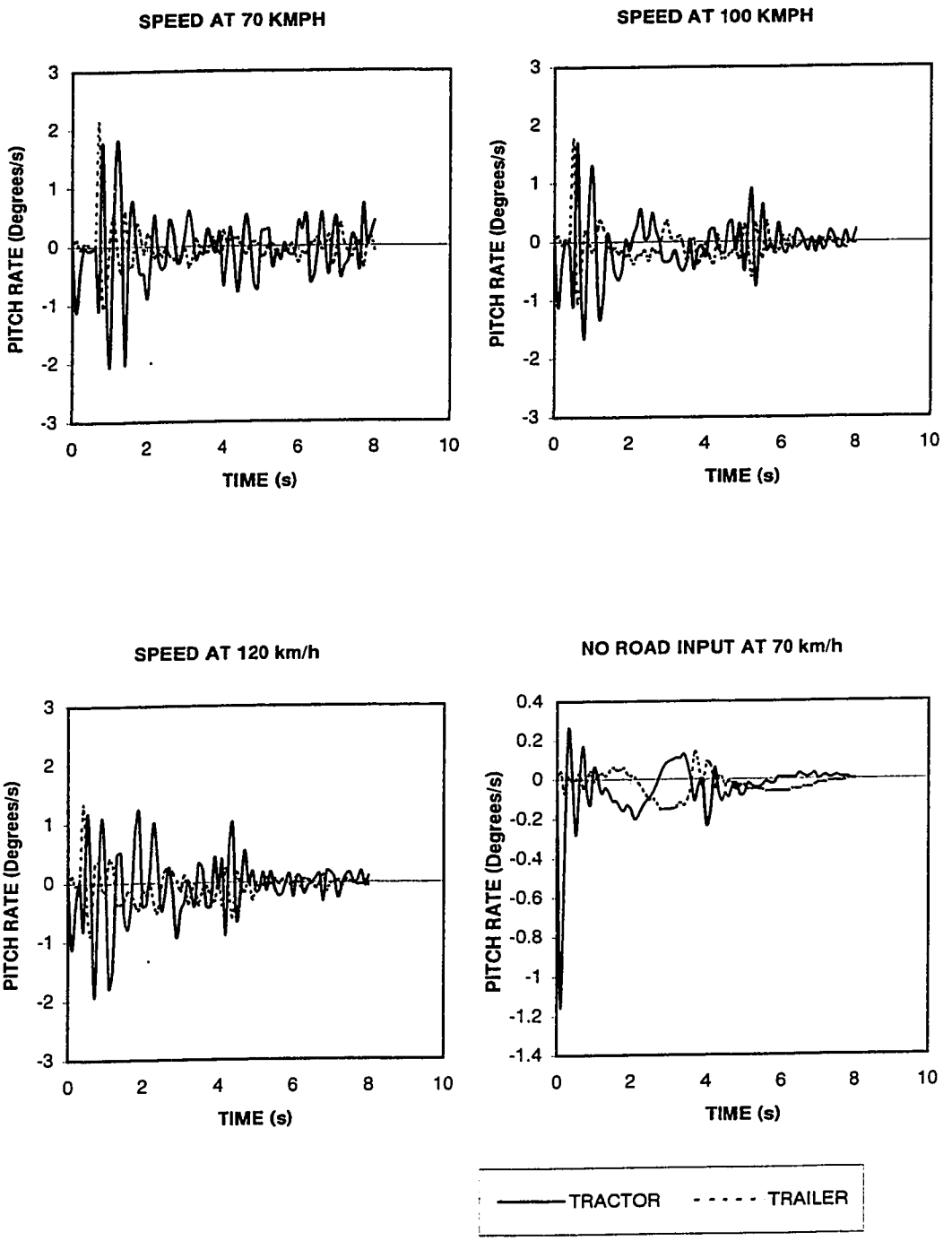

Figure 4.27: Pitch rate response of the vehicle subject to lane change maneuver under rough road.

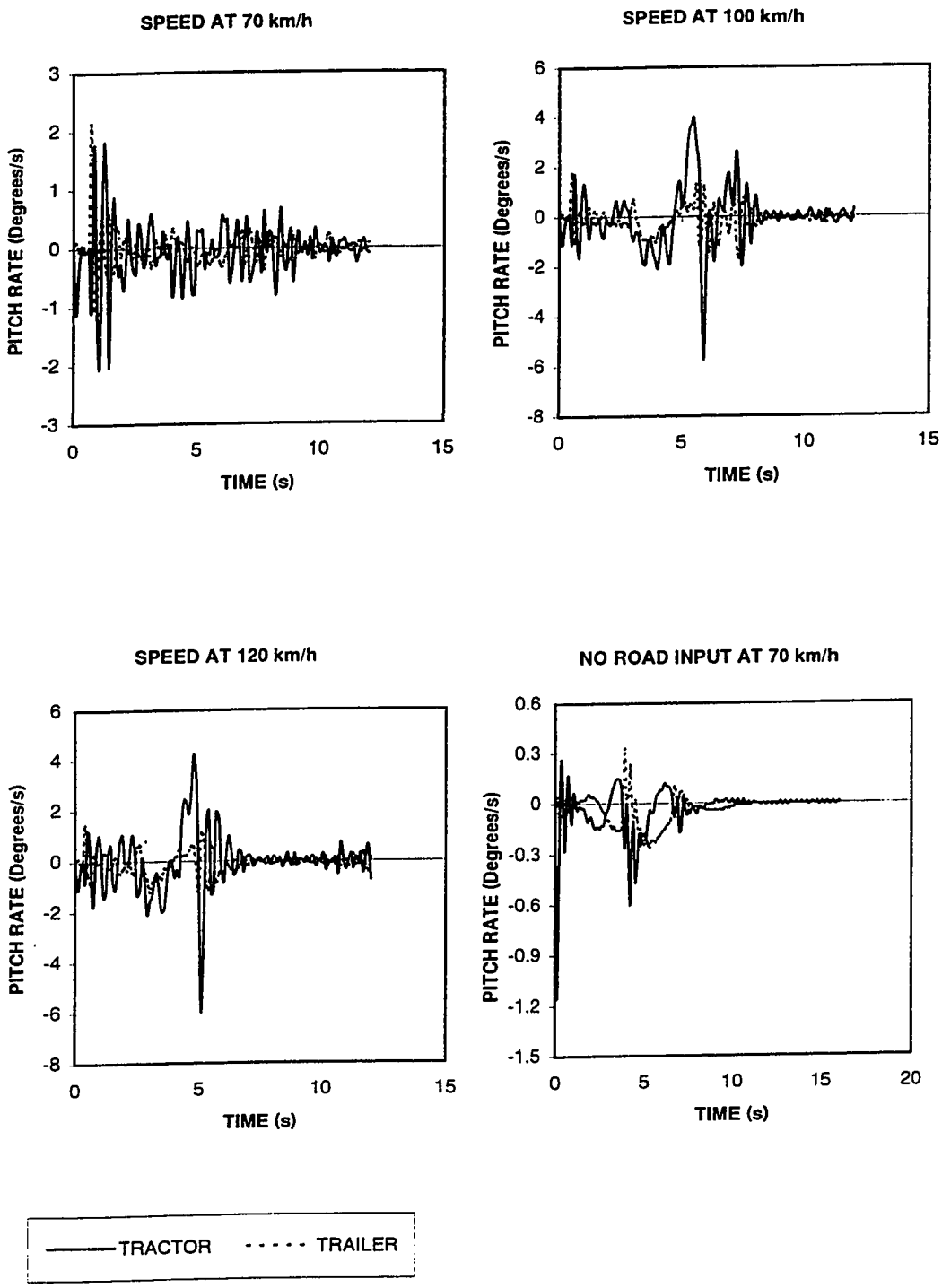

Figure 4.28: Pitch rate response of the vehicle subject to double lane change under rough road.

revealed that performance measures dependant upon the vertical tire-road interactions are strongly influenced by the road roughness. These include roll dynamic measures (LTR), roll rate and pitch rate. The performance measures, which are mostly related to lateral tire-road interactions, are affected by the road roughness in an insignificant manner. These include: rearward amplification, handling and yaw rate. The lateral acceleration of the tractor and the trailer can increase by as much as 10% to 60%, when the vehicle is subject to single or double lane change maneuver on a rough road. However, during a single lane change maneuver the trailer and tractor accelerations increase with increase in vehicles forward speed. During the double lane change maneuver, the lateral acceleration of both tractor and trailer increases significantly with the increase of the speed. The relative increase in lateral acceleration of the two units however, is not linear and thus yields insignificant increase. This hinders the amplification of lateral acceleration at low speeds under rough roads during the single lane change maneuver. During the double lane change maneuver, the amplification of lateral acceleration increases at higher speeds. The road roughness, however, does not influence the roll angle amplification.

The lateral load transfer ratio of different axle increases considerably the influence of road roughness. The LTR values exceed the proposed limiting value of 0.6 under the presence of rough road excitation at 70 km/h. The influence of road roughness ranges from 20% to 40% for entire speed range considered in the study. During the double lane change maneuver, the instantaneous values of LTR approach 1.0 at the speeds of 100 and 120 km/h, irrespective of the road roughness. Although the road roughness affects the handling of the vehicle very slightly, the understeer coefficients of

the two units tend to decrease considerably under medium-rough and rough roads. The road roughness further affects the roll and pitch rates of the vehicle quite significantly. The roll rates of the tractor and semitrailer increase considerably under the influence of road roughness at lower speeds.

Chapter 5

Influence of steering input on the Dynamic Wheel Loads

5.1 General

One element of the criteria used in the design of bridges and pavements is the dynamic loading transmitted to pavements in terms of both magnitude and number of applications during the lifetime of the structure. Among all the concerns, the most crucial is the loading applied to these structures by heavy highway vehicles. Traditionally, the loading element of the design criteria has been accounted for through heavy vehicle weights and dimensions, with addition of overload factors estimated as a percentage of the nominal weight. These loads are equivalent, respectively, to the vehicle static weight and dynamic load. The later has been considered a variable and largely unknown quantity [3].

Although it is assumed that dynamic vertical loads influence the life expectancy of pavement and bridge structures, the degree of influence has been a point of conjecture, because of their unknown nature. As discussed in the literature review, researchers all over the world have undertaken comprehensive studies for subsequent understanding of

the nature and magnitude of heavy vehicle dynamic loads and pavement failure. To gain an understanding of dynamic pavement loading, a study of the factors that may have influence is necessary. These factors are: (1) pavement surface profile, (2) certain characteristics of the vehicles, and (3) the mode of vehicle operation. Pavement surface is the profile, which is traversed by the rolling tire of the vehicle under consideration. Important vehicle characteristics are weight its distribution, method of distributing that weight to the pavement (wheels and tires), and the nature of the elastic suspension system. The important vehicle operating mode that must be considered is speed, steering and braking of the vehicle. The yaw roll model of the heavy articulated vehicle considered in this study under the inputs of road roughness and steering inputs is adapted here to investigate the dynamic wheel load characteristics.

In this chapter, the vehicle response characteristics are analyzed to illustrate the influence of directional maneuvers and the road roughness the dynamic wheel loads. The analyses are performed as per the formulated in chapter 3, while the suspension parameters are held fixed.

5.2 Assessment of Road Damage

Vehicle generated road damage is directly related to the magnitude of tire forces transmitted to the pavement. The tire forces transmitted to the road consist of static load and a fluctuating dynamic load. The static load depends on the geometry and mass distribution of the vehicle, and load sharing characteristics of the suspension systems.

Dynamic tire forces, on the other hand, are the result of the vehicle vibration caused by the road roughness and load shift due to a maneuver. The intensity of these vibrations and hence the severity of the dynamic tire forces primarily depend upon the suspension design as well as vehicle and axle configuration. Dynamic tire forces and their interaction with the pavement is a complex process. The extent of damage caused by these loads to pavements depends on the road structure and material characteristics, as well as the nature of the applied loads. Although number of methods have been proposed to estimate the serviceability index or service lives of pavements, serious concerns have been raised on the validity of the methods [3, 28, 29]. In this study, the dynamic wheel load and road damage potentials are assessed in terms of dynamic load co-efficient, road stress factor and peak resultant forces based on vertical and cornering forces. A detailed discussion of these performance measures is presented in Chapter 3.

5.3 Results and Discussion

The simulation results under various road roughness and maneuvers are extracted in terms of each tire force in order to derive various performance measures. It is well established that the dynamic forces are the prime cause of road damage, where the dynamic component is an oscillating force about the mean of the static force. The parameter used frequently to characterize the magnitude of dynamic tire force is the 'Dynamic Load Coefficient' (DLC), which is defined as the ratio of the root mean square (RMS) of the dynamic tire force to the static tire force. The study focuses on the influence of road roughness and steering input on the value of DLC. The DLC value shows the extent of the variation from the normal, however the effect on the road due to

this variation from the normal is identified by the 'road stress factor'. In assessing the severity of dynamic road loading, the dynamic road stress factor is considered to be lower estimate because it effectively assumes that the pattern of dynamic loading is random. Since dynamic loading responds to pavement profile and heavy vehicle suspension characteristics are, to some extent similar, the higher loads will tend to recur at specific points in the pavement. The 95^{th} percentile load may be estimated quite readily from the DLC, if it is assumed that the dynamic load distribution is normal. The 95^{th} percentile load is referred to as impact factor and the corresponding road stress factor related to this factor is also calculated to determine the damaging effect at an instantaneous point.

5.3.1 Dynamic Load Coefficient

Under normal operating conditions, heavy vehicles typically yield DLC ranging from 0.05 to 0.3 [3]. Many studies have reported that the DLC ranging from 0.05 to 0.3 increases with an increase in road roughness, speed, tire inflation pressure and suspension stiffness [27]. Experimental studies [26] have further established that the properties of heavy vehicle suspensions strongly affect the magnitude of the dynamic loads transmitted to the road surface. The DLC due to tire forces of an air suspension axle is lower than that of an axle with torsion bar suspension, which is also lower than that of an axle with four-leaf suspension. A walking beam suspension yields highest DLC due to tire forces.

The vehicle model considered in this investigation is a typical tractor semi-trailer configuration with leaf spring in the tractor front axle and air springs for the tractor rear s

and semitrailer axles. Heavy vehicle dynamic studies for estimation of DLC typically employ a straight path. Here, the vehicle is simulated under different road roughness conditions at various speeds while performing single and double lane change maneuvers. The findings under different maneuvers are discussed below.

Case I: No steering input

The first set of values shown in the Figure 5.1 present the DLC values for axle # 2 to 5 at forward speeds of 70, 100 and 120 km/h. These results are obtained from various road roughness in the absence of steering input. The results clearly show that on perfectly smooth road the DLC is very low and is slightly affected by speed of the vehicle. This is expected as there is no excitation to the vehicle. With the introduction of road roughness, the DLC values for each axle changes dramatically where the magnitude increases in road roughness. This well-known trend obtained from simulation under no steering input confirms the validity of the model used in this investigation. It can further be noted that for the vehicle configuration and parameters used, the DLC values for each axle on a straight path remain well within the typical value of 0.3.

Case II: Single lane change maneuver

The above simulation is next repeated for a steering input corresponding to a single lane change maneuver. The results for various axles on different road roughness are shown in Figure 5.2. Comparison of these results with those of straight path (Figure 5.1) show that the DLC value for each axle is increased from negligible level to a value of 0.2 under no road inputs. This clearly demonstrates the influence of maneuvers on the level of DLC,

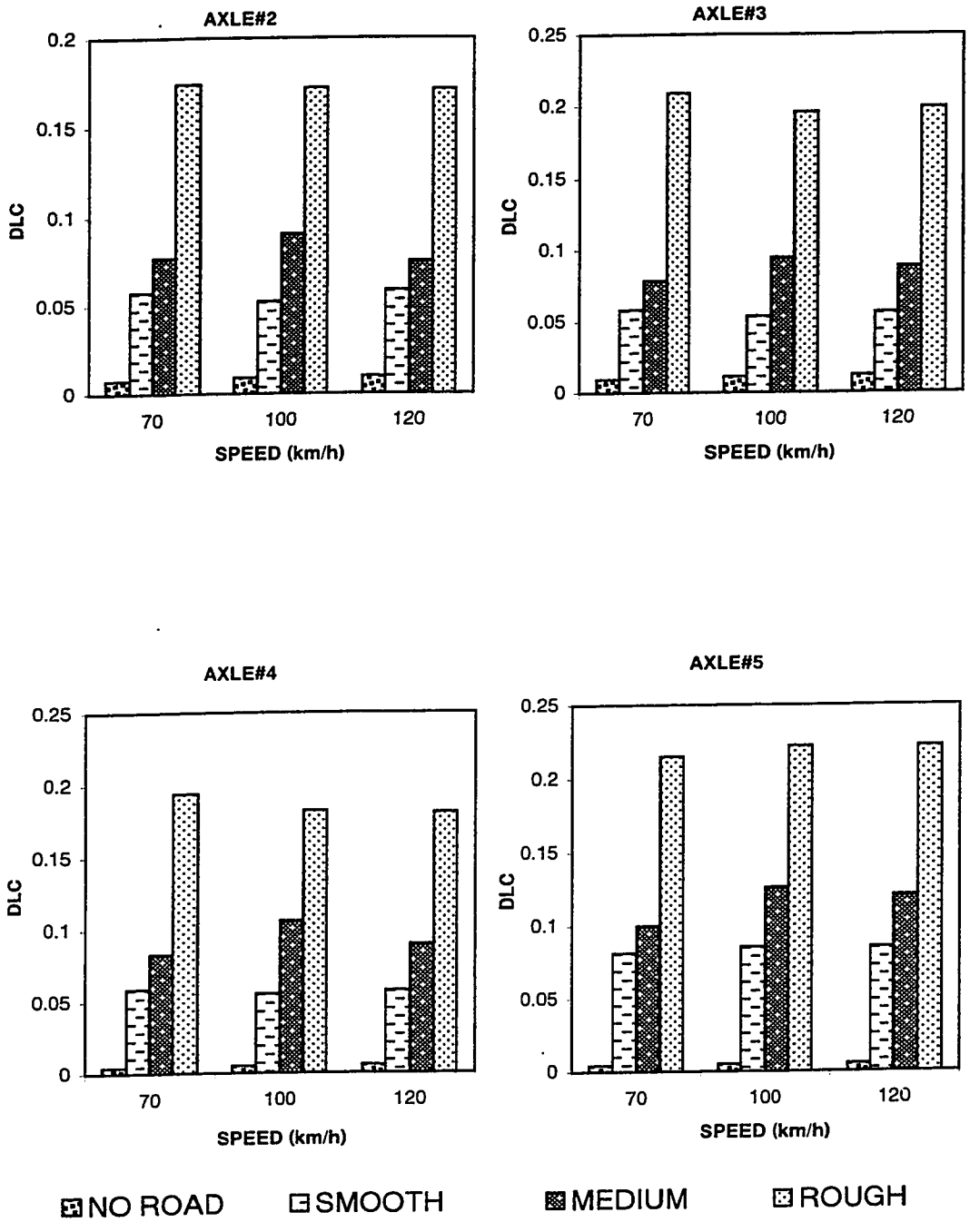

Figure 5.1: Dynamic load coefficient for various axles under different road roughness on straight path.

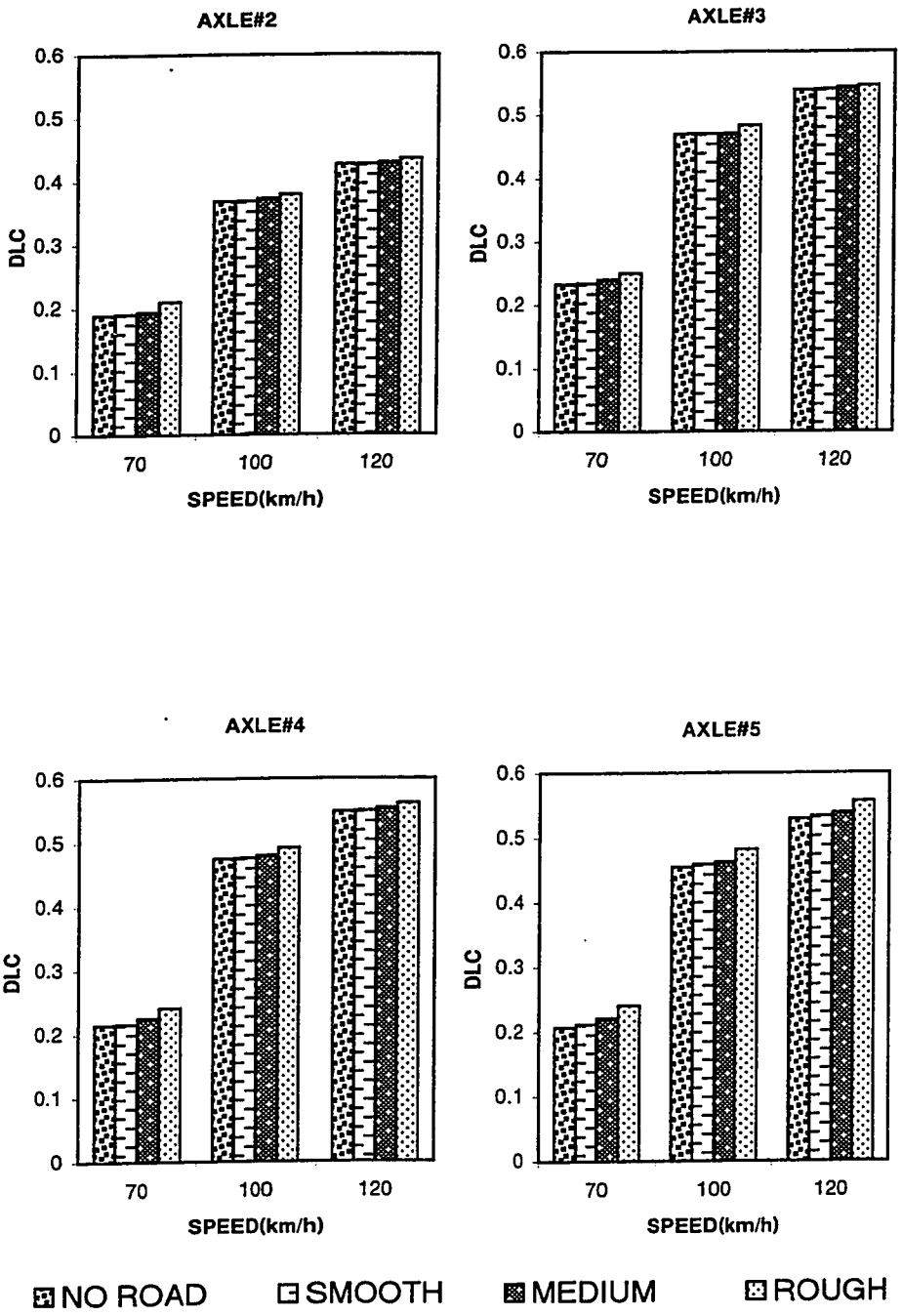

Figure 5.2: Dynamic load coefficient for different axles during single lane change maneuver on different road roughness.

which primarily results from load transfer. For the same reason the DLC show an increasing trend with forward speed of the vehicle. In all cases the load transfer is a dominating factor where road roughness shows a meager influence. It is evident that under a single lane change maneuver, the DLC values at 120km/h can be as high as 0.55 for tractor rear and trailer axles.

Case III: Double lane change maneuver

During the double lane change maneuver, the dynamic load coefficient in trend resembles the single lane change maneuver performance, as shown in Figure 5.3. Due to the severity of the maneuver, DLC value can be as high as 0.8 especially at high speeds. These results further show that the magnitude of DLC increases drastically at 100km/h from that at 70km/h. This again resembles the trends in load transfer characteristics under a double lane change maneuver. The trend in DLC between 100 and 120km/h is found to be very similar to that of load transfer ratio characteristics observed under same inputs.

This part of the study very clearly demonstrates the influence of steering maneuvers on the level of DLC generated. Although the influence of road roughness is visible, its significance is small compared to the severity of the maneuvers. It is clearly evident that a maneuver such as double lane change at a speed of 100km/h can result in a DLC of 0.8 compared to a value of 0.2 that was obtained under similar conditions for straight path. This means that a semitrailer wheel with static load of 45000N can produce average dynamic load as high as 81,000N where the instantaneous load can be significantly higher.

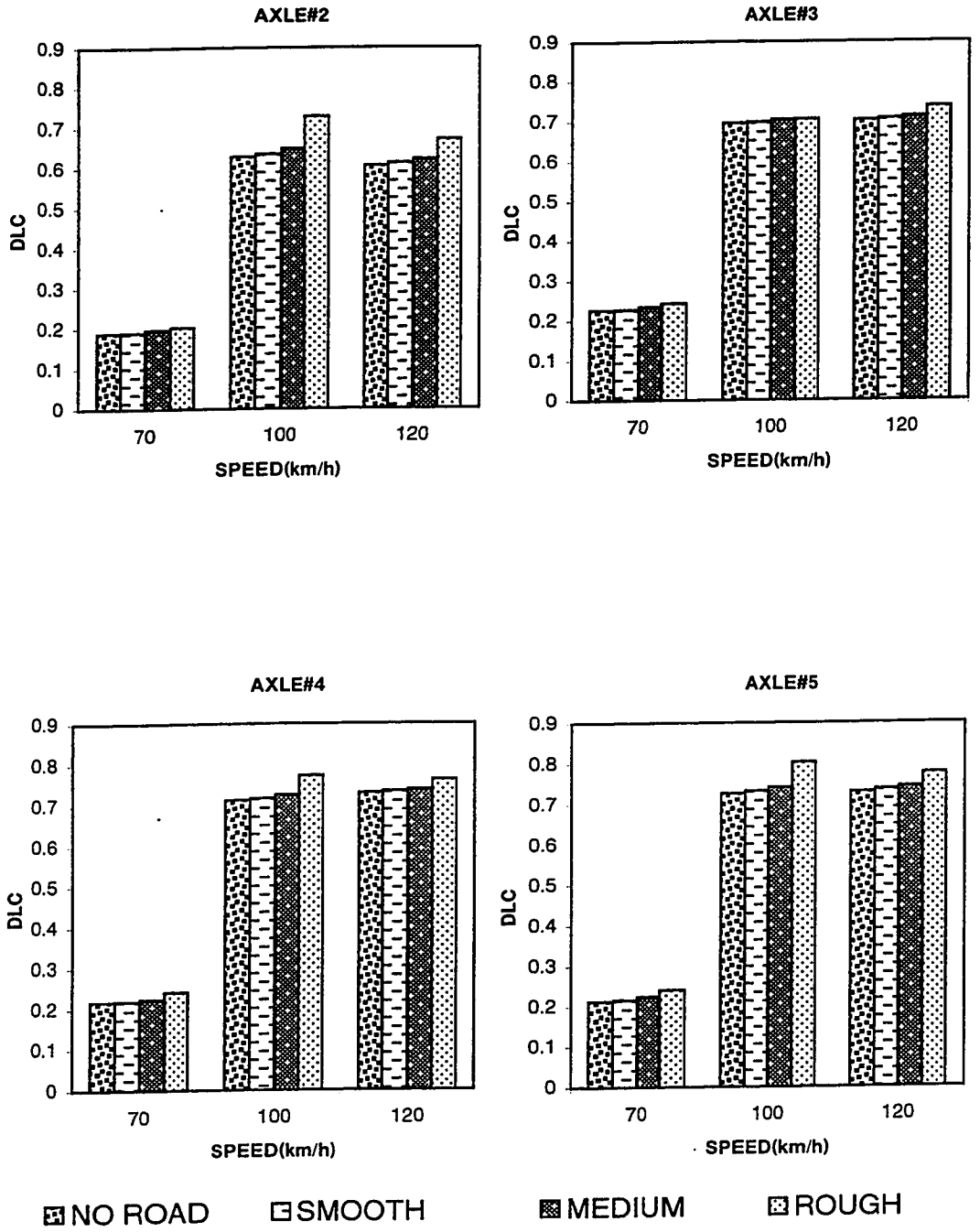

Figure 5.3: Dynamic load coefficient for various axles during double lane change maneuvers on different road roughness.

5.3.2 Road Stress Factor

The measure of road stress factor (RSF) as a performance index for road damage potential of heavy vehicle was discussed in chapter 3. The measure of RSF is based on the fourth power law applied to static load, which is extended to include the dynamic load. This section defines the measure of RSF and presents its magnitude for simulations under different road roughness and maneuvers.

The Fourth Power Law

A common unit for defining the road damage potential of various classes of vehicles has been sought to normalize and objectively compare the extent of damage caused by different classes and vehicle configurations. The first attempts to normalize road damage were based on identification of broad vehicle groups. Each group contains a number of broadly "similar" vehicles, which are assigned a common damage potential index. The most important result to quantify and compare road damage due to static load was attained through extensive road tests conducted by the AASHO [33]. Analysis of measured data revealed that the decrease in pavement "serviceability" caused by heavy vehicles can be related to the fourth power of the static axle load. Consequently the number of *Equivalent Standard Axle Loads (ESAL) N,* attributed to static loads was defined as [10-12]:

$$N = (P_{stat} / P_0)^4$$

Where, P_{stat} is axle static load and P_0 is a reference axle load taken as 80 KN. While the *Fourth Power Law* remains widely used as an effective tool, its validity has been questioned and exponents as high as 12 have been cited . To demonstrate the significance

of the *Fourth Power Law*, consider an axle carrying a static load resulting in N *ESAL*, if N approaches 2^4 when the load is doubled. This indicates that while the static load is only doubled, the damage potential is multiplied by 16. The approach to the problem of estimating the extent of the road damage due to dynamic tire forces was based on an extension of the *Fourth Power Law* to dynamic loads. Using the assumption that the road damage depends on the fourth power of the dynamic wheel force at a point on the road, it has been shown that the expected value of the fourth power of the instantaneous wheel force is given by [32]:

$$\Phi = E[P^2(t)] = (1 + 6\bar{s}^2 + 3\bar{s}^4)\, P_{stat}^4 = RSF \times P_{stat}^4 \qquad (5.1)$$

where,

P(t) is the instantaneous tire force and E is the expectation operator. $\bar{s}$ is the coefficient of variation of dynamic tire forces (DLC), and $RSF = (1 + 6\bar{s}^2 + 3\bar{s}^4)$ is the Road Stress Factor. The RSF approach was used in a limited number of studies to estimate the pavement damage caused by dynamic tire forces and to introduce new legislation relevant to axle configuration and loads. The simulation results obtained in terms of RSF for various roads and operating conditions are discussed below.

<u>Case I: No Steering Input</u>

The first set of results shown in Figure 5.4 present the RSF values for axle # 2 to 5 at forward speeds of 70, 100 and 120km/h. The results are obtained for various road roughness in the absence of steering input. These simulation results on a straight path reveal the influence of road roughness and the forward speed of the vehicle on the RSF

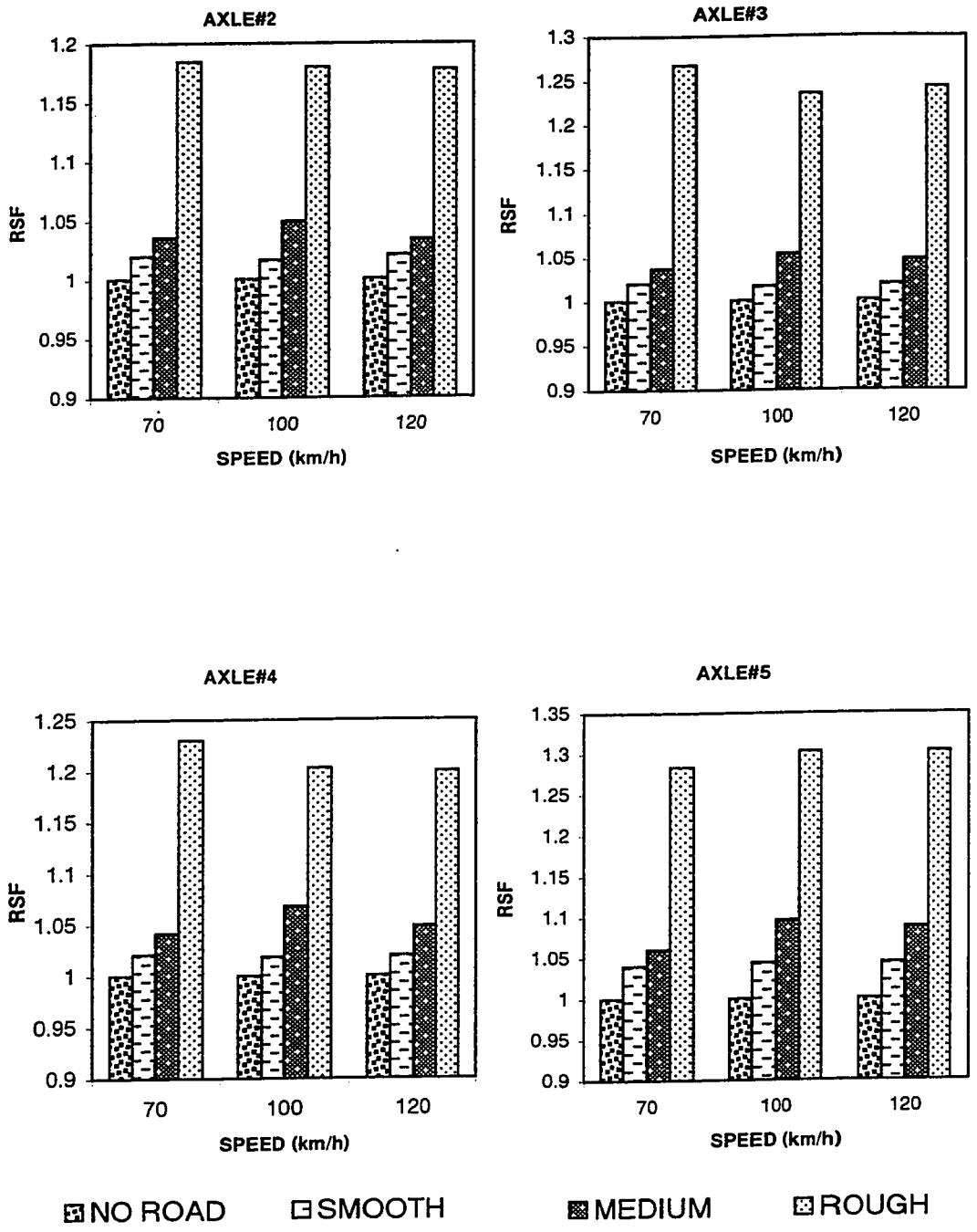

Figure 5.4: Road stress factor for various axles under different road on a straight path.

values. The results show that up to medium road roughness, the RSF values are quite low and are not highly influenced by the speed. This RSF value around 1.0 is indicative of good suspension configuration used for the vehicle. The recommended vale for RSF to ensure minimum damage is specified in the range of 1.1 to 1.4 [3]. These results further demonstrate that rough road may have very significant influence on the RSF vale. The RSF value is observed to be as high as 1.3 for axle #5 on road roughness corresponding to rough road.

Case II: Single lane change maneuver

The above simulation is next repeated for a steering input corresponding to a single lane change maneuver. The results describing the RSF for various axles on different road roughness are shown in Figure 5.5. Comparison of these results with those of straight path (Figure 5.4) show that the 70km/h RSF values for each axle is increased from around 1.0 to around 1.25 due to the maneuver. It is further observed that unlike straight path, RSF is highly sensitive to speed in the presence of steering maneuver. This clearly demonstrates the influence maneuver on the level of RSF, which primarily results from the load transfer, which in turn influences, the DLC. In all cases the load transfer is a dominating factor where road roughness has a meager influence. It is evident that under single lane change maneuver the RSF at 120km/h can be higher than 3.0, which are well beyond the suggested range.

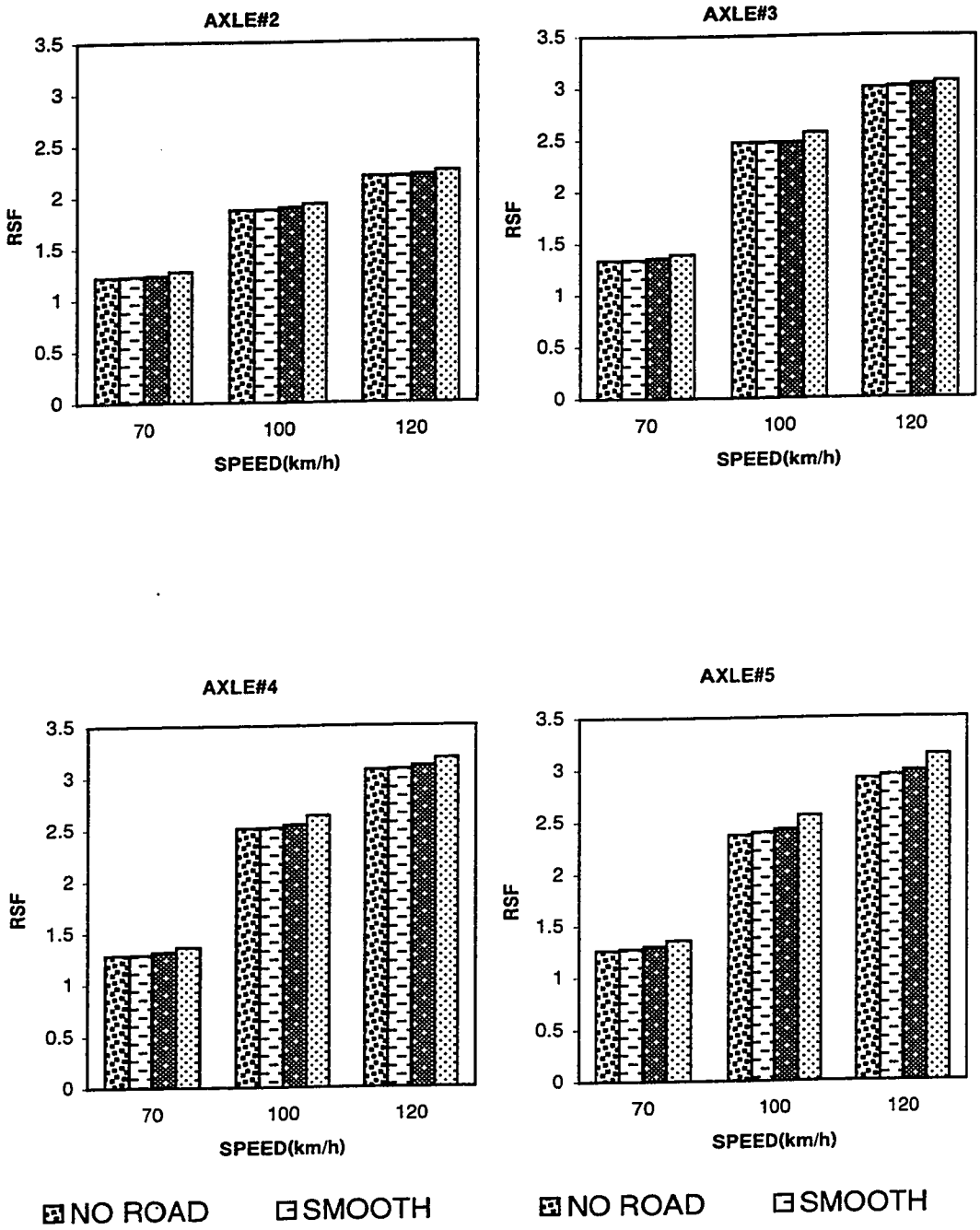

Figure 5.5: Road stress factor for various axles during single lane change maneuver on different road roughness.

Case III: Double lane change maneuver

Under a double lane change maneuver, the trends in RSF resemble those of the single lane change maneuver, as shown in Figure 5.6. Due to the severity of the maneuver, the RSF value can be as high as 6.0 especially at high speeds. These results further show that the magnitude of RSF increases drastically at 100km/h from that of the 70km/h. This resembles the trend of DLC since RSF is closely related to the DLC, which in turn is dictated by the severe load transfer characteristics under a double lane change maneuver. The trend in RSF between 100 and 120km/h is found to be very similar to that of load transfer ratio characteristics observed under the same inputs.

5.3.3 Impact Factor

In assessing the severity of dynamic loading, the dynamic road stress factor presented above is considered to be a lower estimate since it effectively assumes that the pattern of dynamic loading is random. Since the dynamic loading responds to pavement profile, and heavy vehicle suspension characteristics are to some extent, similar, the higher loads will tend to recur at specific points in the pavement. The 95th percentile load may be estimated quite readily from the dynamic load coefficient if it is assumed that the dynamic load distribution is normal. An analysis of wheel force distribution carried out showed small departure from normality. With the assumption of normality, the 95th percentile impact factors may be estimated as follows [3, 26]:

$$IF_{95th} = 1 + 1.645\text{DLC}$$

The road stress factor associated with this level of quasi-static force is given by:

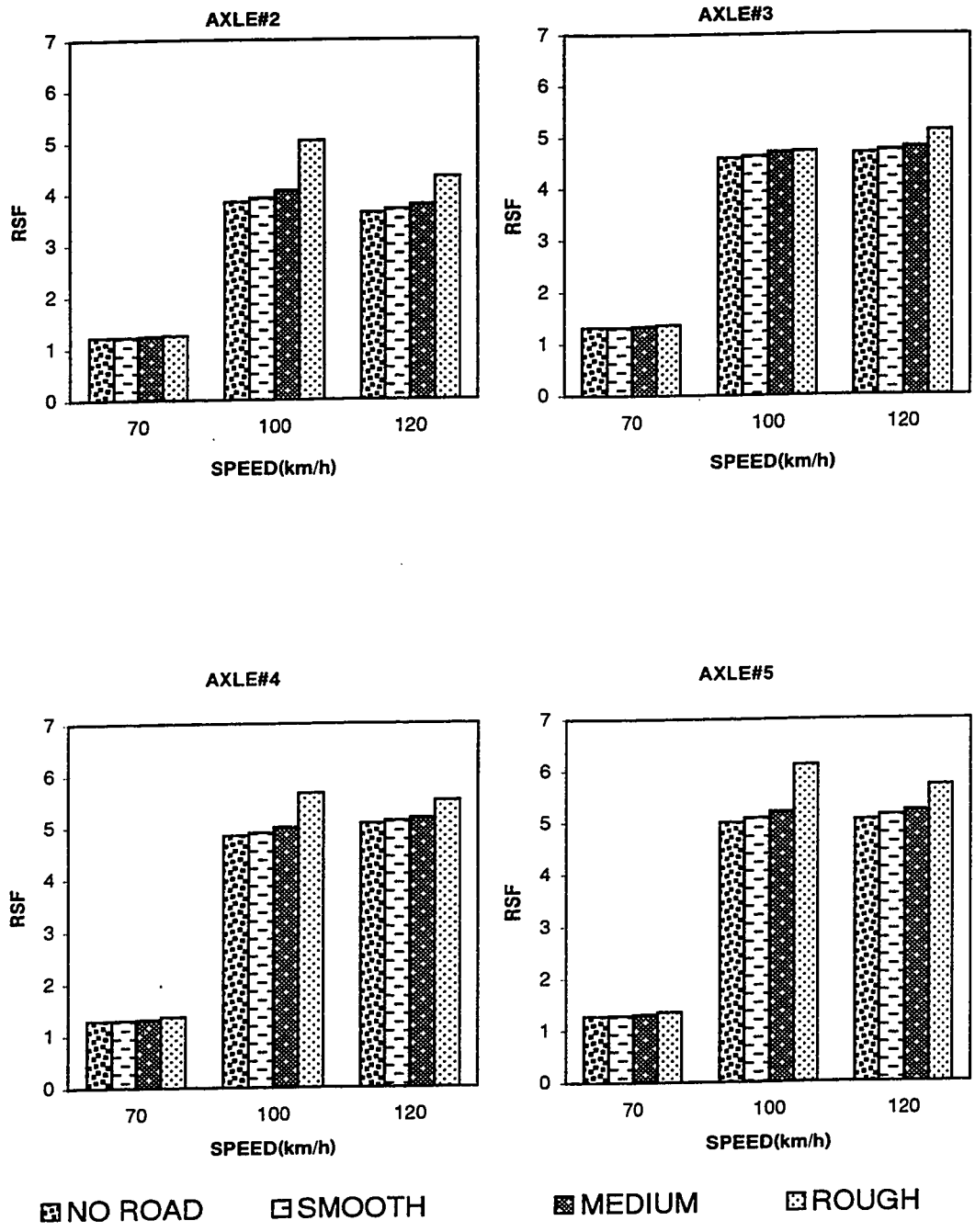

Figure 5.6: Road stress factor for various axles during double lane change maneuver on different road roughness.

$$\Phi_{95th} = (IF_{95th})^4$$

Table 5.1 shows the estimated severity of the dynamic loading for single lane change

Table 5.1: Severity of Dynamic Loading during a single lane change maneuver

Axle	Speed Km/h	Dynamic Road Stress Factor				95th Percentile Road Stress Factor			
		Road Roughness				Road Roughness			
		None	Smooth	Medium	Rough	None	Smooth	Medium	Rough
#2	70	1.218	1.22	1.237	1.274	2.95	2.9838	3.02	3.27
	100	1.869	1.87	1.89	1.92	6.65	6.66	6.76	6.97
	120	2.19	2.19	2.21	2.2537	8.39	8.405	8.49	8.69
#3	70	1.33	1.335	1.366	1.392	3.66	3.67	3.78	3.96
	100	2.476	2.476	2.47	2.569	9.8	9.883	9.88	10.3
	120	2.968	3.0	3.02	3.05	12.6	12.77	12.845	12.98
#4	70	1.272	1.273	1.311	1.35	3.35	3.375	3.523	3.8
	100	2.5	2.51	2.54	2.63	10.06	10.1	10.235	10.786
	120	3.08	3.08	3.11	3.18	13.07	13.11	13.299	13.69
#5	70	1.261	1.27	1.309	1.35	3.221	3.33	3.45	3.9
	100	2.372	2.397	2.42	2.55	9.35	9.426	9.638	10.3
	120	2.921	2.948	2.983	3.14	12.2	12.4	12.608	13.43

maneuvers at different speeds using both dynamic road stress factor and the 95th percentile road stress factor. The 95th percentile road stress factors presented in the Table

5.1, imply that the pavement damage at specific points in the pavement may be increased by 50-500% due to the dynamic tire forces. The results of the double lane change maneuver also resemble the single lane change maneuver, where the magnitudes are even higher.

5.3.4 Peak Vertical Force

The dynamic pavement load and damage potential measures examined so far are based on average force and RMS variation about the mean. The peak dynamic force that may occur for a very short period can further influence the damage process. This section examines the peak vertical force generated at each of the tire/road interface.

Case I: Single lane change maneuver

The peak vertical tire forces under a single lane change maneuver obtained at 70, 100 and 120km/h are presented in Figure 5.7. It is observed that the dynamic load experienced under front axle of the tractor is small, the emphasis can therefore be placed on the tractor rear (drive) axles and semitrailer axles. It should be noted that the static axle load on the front axle is 54000N and rest of the axles carry 90000N each. When a vehicle encounters a single lane change maneuver under no road input the tractor drive axles experience a maximum of 13000 N more than the static load and the semitrailer axles experience as high as 23000 N more than the static load corresponding to the forward speed of 70 km/h. This instantaneous peak force occurs because of the load transfer during the maneuver.

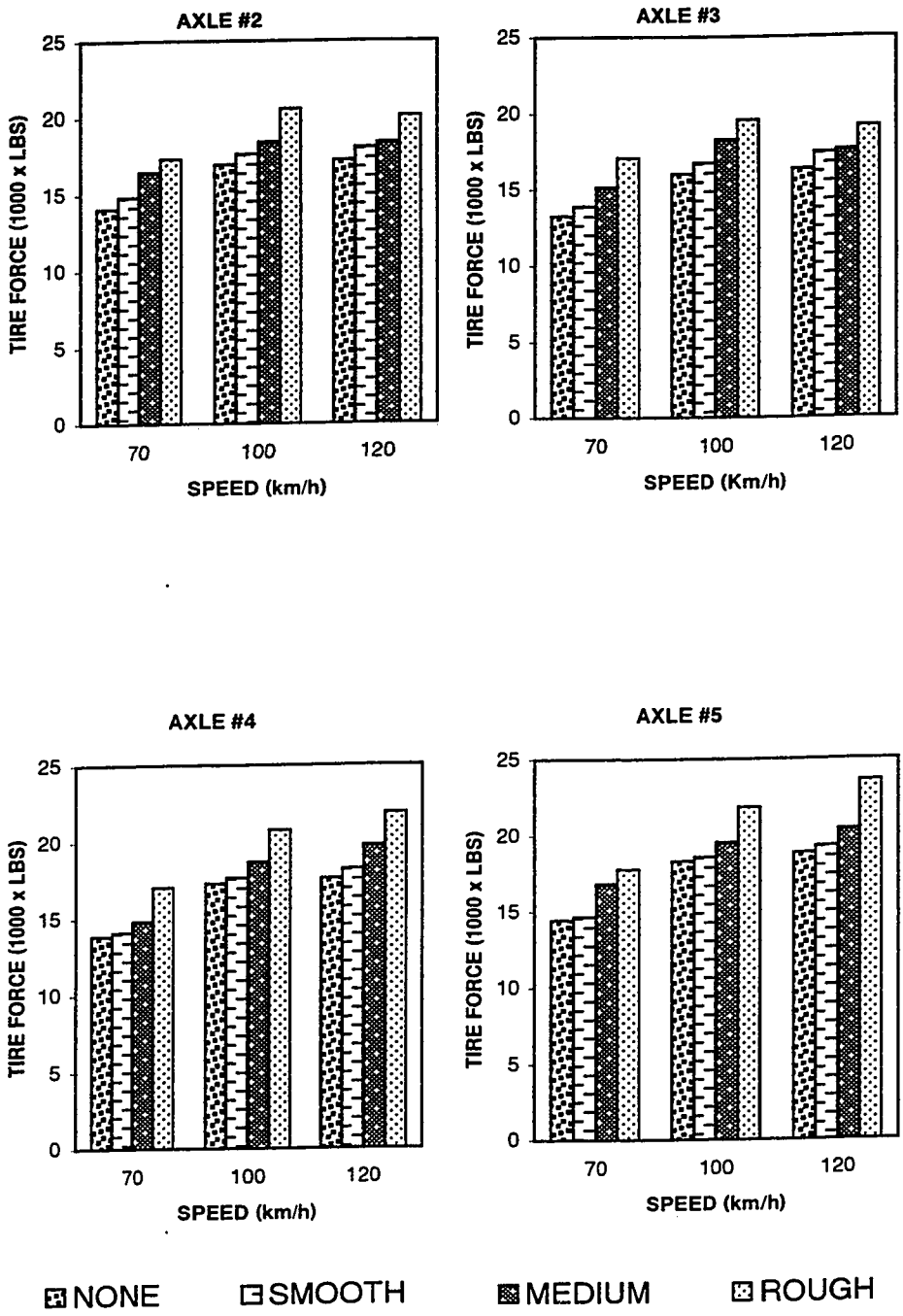

Figure 5.7: Peak vertical tire force for various axles during single lane change maneuver on different road roughness.

The moment the road inputs are brought into consideration the instantaneous peak force changes dramatically. Under the influence of smooth road input, the instantaneous tire force easily exceeds 68000N on all the axles. Under the influence of medium rough roads the peak force reaches as high as 81000N which is 80% more than the static force. It is quiet interesting to note that at 120km/h the peak dynamic tire force under rough roads may reach 110000N as shown in Figure 5.7. In other words if the left or right side wheels experience a load which is greater than the axle load, it is more likely that the wheels on the other side are no longer on the ground. This is the condition of wheel hop, which is the condition of vehicle instability. This condition, however, occurs for a fraction of a second and by other performance it is learnt that the vehicle is stable. The main concern, therefore, is the load transmitted to the ground and not the stability of the vehicle.

Case II: Double lane change maneuver

The above results repeated for a double lane change maneuver are presented in Figure 5.8. During the double lane change maneuver, even under no road influence the peak force reaches as high as 68000N and under the influence of smooth and medium rough roads the instantaneous value may reach as high as 81000N. On roads, at high speeds the wheel hop condition is evident where peak vertical force can be higher than 11000N.

The pavement is designed based on the traffic flow and as well as the axle loading. Research on the dynamic wheel loads carried out invariably employ the assumption that the vehicle is travelling on a straight path. When travelling on a straight path the load transfer from one side of the vehicle to the other side is not present even

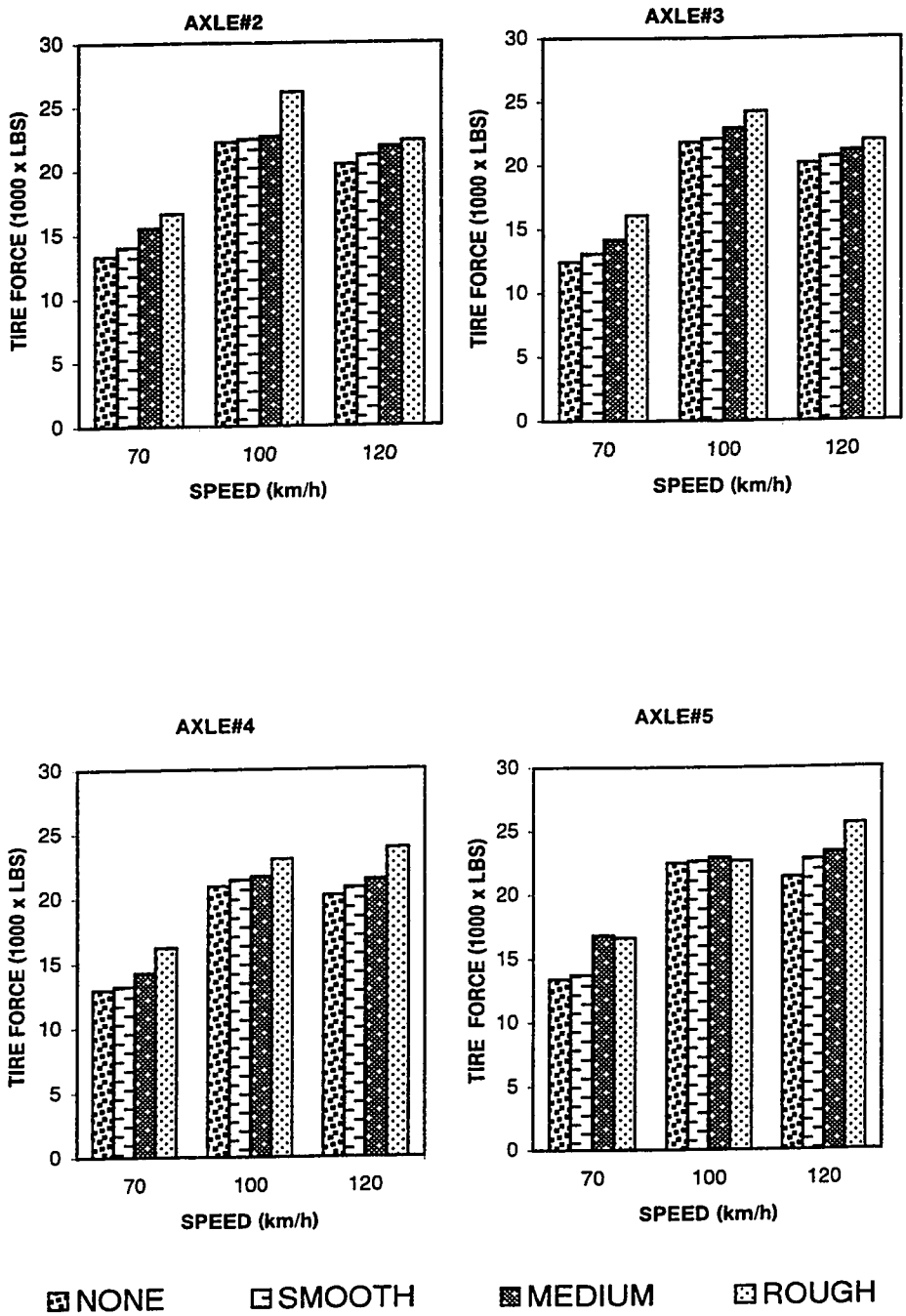

Figure 5.8: Peak vertical tire force of various axles during double lane change maneuver on different road roughness.

under the influence of rough roads. The study presented here clearly show that the dynamic wheel load is strongly influenced by both road roughness and steering maneuver. In certain cases the load may be well above 100% greater than the static load and may contribute very significantly to rapid deterioration of the road.

5.3.5 Peak Cornering Force

Apart from the vertical forces, the tires transmit significant levels of lateral forces to the pavements, when the vehicle is subject to a steering maneuver. The lateral or cornering forces developed at the tire-road interface, in general, increases with an increase in the normal load. The relationship between the cornering force and the normal load however, is quite nonlinear. Thus, the transfer of load from the inside to the outside tire during a turning maneuver may reduce the total cornering force that a pair of tires can develop.

The peak lateral forces of tires transmitted to the pavement may also contribute to road damage. The peak lateral forces and the resultant tire forces are thus analyzed to study the influence of directional maneuvers. When the vehicle encounters a lane change maneuver, the cornering force builds up under the wheel, which carries the higher load. However the cornering force developed during a maneuver is very small when compared to the vertical tire force. The cornering force developed is as high as 10% - 30% of the vertical tire force. From Figure 5.9, it is evident that the cornering force increases with the speed and the road roughness. However, the influence of the cornering force on the pavement damage is found to be negligible from the fact that the contributions of the lateral forces to the resultant DLC are relatively small. The peak lateral forces developed

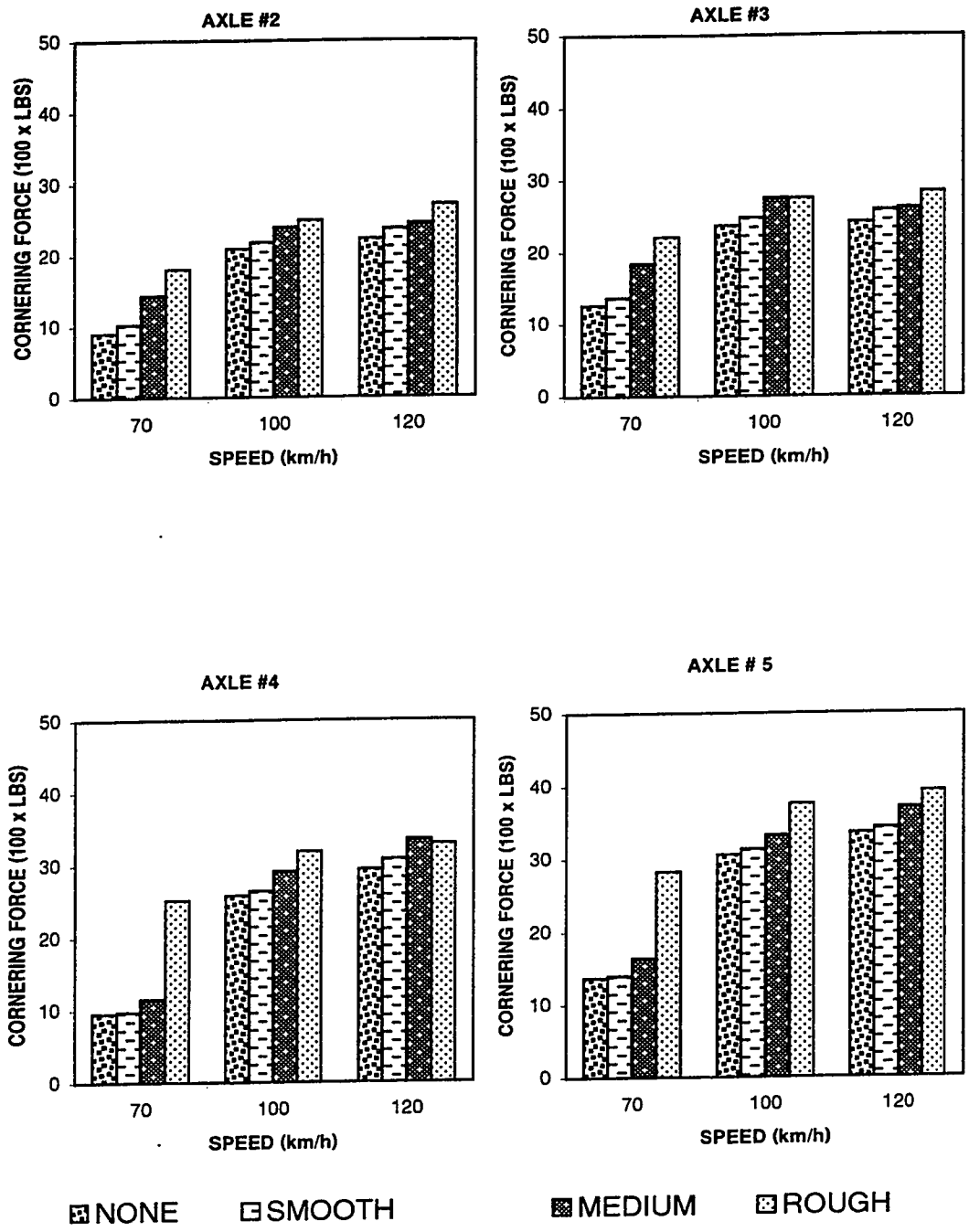

Figure 5.9: Peak cornering forces during single lane change maneuver.

during a double lane change maneuver are also observed to be relatively small and thus are not presented.

5.4 Summary

The influence of steering input on the dynamic wheel loads is thoroughly investigated through various performance measures. It is observed that the dynamic load coefficient (DLC) for this vehicle remains within the suggested values while traveling at different speeds under the influence of different road inputs. The application of steering input, however, yields significant increase in the DLC at all speeds to dynamic load transfer. The road stress factor (RSF) which is a function of DLC increases by two folds of the recommended values. The 95^{th} percentile impact factor increases by 50-500% due to the dynamic forces under steering inputs. The peak vertical force of the dynamic tire forces (tire vertical force) increases by 10-100% because of the lateral load transfer during the maneuver. It is also observed that the peak cornering force developed by the tires is considerably small when compared to vertical forces and thus does not contribute significantly to the resultant DLC.

Chapter 6

Conclusions and Suggestions for Future Research

6.1 General

The handling and directional stability performance of freight vehicles is strongly influenced by their weights and dimensions. A series of performance measures, related to yaw and roll directional stability and braking efficiency, have been proposed to assess the relative safety characteristics of different configurations. These performance measures, however, are invariably evaluated assuming perfectly flat roads. The road-roughness induced vertical and roll dynamics of the vehicle can affect the handling and dynamic roll performance of the vehicle in a significant manner. Moreover, the multiple axle groups of heavy trucks can generate peak dynamic tire loads that are greatly in excess of their static loads due to the road roughness, which results in the deterioration of pavements at a faster rate. The road roughness induced vertical dynamics of the vehicle coupled with the

steering induced roll dynamics can lead to considerable variations in the dynamic wheel loads during a directional maneuver.

In this dissertation, the handling and directional dynamics performance of an articulated freight vehicle is investigated under excitations arising from roads with varying roughness. The response characteristics are analyzed to quantify the influence of road roughness on the directional performance measures, and the dynamic wheel loads developed during different maneuvers.

6.2 Highlights of the Investigations

The steady-state and transient directional dynamics of an articulated vehicle with a multiple axle semitrailer are investigated through simulation of a nonlinear analytical model. A three dimensional nonlinear model of the vehicle incorporating tire interactions with randomly rough roads is developed based upon the Yaw / Roll model reported in the literature. The cornering forces and aligning moments of the radial tires are characterized by a nonlinear describing function in side-slip angles and normal loads. The influence of different road inputs, ranging from smooth to rough roads on the directional dynamics of the vehicle is investigated, while the vehicle is undergoing different maneuvers at different speeds. The influence of steering inputs on the dynamic tire loads of the vehicle subject to excitations arising from road roughness and maneuvers is further investigated. The influence of road roughness on the directional dynamics is characterized by different performance measures related to handling and dynamic roll behavior of the vehicle. The

dynamic wheel loads developed during a directional maneuver are quantified in terms of dynamic load coefficient, DLC.

6.3 Conclusions

Following conclusions are drawn from the results of the study:

6.3.1 Development of a Vehicle Model and Road Roughness Characterization

- Based on the reported surveys of heavy vehicle population in North America, a tractor-semitrailer combination is considered to be the most commonly used heavy vehicle configuration.
- The directional dynamics and dynamic wheel loads of the vehicle can be adequately investigated using the Yaw/Roll model of tractor-semitrailer, with sprung mass possessing five degrees of freedom, namely: lateral, vertical, yaw, roll and pitch, and the unsprung mass having two degrees of freedom, namely: roll and bounce.
- The vertical tire-road interactions can be incorporated into the vehicle model, assuming point-contact with the road and nonlinear force-deflection properties of the tire.
- Relative irregularities of the roads can be characterized by their Roughness Index (RI) values.
- The correlation between the road inputs on the left and right tracks are studied.
- The induced roll excitations present between the road inputs on the left and right tracks are studied.

6.3.2 Influence of road roughness on the directional dynamics of the vehicle

- The excitations arising from front vertical tire-road interactions directly influence the instantaneous normal load on the tires and thus the cornering forces developed by the tires.
- The road-roughness induced roll dynamics of the vehicle yields dynamic lateral load transfer, and roll deflections of the sprung and unsprung masses, which directly influence the directional and dynamic tire load performance of the vehicle.
- The rearward amplification factor of lateral acceleration is strongly influenced by the road roughness. Vehicle interactions with rough roads can reduce the rearward amplification by 40% during a single lane-change maneuver at a speed of 70 kmph.
- During a double lane-change maneuver, the influence of road roughness is significant at the speed of 70 kmph reducing the amplification of lateral acceleration by 30%.
- The influence of the road roughness on the rearward amplification in roll angle of the vehicle, however, is observed to be negligible during single- and double lane-change maneuvers. This may be attributed to the roll excitations arising from the road, cross-slope of the road, and roll dynamics of the vehicle.
- The lateral load transfer ratio, a measure of the dynamic rollover of the vehicle, increases rapidly under the influence of road roughness, irrespective of the vehicle speed and directional maneuver The increase in LTR ranges from 10% to 80%, when the vehicle is subject to a single lane change maneuver on a smooth and medium rough roads, when compared to that obtained for a perfectly smooth surface (no road input). The instantaneous values of LTR, however approaches 1.0, when the vehicle

is maneuvered on rough roads, indicating loss of contact between one or more wheels and the road.

- The LTR response of the vehicle traversing a medium rough road is 30% higher than that encountered under no road roughness condition.
- The peak LTR value of the vehicle under medium road roughness condition remains below the recommended limit of 0.6 at a forward speed of 70 kmph.
- The vehicle exhibits frequent wheel hops (instantaneous LTR = 1.0) under rough road condition.
- While the handling diagram of the vehicle, revealed stable behavior, the trailer approached oversteer conditions when maneuvered on medium rough and rough roads.

6.3.3 Influence of steering inputs on the dynamic tire loads

- The DLC due to tire loads, approach as high as 100% to 300%, during steering. The DLC during steering maneuver surpasses the recommended values of 0.3 even at a lower speed of 70 kmph. However the influence of road roughness increases as much as 30% as compared to the DLC under no road input.
- The road stress factor (RSF) increases by 50-200% during the steering maneuvers. The RSF due to tire loads tends to further increase by 10-30%, road roughness is incorporated in the analysis.
- The influence of cornering force on the dynamic wheel loads is found to be negligible.

- The dynamic wheel loads of certain wheels of the vehicle increase considerably during a steering maneuver due to dynamic load transfer and roll motions.
- The dynamic loads tend to considerably high for relatively short duration of the steering maneuver. The heavy vehicles may thus cause rapid fatigue of sections of roads requiring frequent turning or maneuvering, such as exit and entrance ramps, urban roads intersections, etc.

6.4 Suggestions for Future Research

The study presents a methodology to enhance an understanding of the influence of road roughness and directional maneuvers on the dynamic performance of heavy vehicles. Although the study has clearly demonstrated that the road roughness affects the directional performance measures of the vehicle in an adverse manner. The excessive increase in dynamic wheel loads during turning and lane-change maneuvers is further established. The dissertation research, however, is focussed on few performance measures related to handling and roll dynamics behavior, and DLC of tires under certain maneuvers. The conclusion drawn for this initial study is indicative of strong contributions of the road roughness on the selected performance measures. A thorough study of the influence of road roughness on all the directional performance measures is highly desirable. Furthermore, the methodologies to assess the road damage potentials of heavy vehicles during turning maneuvers need to be developed. It is suggested to enhance the knowledge in this subject through following systematic further investigations.

- Study the influence of road roughness on various performance measures related to yaw, damping, friction demand and braking.
- Analyze the role of damping to suppress the undesirable contribution due to road roughness.
- Study the influence of road roughness on the performance measures of vehicles with different suspension and tire pressures.
- Methods to assess the DLC due to transient dynamic loads encountered during steering maneuvers.

Bibliography

[1] Robert D. Ervin et al. , 'Influence of Size and Weights Variables on the Stability and Control Properties of Heavy Trucks', Report UMTRI-83-10-2, University of Michigan Transportation Research Institute, 1983.

[2] VLk,F. 'Lateral Dynamics of Commercial Vehicle Combinations – a Literature Survey', Vehicle Systems Dynamics, vol. 11, no. 6, pp. 305-324, 1982.

[3] David Cebon, ' Interaction Between Heavy Vehicles and Roads', The Thirty-Ninth L.Ray Buckendale Lecture, 1993.

[4] Huber, L. and Dietz, O. 'Pendelbewegungen Von Lastkraftwagen – Anhangern und iher Vereidung', VDI-Zeitschrift, vol.81, no. 16, pp. 459-463, 1937.

[5] Dietz, O. 'Pendelbewegungen an Strassen-Anhangerzugen', DKF, Heft 16, 1938.

[6] Dietz, O. 'Uber das Spuren und Pendeln von Lastkraftwagen-Anhangern', Atz, vol. 41. No. 15, 1939.

[7] Zeigler, H. 'Die Querschwingungen von Kraftwagenanhagern', Ing. – Archiv, vol. 9, no. 2, pp. 96-108, 1938.

[8] Zeigler, H. 'Der Einfluss von Bremsung und Steigung auf die Querschwingungen von Kraftwagenanhagern', Ing. – Archiv, vol. 9, no. 2, pp. 241- 243, 1938.

[9] Laurien, F. 'Untersuchung der Anhangernseitenschwingungen in Strassinzugen',Dissertation, TH, Hannocer, 1955.

[10] Schmid, I. 'Das Fahrstabilitatsverhalten zwei – und dreigliedriger Fahrzeugketten', Dissertation TH, Stuttgart, 1964.

[11] Jindra, F.'Off-tracking of tractor-trailer Combinations', Automobile Engineer, vol. 53, no. 3, pp. 96-101, 1963.

[12] Gerlach, R. 'Utersuchung der Querschwingungen von Lastzugen auf Analogrechnern', 8.Kraftfahrzeugtechnische Tagung, Karl-Marx-Stadt, Vortrag A9, Kammerder Technik, Fachverband Fahrzeugbau und Verkehr IZV Automobilbau, 1968.

[13] Nordstrom, O., Magnusson, G. and Strandberg, L. ' The Dynamic Stability of Heavy Vehicle Combinations' (in Swedish), VTI Rapport No. 9, Statens Vag-och trafikinstitut, Stockholm, 1972.

[14] Nordstrom, O., and Strandberg, L. 'The Dynamic Stability of Heavy Vehicle Combinations' International Conference of vehicle system Dynamics, Blacksburg, Virginia, Report no. 67A. Statens Vag-och trafikinstitut, Linkoping, 1975.

[15] Nordstrom, O., and Nordmark, S., 'Test procedures for the Evaluation of the Lateral Dynamics of Commercial Vehicle Combinations', Automobile- Industrie, vol 23, no.2, pp. 63-69, 1978.

[16] Bakhmutskii, M. M. and Ganesburg, I. I., 'Relation of Road Train Steering Responses and Handling Performance within System Articulated Vehicle - Driver', vol. 39, no. 2, pp 32-33, 1973.

[17] Mallikarjunarao, C. and Fancher, P. 'Analysis of the Directional Response Characteristics of Double Tanker', Society of Automotive Engineers, Paper no. 81064, pp. 4007-4026, 1979.

[18] Johnson, D.B. and Huston, J.C, 'Nonlinear Lateral Stability Analysis of Road Vehicles Using Liapunov's Second Method', SAE, paper no. 841507, 1984.

[19] Wong, J.Y. and El-Gindy, M., ' Computer Simulation of Heavy Vehicle Dynamic Behavior – User Guide to UMTRI Models', no. 3, Road and Transportation Association of Canada, 1985.

[20] Susemihl, E.A. and Kranter A.I., 'Automatic Stabilization of Tractor Jackknife in Tractor-Semitrailer Trucks', SAE, Paper no 740138, 1974.

[21] M. El-Gindy., ' An Overview of Performance Measures for Heavy Commercial Vehicles in North America', Int. J. of Vehicle Design, vol. 16, Nos. 4/5, 1995.

[22] Wong, J. Y., Theory of Ground Vehicles, Carleton University, Canada, 1993.

[23] A.G. Nalcez and J. Genin, ' Dynamic Stability of Heavy Articulated Vehicles', Int. J. of Vehicle Design, Vol. 5, no. 4, 1984, pp. 417-426.

[24] Gindy, M.,' The use of heavy vehicle performance measures for design and regulation', ASME Winter Annual Meeting, 1992.

[25] Baum, ' Comments on increasing total weights of commercial vehicles from the point of view of road stress'. Road and Traffic Research Institute, Cologne, Report 99, Road Stress Working Committee, (Translated by TRRL as WP/V&ED/87/27), 1983.

[26] Yi, K. and Hendrick, K., ' The Use of Semi-Active Suspensions to Reduce Pavement Damage', Vehicle, Tire, Pavement Interface, ASTM STP, pp. 1-13, 1992.

[27] Wen-Kan Lin, Yen-Cheng Chen, Bohdan T. Kulakowski, and Donald A. Streit 'Dynamic Wheel/ Pavement Force Sensitivity to Variations in Heavy Vehicle Parameters, Speed and Road Roughness', Int. J. of Vehicle Design, Vol. 1, no. 2, 1994, pp. 139-155.

[28] Cebon D, 'Theoretical Road Damage due to Dynamic Tire Forces of Heavy Vehicles. Part 1: Dynamic analysis of vehicles and road surfaces'. Proc I. Mech.E., 202 (C2) pp. 103-108, 1988.

[29] Cebon D, 'Theoretical Road Damage due to Dynamic Tire Forces of Heavy Vehicles. Part 2: Simulated damage caused by a tandem-axle vehicle'. Proc I. Mech.E., 202 (C2) pp. 109-117, 1988.

[30] Sweatman PF, ' A Study of Dynamic Wheel Forces in Axle Group Suspensions of Heavy Vehicles', ARRB, Special Report SR27, 1983.

[31] Woodrooffe JHF, LeBlanc PA and LePiane KR, ' Effects of Suspension Variation on the Dynamic Wheel Loads of a Heavy Articulated Highway Vehicle', Canroad Transportation Research Corporation, Canada, Vehicle Weights and Dimensions Study Vol 11, 1986.

[32] Eisenmann J, 'Dynamic wheel Load Fluctuations – Road Stress'. Strasse und Autobahn, 4 pp. 127-128, 1975.

[33] The AASHO Road Test, Report 5, ' pavement Research', HRB Special Report 61E, National academy of Science, National Research Council Publication 954, 1962.

[34] Eisenmann J, ' Beuteilung der Strassen – beanspuchung'. Strasse und Autobahn, 3 1978.

[35] Alain Piche, 'Detection of Onset of Instabilities for an Early Warning Safety Monitor for Articulated Freight vehicles', M. Eng. Thesis, 1990.

[36] 'A Factbook of the Mechanical Properties of the Components for Single-Unit and Articulated Heavy Trucks', Final Report, National Highway Traffic Safety Administration, 1986.

[37] Gordan D. Gronberg,' Use of Pavement Condition Data in Highway Planning and Road Life Studies', HRB, Highway Research Record 40, pp.37-50, 1963.

[38] Paul H, Thomas L and Keith O,' Random Vibrations, Theory and Practice'.

[39] B. E. Quinn and S. D. Hildebrand,' Effect of Road Roughness on Vehicle Steering', HRB, Highway Research Record 471, pp. 62-75, 1973.

[40] Damien, T.M. et al.,' Pavement Profiling Various Pavements: Ottawa/Smith Falls', John Emery Geotechnical Engineering Report', 1992.